UNIVERSITY OF MICHIGAN
FEB 8 1957
ENGINEERING LIBRARY

JOURNAL OF FLUID MECHANICS

VOLUME 1 PART 6

DECEMBER 1956

Printed and Published by

TAYLOR & FRANCIS LTD

RED LION COURT, FLEET STREET, LONDON, E.C.4

The JOURNAL OF FLUID MECHANICS exists for the publication of theoretical and experimental investigations of all aspects of the mechanics of fluids, and is issued in six parts per volume.

Editor:

Dr. G. K. BATCHELOR, Cavendish Laboratory, University of Cambridge, Cambridge, England.

Assistant Editors:

Dr. T. B. BENJAMIN, Dr. I. PROUDMAN.

Associate Editors:

Prof. G. F. CARRIER, Pierce Hall, Harvard University, Cambridge 38, Massachusetts, U.S.A.

Prof. W. C. GRIFFITH, Palmer Physical Laboratory, Princeton University, Princeton, New Jersey, U.S.A.

Prof. M. J. LIGHTHILL, Department of Mathematics, The University, Manchester, England.

Authors wishing to have papers published in the JOURNAL should communicate them to any one of the persons named above, choosing one in their own country where possible.

Authors are urged to ensure that their papers are written clearly and attractively, in order that their work will be readily accessible to readers.

Manuscripts should be typed in double spacing on one side of the paper only, with references listed at the end in alphabetical order of authors. Drawings should be done on a large scale in Indian ink on tracing cloth or drawing paper, captions being typed on a separate sheet. Proofs of papers from overseas will usually be despatched to authors by airmail. Authors are entitled to receive 50 offprints of a paper in the JOURNAL free of charge, and additional offprints can be purchased from the publisher.

PRICE £1 ($3.00) per part

Subscription, £5 10s. 0d. per volume of six parts, post free ($16.50 in U.S.A. and Canada)

Agents for U.S.A. and Canada:

Academic Press Inc., 111 Fifth Avenue, New York 3, N.Y., U.S.A.

The properties of equilibrium boundary layers

By A. A. TOWNSEND
Emmanuel College, Cambridge

(*Received* 7 *June* 1956)

SUMMARY

The recent work on equilibrium (i.e. self-preserving) turbulent boundary layers in adverse pressure gradients is compared with theoretical predictions based on current generalizations about the turbulent shear flow. Using only assumptions of similarity, it is possible to show that an equilibrium layer can exist only if the free stream velocity varies as a power of distance downstream with an exponent greater than $-\frac{1}{3}$ and if the velocity defect from the free stream is small. Assuming further that the effective eddy viscosity is independent of distance from the wall over the outer part of the layer, most of the properties of equilibrium layers may be computed from the known behaviour of layers in zero pressure gradient. The predicted values of skin friction and the predicted shape and magnitude of the mean velocity distribution are in fair agreement with the observations of Clauser. Finally, the modifications that are necessary if the velocity defect is not small are discussed briefly.

1. INTRODUCTION

Much of the recently published work on turbulent boundary layers has abandoned the long-standing tradition of purely empirical approach based on direct analogy with the behaviour of laminar layers and has begun to use generalizations about the characteristics of turbulent shear flow. The movement began, perhaps, with the work of Ludweig & Tillmann (1949) who established experimentally that the distribution of mean velocity near a smooth wall is independent of the pressure gradient in the free stream, and is determined by the shear stress at the wall and the fluid viscosity. This conclusion, which has since received abundant experimental confirmation (e.g. Coles 1956), is more than an empirical generalization, being a necessary consequence of the mixing-length and similarity theories of turbulence and indeed of any theory of turbulence that assumes net turbulent transfer of energy to be small within the wall region of substantially constant shear stress. At much the same time it was being realized that the apparent variation in shape of the velocity profiles for a constant pressure layer is an illusion, produced by measuring velocities relative to the stationary wall rather than to the free stream. Profiles of velocity defect from the free stream velocity are accurately similar in shape except within the viscous layer next the wall (e.g. Clauser 1954). Again, this 'defect law' is not

only an empirical result but is a consequence of two widely accepted generalizations about turbulent flows, that the general motion of a fully developed turbulent flow is independent of the fluid viscosity*, and that developing flows tend to a condition of moving equilibrium or self-preservation.

Although these two results are in a sense experimental rediscoveries of much earlier theoretical work (see, for example v. Kármán (1930) and Goldstein (1938)), they are none the less valuable, and their application to boundary layers in pressure gradients is of great interest. A fundamental advance in this direction was made by Clauser (1954) who, by trial and error adjustment of the external pressure gradient, constructed 'equilibrium' boundary layers satisfying the defect law and who discussed and analysed their behaviour. It is possible, using only the generalizations employed in inferring the existence of a universal velocity profile near a wall and the defect law for constant pressure layers, to determine the conditions necessary for the existence of an equilibrium boundary layer in a pressure gradient (Townsend 1956). The purpose of this paper is to summarize the results of this analysis, including the consequences of assuming an effective eddy viscosity independent of distance from the wall in the outer layer, and then to compare the predictions of this theory with the results and generalizations of Clauser (1956).

2. Notation

Consider a boundary layer on a smooth flat plate whose surface is the plane, $y = 0$. Oz is the direction of homogeneity at right angles to the two-dimensional mean flow, and Ox is parallel to the surface and in the general direction of the flow. Then,

U, V	are the components of the mean velocity parallel to Ox and Oy respectively,
u, v, w	are the components of the turbulent velocity fluctuation parallel to Ox, Oy, Oz,
P	is the pressure,
ν	is the kinematic viscosity,
U_1, P_1	are the Ox component of the mean velocity and the pressure in the free stream just outside the layer,
τ_0	is the shear stress at the wall,
K, A	are the constants in the universal logarithmic distribution of mean velocity near a smooth wall (equation 3.12),
$c_f = 2\tau_0/U_1^2$	is the local coefficient of skin friction,
$\gamma = \tau_0^{\frac{1}{2}}/KU_1$	is a non-dimensional quantity specifying skin friction,
$u_0 = \tau_0^{\frac{1}{2}}/K$	is the velocity scale of the boundary layer,

* This statement is not inconsistent with the dependence of the velocity profile near the wall on fluid viscosity. The magnitude of the viscosity merely determines a velocity of translation for the fully turbulent part of the flow, and velocity differences within it are unaffected.

$\delta = \nu/\tau_0^{1/2}\exp\left(\frac{1}{\gamma} - A\right)$ is the length scale (or 'thickness') of the layer,

η denotes y/δ,

$f(\eta) = (U - U_1)/u_0$ is a universal function specifying the mean velocity distribution,

g_1, g_2, g_{12} are functions specifying the distributions of turbulent intensities and stresses,

$$I_1 = -\int_0^\infty f(\eta)\, d\eta, \qquad I_2 = \int_0^\infty [f(\eta)]^2\, d\eta,$$

$$Y = K^{-3} I_1 \gamma^{-2} \exp\left(\frac{1}{\gamma} - A\right), \qquad Y_1 = Y\left\{1 + \left(2 + \frac{I_2}{I_1}\right)\gamma\right\},$$

$R_x = \int \frac{U_1\, dx}{\nu} = \frac{U_1 x/\nu}{1+a}$ is the Reynolds number,

ν_T is the effective eddy viscosity in the outer layer,

$R_s = u_0\,\delta/\nu_T$ is a non-dimensional constant relating the effective eddy viscosity to the velocity distribution,

s is a non-dimensional variable of position,

C is a constant determining the scale of the velocity defect.

It should be noted that the pressures and stresses are 'kinematic', that is, they are the ordinary mechanical values divided by the fluid density. Also, since the pressure in the free stream is related to the velocity by

$$U_1 \frac{\partial U_1}{\partial x} = -\frac{\partial P_1}{\partial x}, \tag{2.1}$$

its gradient is specified by the variation of free stream velocity. For the most part, we consider a free stream velocity variation

$$U_1 = Bx^a \quad (x > 0), \tag{2.2}$$

which represents an adverse pressure gradient if the exponent is negative.

3. The conditions for self-preserving development of a boundary layer

The defect law for the mean velocity distribution in a boundary layer is equivalent to the assumption of self-preserving profiles in a wake, i.e.

$$U = U_1 + u_0\, f(y/\delta), \tag{3.1}$$

where u_0 and δ are scales of velocity and length depending on x, and the function is independent of x. For the establishment of a self-preserving flow it is necessary that the distributions of shear stress and turbulent intensities should be expressible in terms of the same scales by other functions independent of distance downstream, say

$$\overline{uv} = u_0^2 g_{12}(y/\delta), \qquad \overline{u^2} = u_0^2 g_1(y/\delta), \qquad \overline{v^2} = u_0^2 g_2(y/\delta). \tag{3.2}$$

Naturally, the distributions must satisfy the equations of mean motion, which, for the boundary layer, and to the approximation usually found

sufficiently accurate, can be reduced to the single equation,

$$U\frac{\partial U}{\partial x}+V\frac{\partial U}{\partial y}+\frac{\partial \overline{uv}}{\partial y}+\frac{\partial(\overline{u^2}-\overline{v^2})}{\partial x}=U_1\frac{\partial U_1}{\partial x}+\nu\frac{\partial^2 U}{\partial y^2}. \tag{3.3}$$

In terms of the self-preserving functions of equations (3.1), and (3.2) this may be written

$$\frac{d(u_0U_1)}{dx}f-\frac{u_0}{\delta}\frac{d(U_1\delta)}{dx}\eta f'+u_0\frac{du_0}{dx}(f^2+2(g_1-g_2))-$$
$$-\frac{u_0}{\delta}\frac{d(u_0\delta)}{dx}f'\int_0 f\,d\eta-\frac{u_0^2}{\delta}\frac{d\delta}{dx}\eta(g_1'-g_2')+\frac{u_0^2}{\delta}g_{12}'=\frac{\nu u_0}{\delta^2}f'', \tag{3.4}$$

where dashes indicate differentiation with respect to η.

This equation may be satisfied exactly by self-preserving functions independent of x if the ratios of the non-zero coefficients are independent of x. For laminar flow, the functions representing the fluctuating motion are identically zero and self-preserving flow is possible either if

$$u_0=U_1\propto x^n,\qquad \delta\propto x^{(1-n)/2}, \tag{3.5}$$

or if

$$u_0=U_1\propto e^{\mu x},\quad \delta\propto e^{-(1/2)\mu x},\quad (\mu>0), \tag{3.6}$$

(Goldstein 1939). If δ is now defined by

$$\frac{\delta^2}{\nu}\frac{dU_1}{dx}=\frac{2a}{1+a}=n\quad \text{say},$$

substitution in equation (3.4) gives an equation for $f(\eta)$,

$$anf-f'\left(\eta+\int_0^\eta f\,d\eta\right)+nf^2=f''. \tag{3.7}$$

(The exponential flow (3.6) corresponds to $n=2$.) When the non-dimensional stream-function defined by

$$\psi'(\eta)=1+f(\eta),$$

is introduced, this becomes the Hartree form of the Falkner–Skan equation,

$$\psi'''+\psi\psi''=n(\psi'^2-1). \tag{3.8}$$

It is known that acceptable solutions satisfying the boundary conditions, $\psi(0)=\psi'(0)=0$, $\psi''(0)=-n$, $\psi'(\infty)=1$, exist only if $n>-0{\cdot}199$ or $a>-0{\cdot}11$ (Hartree 1937). This sets a lower limit to the possible values of the exponent and to the severity of the adverse pressure gradient.

In turbulent flow, a self-preserving flow is possible only if

$$u_0\propto U_1\propto(x_0-x)^{-1},\qquad \delta\propto(x_0-x),\qquad (x_0>x), \tag{3.9}$$

corresponding to the accelerated boundary layer within a wedge. The equation may be satisfied *approximately* if the velocity defect is small, that is, if

$$-u_0f\ll U_1, \tag{3.10}$$

unless $\eta\ll\delta$. Then equation (3.4) may be approximated by

$$\frac{d(u_0U_1)}{dx}f-\frac{u_0}{\delta}\frac{d(U_1\delta)}{dx}\eta f'+\frac{u_0^2}{\delta}g_{12}'=0 \tag{3.11}$$

except very close to the wall where direct viscous stresses are appreciable. The existence of a wall layer within which the velocity distribution is given by

$$U = \frac{\tau_0^{1/2}}{K}\left[\log\frac{\tau_0^{1/2}y}{\nu} + A\right] \tag{3.12}$$

implies that we may choose as scales

$$u_0 = \tau_0^{1/2}/K$$

and

$$\delta = \frac{\nu}{\tau_0^{1/2}}\exp\left(\frac{KU_1}{\tau_0^{1/2}} - A\right). \tag{3.13}$$

It may then be shown that self-preserving flow is only possible for free stream velocity variations of three types,

(*a*) $U_1 = Bx^a \quad (x > 0,\ a > -\frac{1}{3})$,

(*b*) $U_1 = B(-x)^a \quad (x > 0,\ a < -\frac{1}{3})$,

(*c*) $U_1 = Be^{\mu x} \quad (\mu > 0)$.

Of these only the first can represent retarded flow (for $0 > a > -\frac{1}{3}$) and correspond with an equilibrium layer of the type studied by Clauser. For this type of velocity variation, the relation between wall stress and position is given by

$$Y = K^{-3}I_1\gamma^{-2}\exp\left(\frac{1}{\gamma} - A\right) = \frac{1}{3a+1}\frac{U_1 x}{\nu} \tag{3.14}$$

with the approximation (3.10). Here $\gamma = \tau_0^{1/2}/KU_1$ is a friction parameter, and $I_1 = -\int_0^\infty f(\eta)\,d\eta$ is a constant of the flow and a function of a. It should be emphasized that the wall stress is uniquely related to the velocity in the free stream and so to the position. The existence of the proper variation of free steam velocity (or pressure) alone is not sufficient to ensure self-preserving development; the boundary layer must be matched to the pressure gradient.

Clauser has observed that the parameter

$$\Pi = \frac{\delta^*}{\tau_0}\frac{dP_1}{dx}, \quad \text{where } \delta^* = \int_0^\infty\left(1 - \frac{U}{U_1}\right)dy,$$

is independent of x in an equilibrium layer. In the present notation,

$$\Pi = -\frac{I_1 u_0 \delta}{K^2 u_0^2}\frac{dU_1}{dx} = -\frac{a}{1+3a}, \tag{3.15}$$

using equations (3.13) and (3.14). The constancy of this parameter is a simple consequence of this very general theory of boundary layers with a small velocity defect. It is also the condition that the terms in the equation for the momentum integral should preserve a constant ratio.

4. The velocity distribution in the outer part of an equilibrium layer

Experience with other self-preserving free turbulent flow suggests that an acceptable description of the mean velocity distribution may be obtained by assuming an effective eddy viscosity constant over the outer part of the

layer, the mean velocity distribution due to this being joined smoothly to the logarithmic distribution that obtains in the inner layer (Clauser 1956, Townsend 1956). Clauser has done this without assuming the velocity defect to be small. His results can be derived assuming the relation (3.14) between wall stress and position, although this relation is not accurate for finite velocity defect. In the outer layer, the terms of equation (3.4) that involve the turbulent intensities are usually negligible, and then, putting

$$-\overline{uv} = \nu_T \frac{\partial U}{\partial y}, \tag{4.1}$$

where $u_0 \delta/\nu_T = R_s$, a constant depending on a, the equation of mean motion becomes

$$\frac{I_1}{K^2 R_s} f'' - \frac{2a}{1+3a} f + \frac{1+a}{1+3a} f' \left[\eta + \gamma \int_0 f \, d\eta\right] - \frac{a}{1+3a} \gamma f^2 = 0. \tag{4.2}$$

In terms of a new position variable $s = \left(\frac{K^2 R_s}{I_1} \frac{1+a}{1+3a}\right)^{1/2} \eta$, this is

$$\frac{d^2 f}{ds^2} - nf + \frac{df}{ds}\left(s + \gamma \int_0 f \, ds\right) - \tfrac{1}{2} n \gamma f^2 = 0. \tag{4.3}$$

The non-dimensional stream function defined by

$$\psi'(s) = 1 + \gamma f(s)$$

satisfies the equation

$$\psi''' + \psi\psi'' = \tfrac{1}{2} n(\psi'^2 - 1). \tag{4.4}$$

This is the Hartree equation with two differences. The first and obvious one is that the coefficient outside the bracket is half its value in the equation for laminar flow (3.8), and the second is that the boundary condition at $s = 0$ is no longer $\psi'(0) = 0$ but $\psi'(0) = 1 + \gamma f(0)$. This boundary condition is not independent of x, and does not conform to the initial assumption of self-preservation.

For very small velocity defect in the outer layer, the equation for $f(s)$ becomes

$$\frac{d^2 f}{ds^2} + s \frac{df}{ds} - nf = 0. \tag{4.5}$$

The appropriate solution of this equation is a multiple of the function $Hh_n(s)$, defined by

$$Hh_n(s) = \int_0^\infty \frac{t^n}{n!} \exp[-\tfrac{1}{2}(t+s)^2] \, dt. \tag{4.6}$$

The complete variation of mean velocity is obtained by adjusting the multiplying constant of the function describing the variation in the outer layer to give a smooth junction with the velocity distribution in the inner layer where

$$f(\eta) = \log \eta. \tag{4.7}$$

At high Reynolds numbers, part of the region of constant stress is within the region of small velocity defect, so that the mean velocity distribution within this region of overlap must be both self-preserving and identical

with the universal logarithmic profile. The conditions for this have been given as equations (3.13), and this process of matching the velocity profile for constant eddy viscosity to the logarithmic profile is no more than a working approximation consistent with these conditions and the assumptions of self-preservation.

5. The hypothesis of large eddy equilibrium

There is a considerable body of evidence showing that the rate of spread of a turbulent flow into the ambient undisturbed fluid depends on the presence of a system of large eddies which are also responsible for the observed intermittency of turbulent flow near the free stream boundary. The author has postulated that these large eddies are an integral part of the mechanism that regulates the intensity of the turbulent motion and the rate of entrainment of non-turbulent fluid (Townsend 1951, 1956). By assuming a plausible form for these eddies, it is possible to obtain a complete solution for the boundary layer problem in terms of the universal constants, K and A, of equation (3.12) and of two numbers specifying the position and scale of the large eddies with respect to the mean velocity distribution. Estimates of these numbers may be made from a consideration of the origin and dynamics of the large eddies, or they may be determined by analysing experimental measurements of the layers. If it is assumed that these numbers are independent of pressure gradient, all the properties of equilibrium boundary layers can be predicted from the known properties of constant-pressure layers without ambiguity. For details, reference should be made to the full account (Townsend 1956).

To these approximations, the mean velocity distribution consists of the distribution

$$f(\eta) = \log \eta \tag{5.1}$$

in the inner layer (say for $\eta < \eta_0$) and the distribution

$$f(\eta) = -CHh_n(s), \tag{5.2}$$

where

$$s = \left(\frac{K^2 R_s}{I_1(1+n)}\right)^{1/2} \eta, \qquad R_s = \frac{u_0 \delta}{\nu_T},$$

in the outer layer ($\eta > \eta_0$). As Clauser points out, the experimental determination of mean velocity profiles is not sufficiently accurate to make profitable a comparison of the *shapes* of observed and predicted profiles, and the test of a theory must be the prediction of the scales of variation.

If the velocity distribution in the outer layer is extrapolated to the wall, the extrapolated velocity there, U_0, should be given by

$$K \frac{U_1 - U_0}{\tau_0^{1/2}} = CHh_n(0) = C \frac{\sqrt{(\frac{1}{2}\pi)}}{2^{n/2}(\frac{1}{2}n)!}. \tag{5.3}$$

The scale of velocity variation is so defined by the constant C, which is given by

$$C^2 = \frac{1}{1+n}\left[\frac{22}{\sqrt{\pi}}\, 1{\cdot}7^n \left(\frac{1+n}{2}\right)! - \frac{2^{2+n}}{\pi}\left\{\left(\frac{1+n}{2}\right)!\right\}^2\right], \tag{5.4}$$

the constants, 22 and 1.7, being selected to conform to observations of constant-pressure layers. If $(1+n)$ is small,

$$C^2 = \frac{6{\cdot}66}{1+n}. \tag{5.5}$$

Clauser uses two scales of distance from the wall. The first is

$$\Delta = \int_0^\infty \frac{U_1 - U}{\tau_0^{1/2}}\, dy = \frac{I_1}{K}\delta. \tag{5.6}$$

Distances expressed in this scale are related to distances expressed in the scale of the variable s (equation (4.3)) by

$$\frac{y}{\Delta} = \left(\frac{1+n}{I_1 R_s}\right)^{1/2} s = [k(1+n)]^{1/2} s. \tag{5.7}$$

The second scale is δ_0, the total thickness of the layer, presumably the distance from the wall beyond which the mean velocity variation is imperceptible. This scale will be roughly three times the scale of s.

Clauser expresses the eddy viscosity in the outer layer in terms of the non-dimensional constant, k, which is given by

$$\frac{1}{k} = \frac{U_1 \delta^*}{\nu_T} = I_1 R_s = \frac{121\ K^{-2} \quad 1{\cdot}2^{2n}}{\frac{22}{\sqrt{\pi}}\, 1{\cdot}7^n \left(\frac{1+n}{2}\right)! - \frac{2^{2+n}}{\pi}\left\{\left(\frac{n+1}{2}\right)!\right\}^2}. \tag{5.8}$$

The comparison of these predictions with Clauser's measurements is shown in figures 1 and 2, using the values of n in table 1 computed from equation (3.15). This procedure gives a definite value for a, and should

	Π	a	$1-n$	$1-3a$
Distribution I	2	−0·286	0·20	1/7
Distribution II	7	−0·318	0·0667	1/22

Table 1

make some allowance for the effect of a finite velocity defect. These values of a are in fair agreement with the observed distributions of free stream velocity (figure 3).

The computed variation of C agrees fairly well with observation, the difference being most marked for the lesser pressure gradient. The theory also predicts a nearly constant value for k in agreement with Clauser's findings, although the computed values are 20–25% less than the observed values. This is caused by the use of the velocity profile (5.2) to compute I_1. By overestimating the velocity defect near the free stream, this leads to values of I_1 about 10% greater than the true values. The constancy of k is not unexpected as $U_1 \delta^* = \int_0^\infty (U_1 - U)\, dy$ is nearly the simplest possible expression for the product of length and velocity scales for distributions of nearly similar shapes.

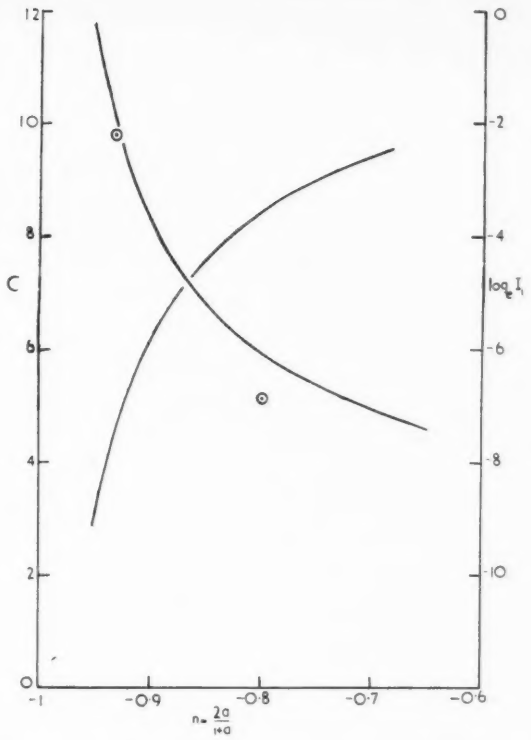

Figure 1. Computed variations of the constants C and I_1 with n (circled points from Clauser's measurements).

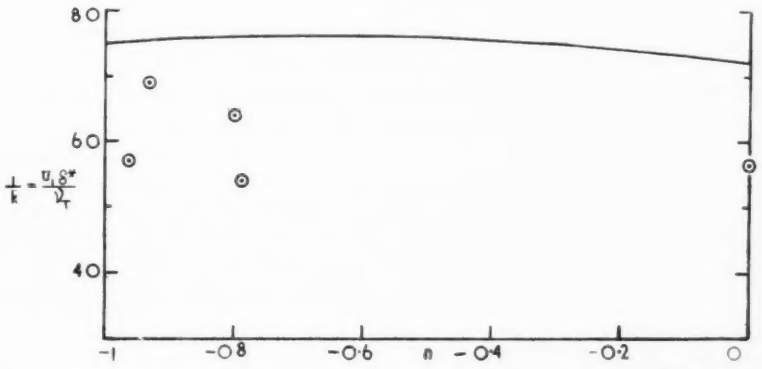

Figure 2. Dependence of effective eddy viscosity on integrated velocity defect (full line from theory, circled points from Clauser 1956).

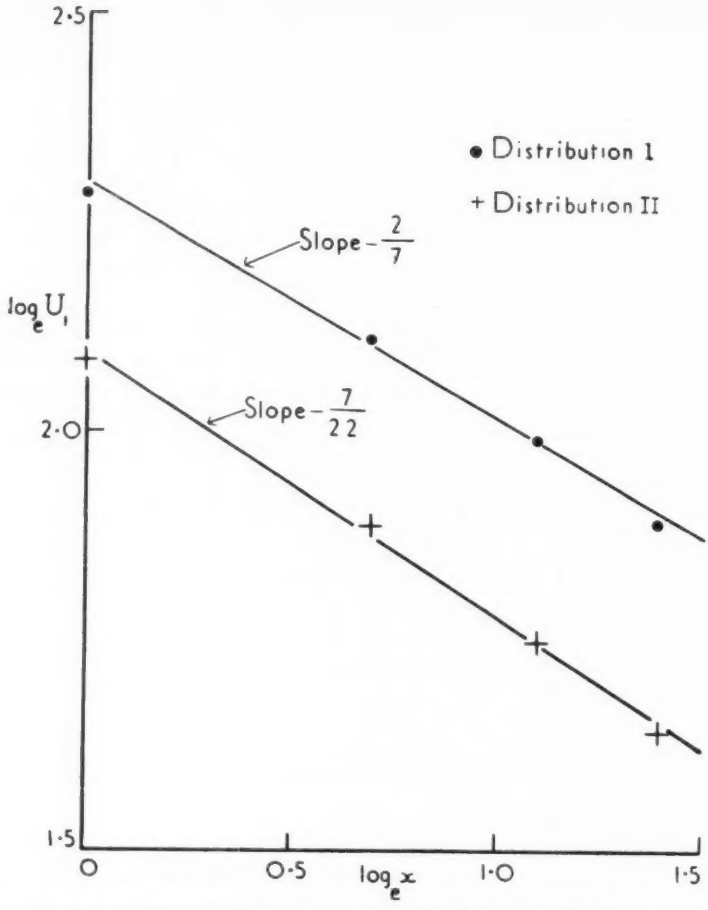

Figure 3. Comparison of Clauser's pressure distributions with the appropriate power laws.

Comparison of predicted and observed scales of distance may be made by computing the position at which the velocity defect is one-half of the extrapolated velocity defect, $U_1 - U_0$, or the position at which the velocity defect is small. Some results of this comparison are shown in table 2.

Lastly, the skin friction may be computed from the friction equation

$$Y = K^{-3} I_1 \gamma^{-2} \exp\left(\frac{1}{\gamma} - A\right) = \frac{1}{1+3a} \frac{U_1 x}{\nu}, \tag{5.9}$$

using values of I_1 given by

$$I_1 = [(1+n)C^2 + 1] \exp\left[1 - \frac{(\frac{1}{2}\pi)^{1/2} C}{2^{n/2} (\frac{1}{2}n)!}\right]. \tag{5.10}$$

If $1+n$ is small, this is nearly

$$I_1 = 7{\cdot}66 \exp\left[1 - \left(\frac{6{\cdot}66}{1+n}\right)^{1/2}\right]. \tag{5.11}$$

	Δ/δ_0	$y_{1/2}/\delta_0$	$s_{1/2}$		s_0	$Hh_n(s_0)$
			Obs.	Calc.	Obs.	
Distribution I	6·35	0·41	1·26	1·18	3·06	0·010
Distribution II	12·0	0·45	1·26	1·18	2·81	0·018
Constant pressure	3·58	—	—	—	2·37	0·025

Table 2

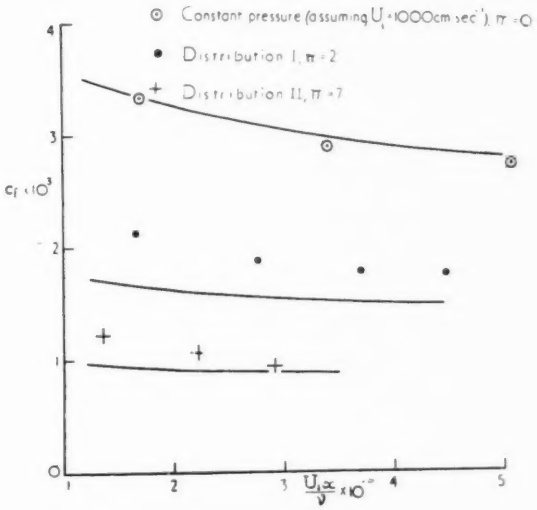

Figure 4. Observed and theoretical distributions of friction coefficient.

Figure 4 compares the predicted values of local friction coefficient with the experimental measurements. The agreement is good only for the larger pressure gradient.

6. The critical value of the power law exponent

The theory for small velocity defect in the outer layer, which is valid at extremely high Reynolds numbers (equation (3.14) shows γ to decrease indefinitely with increasing Reynolds number), predicts that equilibrium layers exist only if $a > -\frac{1}{3}$. The basis of this prediction is the necessity for a positive value of the friction function Y. If the effective eddy viscosity is constant within the outer layer, equation (4.6) shows that self-consistent velocity profiles exist, the critical profile for $a = -\frac{1}{3}$ being

$$f(s) = -Ce^{-1/2s^2}, \tag{6.1}$$

which has a zero gradient at the wall indicating zero wall stress.

There are two simple ways of looking at the consequences of finite velocity defect, viz. by including second-order terms in the derivation of the stress-position relation (assuming self-preservation of velocity profiles and wall stress) or by finding the range of a for which the modified Hartree equation (4.4) has acceptable solutions (assuming that the coefficients of equation (3.4) may be computed from the relation (3.14)). Ideally, both should be investigated but the result is a modified form of equation (4.4) whose solutions have not been studied.

The equation for the momentum integral is

$$\frac{d}{dR_x}\left[\{I_1-(2I_1+I_2)\gamma\}\gamma^{-2}\exp\left(\frac{1}{\gamma}-A\right)\right]+ \\ +\frac{\nu}{U_1^2}\frac{dU}{dx}(2I_1-I_2\gamma)\gamma^{-2}\exp\left(\frac{1}{\gamma}-A\right)=K^3, \quad (6.2)$$

where terms of order less than γ have been omitted. With the use of friction function

$$Y_1 = K^{-3}[I_1-(2I_1+I_2)\gamma]\gamma^{-2}\exp\left(\frac{1}{\gamma}-A\right), \quad (6.3)$$

it becomes

$$\frac{dY_1}{dR_x}+\frac{2a}{1+a}[1+(2+\tfrac{1}{2}I_2/I_1)\gamma]\frac{Y_1}{R_x}=1 \quad (6.4)$$

to the same approximation. Since γ is a slowly varying quantity, an approximate solution may be obtained by neglecting its variation. This is

$$Y_1 = R_x\frac{1+a}{1+3a+2a\gamma(2+\tfrac{1}{2}I_2/I_1)}, \quad (6.5)$$

which has meaning only if

$$a > -\frac{1}{3+2a\gamma(2+\tfrac{1}{2}I_2/I_1)}. \quad (6.6)$$

The quantity $\gamma I_2/I_1$ is nearly proportional to the velocity defect ratio $(U_1-U_0)/U_1$. For the critical velocity profile defined by equation (6.1),

$$\frac{I_2}{I_1}\gamma = \frac{C}{\sqrt{2}}\gamma = \frac{1}{\sqrt{2}}\frac{U_1-U_0}{U_1}. \quad (6.7)$$

Alternatively, we may suppose the development of the layer to be described by the theory for small velocity defect, and look at the conditions for acceptable solutions of the modified Hartree equation (4.4) for various defect ratios. Numerical solutions quoted by Clauser (1956) show that the critical value of the exponent varies with defect ratio in the way shown in figure 5. A comparison with critical values obtained from equations (6.6) and (6.7) shows fair agreement between the two estimates only for small velocity defect ratios.

Neither of these arguments is altogether satisfactory and further work is desirable.

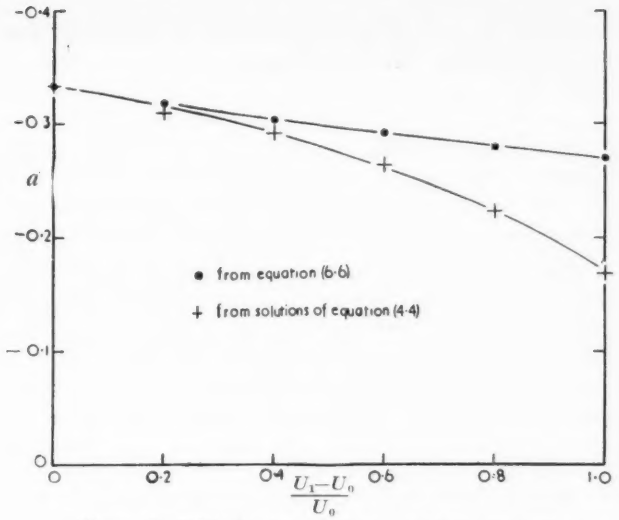

Figure 5. Critical values of the power-law exponent.

7. Concluding remarks

The properties of self-preserving or equilibrium boundary layers may well prove to be of considerable importance in the understanding of the general behaviour of boundary layers in pressure gradients. The theory based on the assumptions of small velocity defect and large eddy equilibrium fits the observations of Clauser as well as can be expected in view of the comparative crudity of the theory and the absence of disposable constants. It should be noted that the hypothesis of large eddy equilibrium is very nearly equivalent to assuming eddy viscosity to be a universal multiple of the integral of the velocity defect.

The condition that the velocity defect is small is satisfied very weakly in the experimental layers, and better agreement between theory and experiment might be obtained by considering the effects of finite defect.

References

Clauser, F. H. 1954 *J. Aero. Sci.* **21,** 91.

Clauser, F. H. 1956 *Advances in Applied Mechanics* **4,** 1.

Coles, D. 1956 *J. Fluid Mech.* **1,** 191.

Hartree, D. R. 1937 *Proc. Camb. Phil. Soc.* **33,** 223.

Goldstein, S. (Ed.) 1938 *Modern Developments in Fluid Dynamics.* Oxford: Clarendon Press.

Goldstein, S. 1939 *Proc. Camb. Phil. Soc.* **35,** 338.

Ludwig, H. & Tillmann, W. 1949 *Ing. Arch.* **17,** 288.

Kármán, T. v. 1930 *Proc. 3rd Inter. Congr. Appl. Mech.* **1,** 85.

Townsend, A. A. 1950 *Phil. Mag.* **41,** 890.

Townsend, A. A. 1956 *The Structure of Turbulent Shear Flow.* Cambridge University Press.

The generation of edge waves by moving pressure distributions

By H. P. GREENSPAN
Harvard University, Cambridge, Massachusetts

(*Received* 1 *August* 1956)

SUMMARY

An analytical study is made of the resurgent wave motion induced by pressure distributions moving parallel to a straight coast line. The resurgence is shown to consist of an infinite number of edge wave modes; expressions for these modes are given and the wavelengths, frequencies and amplitudes are shown to be in agreement with experimental results. The effects of a Gaussian pressure distribution are analysed. For large-scale disturbances off the east coast of the United States only the fundamental mode is excited. Conditions, such as storm size, speed and distance from shore, for maximum induced wave amplitudes are derived.

1. INTRODUCTION

It has been observed that hurricanes and other similar phenomena travelling approximately parallel to a neighbouring coast line sometimes induce a resurgent wave motion. These waves are characterized by the facts that they propagate along the shore line, are essentially confined within a distance of one wavelength from the coast (hence the name 'edge waves'), have wavelengths measured in miles, amplitudes measured in feet, and periods measured in hours.

Munk, Snodgrass & Carrier (1956) conjectured that this resurgence was primarily due to the deviation of the storm pressure distribution from normal atmospheric pressure, and was neither wind-generated nor a consequence of other effects. Using a simple mathematical model for the pressure deviation, with the assumption of quasi-steady state conditions (that the disturbance has been in existence and in motion for an infinite time interval), they obtained results in agreement with experimental evidence. Computed periods, and amplitudes agreed with known values. Their original conjecture concerning the cause of the resurgence was thereby substantiated.

In this paper, the transient problem (i.e. with the disturbance originating at a finite time) is considered and applied to a more precise physical model.

2. THE FUNDAMENTAL EQUATION AND ITS SOLUTION

In order to motivate the choice of an appropriate model on which to base our calculations, we anticipate (as indicated in the introduction) that

the hurricane generated surface waves will display an amplitude η of the order of 3 feet, a wavelength λ of about 200 miles, and a period of about 6 hours. The extremely long wavelengths and small wave heights suggest that the linear shallow water theory may be applied. In order that this theory may provide a valid approximation, the wavelength of a progressive wave propagation must be large compared to the ocean depth, the ocean depth must be large compared to the wave height, and the gradients of the wave height and depth must be small compared to unity. Simple estimates of the orders of magnitude involved show that in the phenomena in question these conditions are satisfied.

The linearized theory essentially eliminates the depth variable z from the exact analysis by averaging the velocity components over the depth. The pressure is then hydrostatic (see Lamb 1945 for a more complete analysis).

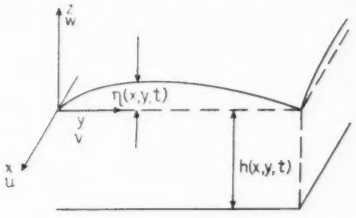

Figure 1. Fluid with a fixed boundary and a free surface.

With the meaning of the symbols shown in figure 1, and with uniform density ρ, the conservation equations of mass and momentum are

$$\frac{\partial \eta(x,y,t)}{\partial t} = -\frac{\partial (uh)}{\partial x} - \frac{\partial (vh)}{\partial y}; \tag{1}$$

$$\frac{\partial u(x,y)}{\partial t} = -\frac{1}{\rho}\frac{\partial P(x,y,z,t)}{\partial x}; \qquad \frac{\partial v}{\partial t} = -\frac{1}{\rho}\frac{\partial P(x,y,z,t)}{\partial y}, \tag{2}$$

where $P(x,y,z,t) \doteqdot P(x,y,0,t)+g\rho(\eta-z)$, and $P(x,y,0,t)$ is the applied surface pressure. We may eliminate u and v to obtain

$$\nabla.(h\nabla\eta) - \frac{1}{g}\frac{\partial^2\eta}{\partial t^2} = -\frac{1}{\rho g}(h\nabla^2 P + \nabla h.\nabla P). \tag{3}$$

Here and in the following, $P(x,y,0,t)$ is replaced by P or $P(x,y,t)$. We can also define a potential function by the relations $u = \partial\phi/\partial x$, $v = \partial\phi/\partial y$, and eliminate η to obtain an equation for ϕ:

$$\nabla.(h\nabla\phi) - \frac{1}{g}\frac{\partial^2\phi}{\partial t^2} = \frac{1}{\rho g}\frac{\partial P}{\partial t}, \tag{4}$$

the wave height being

$$\eta = -\frac{P}{\rho g} - \frac{1}{g}\frac{\partial\phi}{\partial t}. \tag{5}$$

It remains to specify the ocean depth h, and to linearize the topography. We consider only a straight coast line, and take the ocean depth to be a

linear function of distance from shore y, i.e. $h = \alpha y$. For the constant α, we choose the average slope of the ocean depth over the first 120 miles. Munk, Snodgrass & Carrier (1956) have shown that since the wave motion under investigation is sensibly zero farther than $\lambda/2\pi$ from shore, it is essentially independent of the manner in which the ocean depth varies at these large distances. Since the phenomenon in which we are primarily interested is essentially confined to the continental shelf, the approximation of constant slope is adequate. The total linearization of the actual topography is then a straight coast line and a constant slope depth (figure 2).

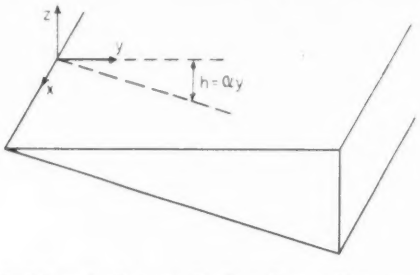

Figure 2. Linearized ocean depth and coast line topography.

With $h = \alpha y$, equation (3) becomes

$$y\nabla^2\eta + \frac{\partial\eta}{\partial t} - \frac{1}{\alpha g}\frac{\partial^2\eta}{\partial t^2} = -q_1(x,y,t) = -\frac{1}{\rho g}\left(\frac{\partial P}{\partial y} + y\nabla^2 P\right), \tag{6}$$

and equation (4) becomes

$$y\nabla^2\phi + \frac{\partial\phi}{\partial t} - \frac{1}{\alpha g}\frac{\partial^2\phi}{\partial t^2} = -q_2(x,y,t) = \frac{1}{\rho g\alpha}\frac{\partial P}{\partial t}. \tag{7}$$

Given that $P(x,y,t) = 0$ for $t < 0$, the correct boundary conditions are: $\eta(x,y,0) = 0$, $\partial\eta(x,y,0)/\partial t = 0$, $\eta(x,y,t) \to 0$ as $|x| \to \infty$ for all positive y, and also as $y \to \infty$ for all x (the phenomenon is confined to the shelf), and finally that the wave height is finite at the shore line. This finiteness condition is the most liberal physical requirement one can apply in the coastal region where the linearized differential equations are not a valid description.

Since equations (6) and (7) differ only in the form of the forcing function, we need only solve the former; the solution to the latter is obtained by replacing η by ϕ and $q_1(x,y,t)$ by $q_2(x,y,t)$. We can now take Fourier and Laplace transforms of equation (6). Defining

$$\left.\begin{aligned} f(k,y,s) &= \int_{-\infty}^{\infty} e^{ikx}\,dx \int_0^{\infty} e^{-st}\eta(x,y,t)\,dt \\ Q_j(k,y,s) &= \int_{-\infty}^{\infty} e^{ikx}\,dx \int_0^{\infty} e^{-st}q_j(x,y,t)\,dt, \end{aligned}\right\} \tag{8}$$

where $j = 1, 2$, we obtain

$$y\frac{d^2f}{dy^2} + \frac{df}{dy} - \left(\frac{s^2}{\alpha g} + k^2 y\right)f = -Q_1(k,y,s). \tag{9}$$

The boundary conditions become $|f(k,0,s)| < \infty$ and $f(k,y,s) \to 0$ as $y \to \infty$. Anticipating difficulties with the inverse Fourier transform, we shall solve, instead of equation (9),

$$y\frac{d^2f}{dy^2} + \frac{df}{dy} - \left(\frac{s^2}{\alpha g} + k_*^2 y\right)f = -Q_1(k,y,s), \tag{10}$$

where

$$k_* = (k^2+\epsilon^2)^{1/2}, \tag{11}$$

subject to the same boundary conditions. After taking the inverse Laplace and Fourier transforms of the solution of equation (10), we shall let ϵ tend to zero to obtain the solution of equation (6). If it is convenient and proper, we can also perform this limiting process at some intermediate step. The function k_* is not single-valued in the complex k plane and we restrict its possible values by two branch lines originating at $\pm i\epsilon$ and extending to $\pm i\infty$ respectively. The reasons for this particular choice will become evident shortly. We choose the Riemann sheet for which $k_* \geqslant 0$ on the entire real axis.

A few simple substitutions will enable us to rewrite equation (10) in a more convenient form. Let

$$\left.\begin{aligned} f(k,y,s) &= \exp(-k_* y)\,p(k,y,s), \\ u &= 2k_* y, \\ p_1(k,u,s) &= p(k, \tfrac{1}{2}u/k_*, s), \end{aligned}\right\} \tag{12}$$

and equation (10) becomes

$$up_1'' + (1-u)p_1' - \left(\frac{1}{2} + \frac{s^2}{2\alpha g k_*}\right)p_1 = -\frac{\exp(\frac{1}{2}u)}{2k_*}Q_1(k, \tfrac{1}{2}u/k_*, s). \tag{13}$$

The boundary conditions become $\exp(-\frac{1}{2}u)p_1(u) \to 0$ as $u \to \infty$ and $|p_1(k,0,s)| < \infty$*. To solve (13), we expand $p_1(k,y,s)$ and

$$-\frac{\exp(\frac{1}{2}u)}{2k_*}Q_1(k, \tfrac{1}{2}u/k_*, s)$$

in terms of Laguerre polynomials (see Courant & Hilbert 1953), and then use the differential equation to determine the unknown coefficients. The expansions are

$$p_1(u) = p_1(k,u,s) = \sum_{n=0}^{\infty} A_n L_n(u), \tag{14}$$

$$-\frac{\exp(\frac{1}{2}u)}{2k_*}Q_1(k, \tfrac{1}{2}u/k_*, s) = \sum_{n=0}^{\infty} B_n L_n(u), \tag{15}$$

where

$$L_n(u) = e^u\left(\frac{d^n}{du^n}\right)(u^n e^{-u}), \tag{16}$$

* We can consider k and s to be real numbers until it is necessary to invert the Fourier and Laplace transforms.

and

$$\left.\begin{aligned} A_n &= \frac{1}{(n!)^2}\int_0^\infty e^{-u}p_1(u)L_n(u)\,du, \\ B_n &= -\frac{1}{(n!)^2}\int_0^\infty \frac{\exp(-\frac{1}{2}u)}{2k_*}\,Q_1(k,\tfrac{1}{2}u/k_*,s)L_n(u)\,du. \end{aligned}\right\} \tag{17}$$

Substituting these expansions into equation (13) and using the fact that $L_n(u)$ satisfies Laguerre's differential equation

$$uL_n''(u)+(1-u)L_n'(u)+nL_n(u) = 0, \tag{18}$$

we obtain

$$\sum_0^\infty A_n\left(-n-\tfrac{1}{2}-\frac{s^2}{2\alpha g k_*}\right)L_n(u) = \sum_0^\infty B_n L_n(u). \tag{19}$$

We use the orthogonality relation

$$\int_0^\infty e^{-u}L_n(u)L_m(u)\,du = (n!)^2\delta_{mn} \tag{20}$$

to equate coefficients, and hence determine that

$$A_n = \frac{-B_n}{(n+\frac{1}{2}+s^2/2\alpha g k_*)}. \tag{21}$$

This implies that

$$p_1(u) = p_1(k,u,s) = -\sum_{n=0}^\infty \frac{B_n L_n(u)}{(n+\frac{1}{2}+s^2/2\alpha g k_*)} \tag{22}$$

($p_1(u)$ satisfies the boundary conditions, since each $L_n(u)$ does) or

$$f(k,y,s) = \exp(-k_*y)\sum_{n=0}^\infty \frac{\displaystyle\int_0^\infty L_n(u)\exp(-\tfrac{1}{2}u)Q_1(k,\tfrac{1}{2}u/k_*,s)\,du}{(n+\frac{1}{2}+s^2/2\alpha g k_*)2k_*(n!)^2}\,L_n(2k_*y). \tag{23}$$

The wave height is then obtained by inverting the Fourier and Laplace transforms; i.e.

$$\eta(x,y,t) = \frac{1}{4\pi^2 i}\int_{-\infty}^{\infty} e^{-ikx}\,dk\int_{-i\infty+\epsilon_0}^{i\infty+\epsilon_0} e^{st}f(k,2,s)\,ds. \tag{24}$$

The path of integration in the k plane for the inverse Fourier transform must lie within a strip containing the real axis. The function k_* has been defined with this in mind; i.e. the inversion contour can pass between the two branch points $\pm i\epsilon$ without crossing a branch line.

There are other ways to solve equation (13); methods involving the solutions of the homogeneous equation (i.e. confluent hypergeometric functions) lead to extremely difficult integrations. A Green's function technique for solving (6), although of little practical value, reduces to an interesting eigenvalue problem, one with both a discrete and a continuous spectrum; this will be the subject of a future paper. The advantage of the method used lies in the fact that we shall be able to consider separately the effects of a pressure distribution on the individual edge wave modes, easily eliminating extraneous parts of the solution. The wave motion can be determined with little difficulty.

3. Application to the model of Munk, Snodgrass & Carrier

Let us now consider this model, adjusted so that it arises at some finite time. The surface pressure is

$$P(x,y,t) = \frac{P_0 a(y+a)}{(x-Ut)^2+(y+a)^2} H(t), \tag{25}$$

where $H(t)$ is the Heaviside function, U is the velocity at which the disturbance moves parallel to the coast, and a is the half-pressure radius. The resemblance to actual hurricanes is poor, but the Fourier transform is simple. We shall solve for the wave height η directly. The forcing function is, from equation (6),

$$q_1(x,y,t) = \frac{P_0 a}{\rho g} \frac{(x+Ut)^2-(y+a)^2}{[(x-Ut)^2+(y+a)^2]^2},$$

and its transform is

$$Q_1(k, \tfrac{1}{2}u/k_*, s)\frac{\exp(\frac{1}{2}u)}{2k_*} = -\frac{\pi P_0 a}{\rho g}\frac{k_* \exp(-ak_*)}{(s-ikU)2k_*},$$

which is constant, so that

$$B_0 = \frac{\pi P_0 a}{\rho g}\frac{k_* \exp(-ak_*)}{2k_*(s-ikU)}, \quad \text{and } B_n = 0 \text{ for } n \neq 0.$$

Thus the expansion of equation (22) reduces to one in which only the 'first' Laguerre polynomial, $L_0(u) = 1$, appears. This implies, as we shall see, that this pressure distribution can excite only the fundamental edge wave mode. The Fourier Laplace transform of η is

$$f(k,y,s) = \frac{\gamma k_* \exp\{-k_*(y+a)\}}{(s-ikU)(s^2+\alpha g k_*)}, \tag{26}$$

where

$$\gamma = -\frac{\alpha\pi P_0 a}{\rho}. \tag{27}$$

The wave height is determined by taking inverse Laplace and Fourier transforms as in equation (24). The function $f(k,y,s)$ is not meromorphic in k, but is in the variable s, having simple poles at $s = ikU$, $s = \pm i(\alpha g k_*)^{1/2}$. It is, therefore, much simpler to compute first the inverse Laplace transform. We set

$$r(k,y,t) = \frac{1}{2\pi i}\int_{-i\infty+\varepsilon_0}^{i\infty+\varepsilon_0} f(k,y,s)e^{st}\,ds,$$

and upon performing the integration we obtain for $t > 0$

$$r(k,y,t) = -\gamma k_* \exp\{-k_*(y+a)\}\left\{\frac{\exp(ikUt)}{k^2U^2-\alpha g k_*} + \right.$$
$$\left. + \frac{\exp\{i(\alpha g k_*)^{1/2}t\}}{2(\alpha g k_*)^{1/2}\{(\alpha g k_*)^{1/2}-kU\}} + \frac{\exp\{-i(\alpha g k_*)^{1/2}t\}}{2(\alpha g k_*)^{1/2}\{(\alpha g k_*)^{1/2}+kU\}}\right\}, \tag{28}$$

and $r(k,y,t) = 0$ for $t < 0$.

As a function of k, $r(k,y,t)$ has *no* poles on the real axis. The solution of the problem is then

$$\eta(x,y,t) = \frac{1}{2\pi}\int_\Gamma e^{-ikx} r(k,y,t)\,dk, \tag{29}$$

or

$$\eta(x,y,t) = -\frac{\gamma}{2\pi}(I+II+III), \tag{30}$$

where

$$\left.\begin{aligned} I &= \int_\Gamma f_I\,dk = \int_\Gamma \frac{\exp\{-k_*(y+a)\}\exp\{-ik(x-Ut)\}}{(k_* U^2-\alpha g)}\,dk, \\ II &= \int_\Gamma f_{II}\,dk = \int_\Gamma \frac{\exp[-i\{kx-(\alpha g k_*)^{1/2}t\}]k_*\exp\{-k_*(y+a)\}}{2(\alpha g k_*)^{1/2}\{(\alpha g k_*)^{1/2}-kU\}}\,dk, \\ III &= \int_\Gamma f_{III}\,dk = \int_\Gamma \frac{\exp[-i\{kx+(\alpha g k_*)^{1/2}t\}]k_*\exp\{-k_*(y+a)\}}{2(\alpha g k_*)^{1/2}\{(\alpha g k_*)^{1/2}+kU\}}\,dk, \end{aligned}\right\} \tag{31}$$

Although the original integrand has no poles, and the path Γ may be the real axis, each individual term does have one or more poles; Γ must therefore be suitably altered. We can easily verify that (30) is a solution of equation (6) by formally carrying out the differentiations.

Our task is now to evaluate and interpret these integrals. I is the easiest and we evaluate it first. This term represents the quasi-steady state solution derived by Munk, Snodgrass & Carrier (1956). (The terms due to a finite starting time are therefore the last two integrals.) The best contour to take is one that minimizes the effect in front of the pressure spot and produces a reaction behind it. Any contour will finally give a correct result for η provided we are consistent; however, we wish to give a definite physical meaning to I, independent of II and III. The poles of f_I are located at $k_* U^2-\alpha g = 0$, i.e.

$$\left.\begin{aligned} k_r &= k_0 = \frac{\alpha g}{U^2}, \\ k_l &= -k_0 = -\frac{\alpha g}{U^2}, \end{aligned}\right\} \tag{32}$$

for $\epsilon = 0$; k_r is located in the right half plane, and k_l in the left half plane. The best contour is one that goes under both of these singularities as in figure 3. For $x > Ut$, we may close the contour Γ in the lower half plane by the quadrants, Γ_1, Γ_1', the two sides of the branch line Γ_4, and the circular path about the branch point, as shown; for $x < Ut$ we may similarly close the contour in the upper half plane. The poles contribute values for $x < Ut$ only. The integrals about the branch lines are easily computed. The integrals over connecting quadrants tend to zero as $|k| \to \infty$, and the

integrals round the small circles about branch points tend to zero as the radius $|k|$ tends to zero. The result is

$$\left.\begin{aligned} I &= \frac{2}{U^2}\operatorname{Re}\Psi(1,1,ik_0[|x-Ut|+i(y+a)]) \quad x<Ut, \\ I &= \frac{4\pi}{U^2}\exp\{-k_0(y+a)\}\sin k_0(x-Ut)+ \\ &\quad +\frac{2}{U^2}\operatorname{Re}\Psi(1,1,ik_0[|x-Ut|+i(y+a)]) \quad x<Ut \end{aligned}\right\} \tag{33}$$

where Ψ is the confluent hypergeometric function of the second kind (see Erdelyi 1954). Asymptotically, for large values of $(x-Ut)^2+(y+a)^2$,

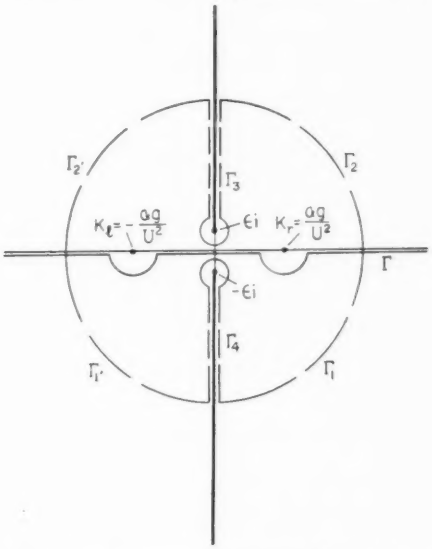

Figure 3. Fourier inversion contours for $X<$ or >0.

Ψ is proportional to the surface pressure $P(x,y,t)$. The result consists of a resurgence for $x<Ut$, together with a motion restricted to the immediate neighbourhood of the pressure spot for which the wave height is the direct effect of the distribution on the ocean surface.

We now show that *II* and *III* essentially yield a cancelling wave, $-(4\pi/U^2)\exp\{-k_0(y+a)\}\sin k_0(x-Ut)$ for $x<\frac{1}{2}Ut$, implying that the resurgence is given asymptotically by

$$\eta \sim \frac{2\pi P_0 a k_0}{\rho g}\exp\{-k_0(y+a)\}\sin k_0(x-Ut) \quad \text{for } \tfrac{1}{2}Ut<x<Ut$$

$$\eta \sim 0 \text{ elsewhere,}$$

where k_0 is $\alpha g/U^2$ as in (32).

The integral to be evaluated is

$$II = \int_\Gamma \frac{\exp[-i\{kx-(\alpha g k_*)^{1/2}t\}-k_*(y+a)]}{2(\alpha g k_*)^{1/2}\{(\alpha g k_*)^{1/2}-kU\}}\, k_*\, dk.$$

To obtain results which are applicable when x and Ut are both large compared to $y+a$, we use a steepest descent procedure; it is noted that if

$$\exp\{-k_*(y+a)\}$$

were not present, we could integrate explicitly. The method of steepest descents is used to remove $\exp\{-k_*(y+a)\}$ from the integrand, and the remaining integral is then evaluated.

Let $x < 0$, $t = x/\beta$, then $II = \int_\Gamma \exp\{xf(k)\}\psi(k)\, dt$,

where

$$f(k) = -i\left(k - \frac{(\alpha g k_*)^{1/2}}{\beta}\right), \quad \text{and} \quad \psi(k) = \frac{\exp\{-k_*(y+a)\}k_*}{2(\alpha g k_*)^{1/2}\{(\alpha g k_*)^{1/2}-kU\}}.$$

We are interested in x and Ut large compared to $y+a$; accordingly $\exp\{-k_*(y+a)\}$ is included in the slowly-varying function $\psi(k)$. The saddle point, determined from the condition $f'(s_0) = 0$ is

$$s_0 = \frac{\alpha g}{4\beta^2}. \tag{34}$$

The path of steepest descent is (if $k = \xi + i\mu$, and $\epsilon = 0$) the parabola

$$\xi^2 - \left(\frac{\alpha g}{4\beta^2}\right)^2 = -\frac{\alpha g \mu}{2\beta^2}. \tag{35}$$

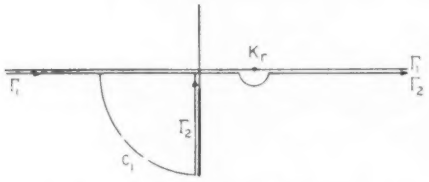

Figure 4. Contour deformation of the inversion path.

By considering the properties of the integrand f_{II}, and, specifically, the behaviour of the factor

$$\exp[-ikx+(\alpha g k_*)^{1/2}-k_*(y+a)]$$

as $|k|$ tends to infinity in the third quadrant, we can show that

$$\int_\Gamma f_{II}\, dk = \int_{\Gamma_3} f_{II}\, dk$$

(see figure 4). Thus far it has been essential to keep one branch line in the upper half plane, and the other in the lower half plane. The branch line from $i\epsilon$ to $i\infty$ can now be turned into the third quadrant (figure 5); and, for computing purposes, it will be taken to be the ray $\theta = \frac{3}{2}\pi$, where the angle θ has its usual meaning. We use the contour Γ_3 about the branch

line and the paths Γ_4 and Γ_5, which are the arcs of a circle of radius R, to form a closed loop (in the limit as $R \to \infty$) with the path of steepest descent. Cauchy's theorem states that

$$\oint f_{II}\, dk = 2\pi i \sum \text{res}\, f_{II}, \tag{36}$$

and thereby relates $\int_{\Gamma_1} f_{II}\, dk$ to the integral over the path of steepest descent $\int_{S.D.} f_{II}\, dk$ (the directions of integration are shown in figure 5). The integrals over the connecting arcs tend to zero as R tends to infinity, with the result that

$$\int_{\Gamma_1} f_{II}\, dk = \int_{S.D.} f_{II}\, dk + \int_{\Gamma_3} f_{II}\, dk + 2\pi i \sum \text{res} f_{II}, \tag{37}$$

where the residues are evaluated only at those singularities contained within the closed contour. The pole of f_{II} ($k_r = k_0 = \alpha g/U^2$) is within the contour only when $s_0 > k_r$, i.e. for $\beta < \frac{1}{2}U$ or $x < \frac{1}{2}Ut$. For x large, the integral

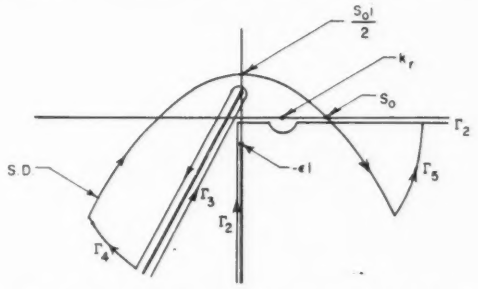

Figure 5. Conversion from the fundamental contour to the path of the steepest descent.

about the branch line is negligible compared with the integral along the path of steepest descent in the neighbourhood of the saddle point, and with the residue. (This is the advantage of the 'deformed branch line–steepest descent' method over other more direct estimations.) Hence we obtain

$$II \sim \int_{S.D.} f_{II}\, dk \tag{38}$$

$$-\frac{2\pi i}{U^2} \exp[-ik_0 x + i(\alpha g k_0)^{1/2} t - k_0(y+a)] H(\tfrac{1}{2}U - \beta),$$

where H is the Heaviside unit function. If the integral over the path of steepest descent were evaluated by conventional means as detailed by Morse & Feshbach (1953), the result would be

$$II \sim \left(\frac{\pi\alpha g}{x\beta^2}\right)^{1/2} \frac{1}{2\alpha g(1 - U/2\beta)} \exp[-\tfrac{1}{4}\alpha g(y+a)/\beta^2 + \tfrac{1}{4}i\alpha g x/\beta^2 - \tfrac{1}{4}i\pi] -$$

$$-\frac{2\pi i}{U^2} \exp[-ik_0 x + i(\alpha g k_0)^{1/2} t - k_0(y+a)] H(\tfrac{1}{2}U - \beta). \tag{39}$$

In the neighbourhood of $s_0 = k_r$ ($\beta = \frac{1}{2}U$ or $x = \frac{1}{2}Ut$), this approximation fails, since the pole of the integrand is too near the saddle point, i.e. the 'slowly' varying function is the dominant factor. We can avoid this difficulty by slightly modifying the conventional technique. Instead of evaluating the *entire* integrand at the saddle point, we evaluate only part of it, i.e. $\exp[-k_*(y+a)]$. We obtain

$$\int_{S.D.} \frac{k_* \exp[-ikx + i(\alpha g k_*)^{1/2}t - k_*(y+a)]\, dk}{2(\alpha g k_*)^{1/2}\{(\alpha g k_*)^{1/2} - kU\}}$$

$$\sim \exp[-s_0(y+a)] \int_{S.D.} \frac{k_* \exp[-ikx + i(\alpha g k_*)^{1/2}t]\, dk}{2(\alpha g k_*)^{1/2}\{(\alpha g k_*)^{1/2} - kU\}}$$

$$= \exp[-s_0(y+a)] \int_{S.D.} g_{II}\, dk, \quad \text{say.} \quad (40)$$

The last integral is equivalent to an integral over the contour Γ_2' (figure 6), provided we again add the appropriate residue term when $s_0 < k_0$ or $x < \frac{1}{2}Ut$; i.e.

$$\int_{S.D.} g_{II}\, dk = \int_{\Gamma_2'} g_{II}\, dk + \frac{2\pi i}{U^2} \exp[-ik_0 x + i(\alpha g k_0)^{1/2}t] H(\tfrac{1}{2}U - \beta). \quad (41)$$

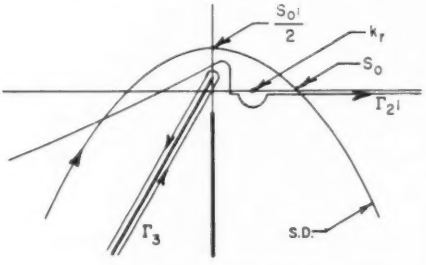

Figure 6. Equivalent inversion path.

The integral over Γ_2' may be evaluated by using formula 809 of Foster & Campbell (1954):

$$\int_{\Gamma_2'} g_{II}\, dk = \frac{1}{2\alpha g} \int_{-\infty}^{\infty} \frac{\exp[-ikx + i(\alpha h k)^{1/2}t]}{1 - U(k/\alpha g)^{1/2}}\, dk$$

$$= \frac{\pi i}{U^2} \exp[-ik_0(x - Ut)] \operatorname{erfc}[(\alpha g/U^2 ix)^{1/2}(\tfrac{1}{2}Ut - x)] +$$

$$+ (\alpha g/i\pi U^2 x)^{1/2} \exp[i(g\alpha t^2/k_0 x)] - \frac{2\pi i}{U^2} \exp[-ik_0(x - Ut)]. \quad (42)$$

Asymptotically, the final result becomes

$$II \sim \frac{2\pi i}{U^2} \exp[-s_0(y+a) - ik_0(x - Ut)]\{\tfrac{1}{2} \operatorname{erfc}[(\alpha g/U^2 ix)^{1/2}(\tfrac{1}{2}Ut - x)] - 1\} +$$

$$+ \frac{2\pi i}{U^2} H(\tfrac{1}{2}U - \beta) \exp[-ik_0(x - Ut)]\{\exp[-s_0(y+a)] - \exp[-k_0(y+a)]\} \quad (43)$$

where $s_0 = \alpha g/4\beta^2$, $k_0 = \alpha g/U^2$, $t = x/\beta$, and

$$\operatorname{erfc} u = 1 - \frac{2}{\sqrt{\pi}} \int_0^u \exp(-v^2)\, dv.$$

For $x \gg \frac{1}{2}Ut$, we have $II \sim 0$; for $0 < x \ll \frac{1}{2}Ut$,

$$II \sim -(2\pi i/U^2) \exp[-k_0(x-Ut) - k_0(y+a)].$$

Thus, for $x < \frac{1}{2}Ut$, II just cancels that contribution of I which arises from the pole at k_r. It may also be shown that $III = II^*$ (complex conjugate). The wave height is therefore

$$\eta = -\frac{\gamma}{2\pi}(I + 2\operatorname{Re} II); \tag{44}$$

and the wave height of the resurgent phenomenon is given asymptotically by

$$\left.\begin{aligned} &\eta_w \sim 0, && x > Ut; \\ &\eta_w \sim \frac{2\pi P_0 a k_0}{\rho g} \exp[-k_0(y+a)] \sin k_0(x-Ut), && \tfrac{1}{2}Ut < x < Ut; \\ &\eta_w \sim 0, && x < \tfrac{1}{2}Ut. \end{aligned}\right\} \tag{45}$$

The other contributions to the solution η do not contribute significantly to the resurgence.

Name	*CAROL*	*EDNA*	—	—
Date	30 Aug.–1 Sept. 1954	11–12 Sept. 1954	14–15 Sept. 1944	21–22 Sept. 1938
Velocity U (knots)	32–34	32	33	40
Wave Period T (hours)				
comp.: $\alpha = 5{\cdot}0 \times 10^{-3}$	5·8–6·1	5·8	6·0	7·3
$\alpha = 4{\cdot}2 \times 10^{-3}$	6·9–7·2	6·9	7·1	8·6
obs.: Atlantic City	5·5	6·0	5·6	—
Sandy Hook	7·0	7·0	7·2	8·0
Duration				
comp.	16–24	17–24	11–12	9
obs.: Atlantic City	20	23	23	—
Sandy Hook	26	—	30	16

Table 1. Periods and durations of sea level disturbance due to four hurricanes.

The resurgent wave motion induced by this simple pressure distribution, equation (25), is essentially restricted to the interval $\frac{1}{2}Ut < x < Ut$, and is characterized by a single wave number $k_0 = \alpha g/U^2$ (that of the fundamental edge wave mode) or the corresponding period $T = 2\pi U/(\alpha g)$. The duration D, which is the time taken for the resurgence to pass a given point, is equal to the total time t for which the disturbance has been in existence and in motion. The periods and durations of the resurgences of several hurricanes have been computed by Munk, Snodgrass & Carrier; the observation points were Atlantic City, where $\alpha = 5{\cdot}0 \times 10^{-3}$, and Sandy Hook, where $\alpha = 4{\cdot}2 \times 10^{-3}$. Their results are presented in table 1.

Although the model of equation (25) bears little resemblance to an actual disturbance, the results are in agreement because, evidently, hurricanes also excite only the fundamental edge wave mode (see § 4). The computed periods of the fundamental mode are in excellent agreement with the observed periods.

Mathematically, the existence of a resurgence is due to the fact that the integrand of the Fourier inversion integral has poles at k_r and k_l. The analytic form of the waves is obtained by evaluating the residues of the integrand at these poles. These results may be generalized to the case of an arbitrary pressure distribution which affects all the edge wave modes. The analysis of each integral arising from the inverse Laplace transform of the infinite series, equation (23), is substantially the same as that already performed in equation (26) et seq. The integrals involving the nth Laguerre polynomial give rise to the nth edge-wave mode. The analytic form of the resurgence is again obtained from an evaluation of the residues of the Fourier inversion integral. The final result is that, for disturbances originating at $t = 0$ and travelling parallel to the coast with constant velocity U, the resurgence, which is a sum of all the edge-wave modes, is asymptotically given by

$$\left.\begin{aligned} &\eta_w \sim 0, && x > Ut; \\ &\eta_w \sim \sum_0^\infty \bar{A}_n(k_n) \exp(-k_n y) L_n(2k_n y) \sin k_n(x - Ut), && \tfrac{1}{2}Ut < x < Ut; \\ &\eta_w \sim 0, && x < \tfrac{1}{2}Ut, \end{aligned}\right\} \quad (46)$$

where $\exp(-k_n y) L_n(2k_n y) \sin k_n(x - Ut)$ is the nth mode, its amplitude being $\bar{A}_n(k_n)$, $k_n = (2n+1)\alpha g/U^2 = (2n+1)k_0$. The resurgence is confined to the interval $\frac{1}{2}Ut < x < Ut$; the front moves with the speed of the storm U, and the rear moves with group velocity $\frac{1}{2}U$. The duration is the same as that previously calculated.

We may now apply these results to a more exact mathematical model, no new techniques being needed.

4. The Gaussian pressure distribution

To investigate how the various modes are stimulated by a real disturbance, we need a more realistic model. We consider, therefore, the effects of a travelling pressure taken to have a Gaussian distribution given by

$$P(x, y, t) = P_0 \exp\left[- \frac{(x - Ut)^2 + (y - y_0)^2}{a^2} \right], \quad (47)$$

where P_0 is the maximum pressure deviation, and $a = 1{\cdot}19 r_0$, r_0 being the half-pressure radius. It is advantageous to use the potential-function formulation of equation (4). The wave height is then given by equation (5). On transforming to a moving coordinate system ($x' = x - Ut$, $y' = y$, $t' = t$) and then dropping the primes, equation (4) becomes

$$y\left(\frac{\partial^2 \phi}{\partial x^2} + \frac{\partial^2 \phi}{\partial y^2}\right) + \frac{\partial \phi}{\partial y} - \frac{1}{\alpha g} \frac{\partial^2 \phi}{\partial t^2} + \frac{2U}{\alpha g} \frac{\partial^2 \phi}{\partial x^2} = - \frac{U}{\rho g a} \frac{\partial P}{\partial x}. \quad (48)$$

In this coordinate system, the pressure is independent of t. By taking Fourier and Laplace transforms, we obtain

$$y\frac{d^2\Phi}{dy^2}+\frac{d\Phi}{dy}-\left\{yk^2+\frac{(s+iUk)^2}{\alpha g}\right\}\Phi = \frac{Uik}{\alpha\rho g s}P_0\exp[-(y-y_0)^2/a^2]\,a\sqrt{\pi}\exp(-a^2k^2/4), \quad (49)$$

where

$$\Phi=\int_{-\infty}^{\infty}e^{ikx}\,dx\int_0^{\infty}e^{-st}\,\phi\,dt=\int_{-\infty}^{\infty}e^{-st}\,\bar{\phi}(k,y,t)\,dt.$$

The solution of this equation (we actually solve a modified equation with yk_*^2 in place of yk^2) is, from equation (13),

$$\Phi=-\frac{2\sqrt{\pi}iUP_0ak_*}{\rho}\exp(-k_*y)\sum_0^{\infty}\frac{A_n'(k)L_n(2k_*y)}{(n!)^2s\{(s+iUk)^2+(2n+1)k_*\alpha g\}} \quad (50)$$

where

$$A_n'(k)=k\exp(-a^2k^2/4)\int_0^{\infty}L_n(2k_*y)\exp(-k_*y)\exp\{-(y-y_0)^2/a^2\}\,dy. \quad (51)$$

The coefficient $A_n'(k)$ has no poles in the finite k-plane; its branch line and branch points coincide with those of k_*. Taking an inverse Laplace transform, we find that

$$\bar{\phi}(k,y,t)=-\frac{2\sqrt{\pi}iUP_0ak_*\exp(-k_*y)}{\rho}\sum_0^{\infty}\frac{A_n'(k)L_n(2ky)}{(n!)^2}\times \times\left\{\frac{1}{U^2k^2-(2n+1)\alpha g}+\ldots\right\}. \quad (52)$$

We have written only the first term of three in the brackets, because, as we have mentioned, it may be shown that this term gives the wave motion for $x<Ut$; the other terms add to yield a cancelling wave in the region $x<\frac{1}{2}Ut$. To determine the induced modal amplitudes, we need compute only the wave function arising from the first term, since all additional terms yield the *same* wave.

To compute the amplitudes of the waves constituting the resurgence, we perform the inverse Fourier transform and evaluate the residues arising from the poles, which are at

$$k=\pm k_n=\pm(2n+1)k_0=\pm(2n+1)\alpha g/U^2. \quad (53)$$

In the original coordinates, the result is

$$\left.\begin{aligned}\phi(x,y,t)&=\sum_0^{\infty}\phi_n(x,y,t)+\int F\,dk, && \tfrac{1}{2}Ut<x<Ut;\\ \phi(x,y,t)&=\int F\,dk, && \text{elsewhere,}\end{aligned}\right\} \quad (54)$$

where ϕ_n is the wave motion of the nth mode, determined, as we have said, by evaluating the residues of the integrand at the poles $k=\pm k_n$; thus

$$\phi_n(x,y,t)=-\frac{2}{U^2}\left(-\frac{2\sqrt{\pi}UP_0a}{\rho}\right)A_n'(k_n)\cos k_n(x-Ut)L_n(2k_ny)\exp(-k_ny). \quad (55)$$

The integral in (54) represents all the other terms, which do not contribute to the resurgence. Since the wave height is related to the potential function by equation (5), the amplitude of the nth edge-wave mode, as defined in equation (45), is

$$\bar{A}_n(k_n) = -\frac{2}{U}\left(-\frac{2\sqrt{\pi}UP_0 a}{\rho}\right)A_n'(k_n)k_n. \tag{56}$$

The amplitude ratio of the nth mode to the mth is

$$\frac{\bar{A}_n}{\bar{A}_m} = \frac{(m!)^2 k_n^2 \exp(-a^2k_n^2/4)}{(n!)^2 k_m^2 \exp(-a^2k_m^2/4)} \times \times \frac{\int_0^\infty L_n(2k_n y')\exp(-k_n y')\exp[-(y'-y_0)^2/a^2]\,dy'}{\int_0^\infty L_m(2k_m y')\exp(-k_m y')\exp[-(y'-y_0)^2/a^2]\,dy'}. \tag{57}$$

The amplitude ratios $\bar{A}_1/A_0$ and $\bar{A}_2/\bar{A}_0$ are plotted in figures (7) and (8) as functions of $k_0 a$ for $y_0 = 0$ (storm centred on the coast line).

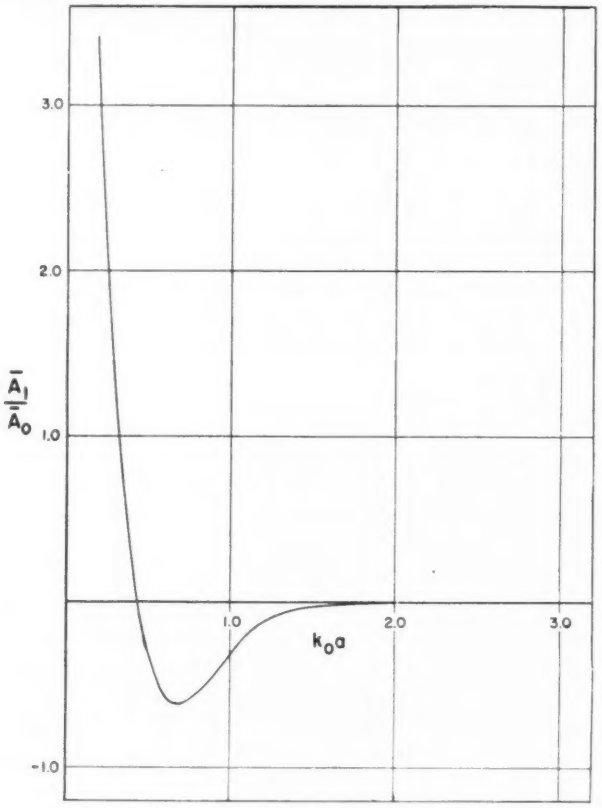

Figure 7. Amplitude ratio of the first harmonic to the fundamental *vs* $k_0 a$.

We shall interpret these results in terms of the half-pressure radius r_0 and the speed of propagation U. For $y = 0$, $P = P_0 \exp(-r^2/a^2)$, or $r = 0{\cdot}837a$. For hurricanes travelling parallel to the east coast of the United States* at 32–34 knots, which is typical, k_0^{-1} lies in the range $30 < k_0^{-1} < 40$ miles. The half-pressure radius of these disturbances is

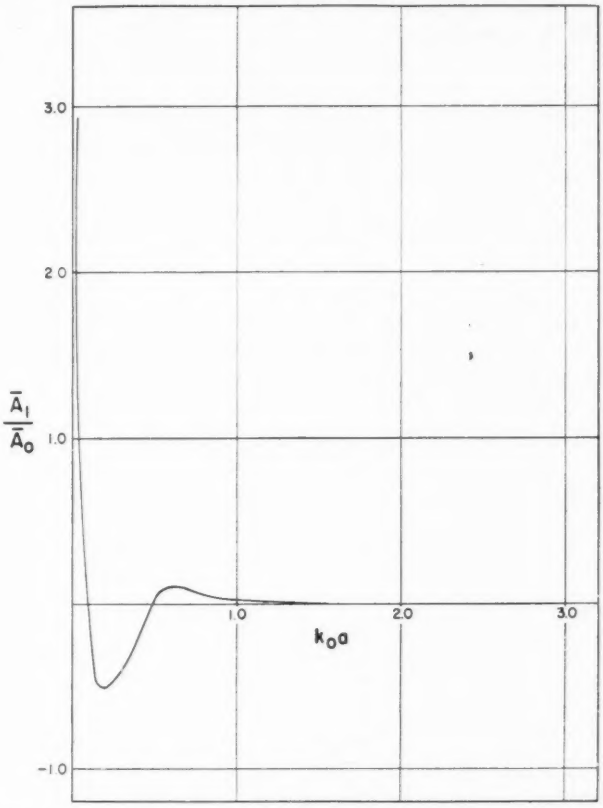

Figure 8. Amplitude ratio of the second harmonic to the fundamental *vs* $k_0 a$.

of the order of 100 miles, which means that $a \doteqdot 120$ miles, or that $3 < k_0 a < 4$. From figures 7 and 8 it is immediately apparent that for these values of $k_0 a$ only the fundamental edge wave,

$$L_0(2k_0\, y) \exp(-k_0\, y) \sin k_0(x - Ut),$$

is excited. All other modes are negligibly small. These results also show that for a disturbance of hurricane proportions to be an effective generator

* Henceforth we shall refer exclusively to hurricanes in this location. In analysing the effects of disturbances off other coasts, the appropriate values of α, U, a, etc. must be used.

of the first harmonic, it must travel at 70 knots at least. To excite the second harmonic, it must have speeds of 120 knots or more. We may draw the conclusion that hurricanes will never effectively stimulate any other mode except the fundamental edge wave. For smaller disturbances the higher modes may be generated. A storm with a half-pressure radius of approximately 25 miles and a speed of 34 knots has a value of $k_0 a$ between 0·75 and 1; k_0 is thus located exactly in the region where higher harmonics are stimulated. To induce still higher harmonics, disturbances must travel faster or be smaller in size or both.

Let us investigate the fundamental mode, and determine the conditions (size, distance from shore, etc.) for optimum edge-wave generation. The wave form of the fundamental mode is given by

$$\eta_0 = \left[\frac{2\pi P_0}{\rho g}(k_0 a)^2 \exp(-k_0 a)\operatorname{erfc}\left(-\frac{y_0}{a}+\frac{k_0 a}{2}\right)\right]\exp(-k_0 y)\sin k_0(x-Ut). \tag{58}$$

The bracketed expression is the wave amplitude. To find the storm position y_0 that produces optimum amplitudes (with constant $k_0 a$), we must determine the value of y_0, say $y_0^{\max}$, which maximizes

$$f(y_0) = \exp(-k_0 y_0)\operatorname{erfc}\left(-\frac{y_0}{a}+\frac{k_0 a}{2}\right),$$

that is, for which $f'(y_0) = 0$. Hence, we need to solve

$$\operatorname{erfc} u = \frac{2}{\sqrt{\pi}}\frac{\exp(-u^2)}{k_0 a}, \quad \text{where } u = -y_0/a + \tfrac{1}{2}k_0 a.$$

For $k_0 a = 2, 2{\cdot}5, 3{\cdot}0, 3{\cdot}5$, we find $u \doteqdot 0{\cdot}6, 0{\cdot}9, 1{\cdot}2, 1{\cdot}5$. In general these results yield maximum wave heights for y_0 in the range 25 to 35 miles. Table 2 summarizes these results, giving the maximum wave height in terms of the coefficient $2\pi P_0/(\rho g)$. For a maximum pressure difference of one pound per square inch, the resulting wave heights, in the hurricane region $k_0 a = 3{\cdot}5$, are approximately 2·5 ft. It is seen that the wave height measured at the coast varies slightly with the distance of the storm centre from shore, being 2·3 ft. for $y_0 = 0$, and rising to a maximum of 2·5 ft.

Knowing that maximum wave heights are induced by hurricanes 24 to 35 miles from shore, we can now determine what size disturbance in this region will produce the largest effects. We maximize the wave amplitude with respect to the variable a, holding k_0 and y_0 fixed. This leads to the equation

$$\sqrt{\pi}\operatorname{erfc}(-y_0/a+\tfrac{1}{2}k_0 a) = (y_0/a+\tfrac{1}{2}k_0 a)\exp[-(y_0/a-\tfrac{1}{2}k_0 a)^2].$$

For $k_0 = 0{\cdot}025$ and $y_0 = 30$, $a \doteqdot 68$ miles, and the half-pressure radius is $r_0 \doteqdot 54$ miles. Our conclusion is that hurricanes are too big to produce

maximum wave heights; 'smaller' storms ($r_0 \doteqdot 50$ miles) 25 to 35 miles from shore produce the largest waves (for a given pressure deviation P_0).

$k_0 a$	Maximum amplitude	k_0 and a	Storm centre (y_0^{max})
2·0	$0{\cdot}712\ \frac{2\pi P_0}{\rho g}$	1/30 & 60 1/40 & 80	22·8 30·4
2·5	0·529 (,,)	1/30 & 75 1/40 & 100	25·0 34·0
3·0	0·328 (,,)	1/30 & 90 1/40 & 120	27·0 36·0
3·5	0·170 (,,)	1/30 & 105 1/40 & 142	26·2 37·0

In particular, if $P_0 = 1$ lb/in.^{2}, and $\rho g = 62{\cdot}5$ lb/ft.^{3}, then $2\pi P_0/(\rho g) = 14{\cdot}5$, and the following wave heights are computed for various distances y_0.

$k_0 a$	$y_0 = 0$	$y_0 = y_0^{max}$	$y_0 = 100$
2·0	—	10·4	—
2·5	—	7·65	—
3·0	4·44	4·75	2·7–3·7
3·5	2·3	2·46	1·65–2·02

Table 2. Maximum wave heights in fundamental mode : a and y_0 are in miles, and wave heights in feet.

5. Conclusion

We can now predict the effects of any particular distribution on the resurgence from a knowledge of the maximum pressure difference, half-pressure radius, and speed. One should hence be able to calculate the positions of highest tide along the east coast following hurricanes. While the amplitude of the resurgence is not in itself remarkable, the extremely long periods enable these waves to be effectively superimposed upon an incoming tide; this is a dangerous situation, especially in those areas where there are resonant phenomena. A two foot or three foot crest coming several hours after the passage of a storm (and therefore somewhat unexpectedly), and superimposed upon the incoming tide, may greatly enlarge existing resonant wave motions (in bays, estuaries, etc.). While these situations cannot be avoided, it may be possible to reduce their effects by predicting their occurrence.

It should be noted that in order to simplify the mathematical analysis the effect of the earth's rotation has been neglected. This approximation is quite proper for the study of wave motion whose period is a few hours or less. However in the application of the theory to hurricane resurgences it is estimated that errors of 15 % are probable. That we were able to obtain such excellent and consistent agreement between observation and theory with so glaring an omission is, to say the least, peculiar. At present those additional effects which presumably nullify the rather large contribution from rotation are unknown.

The author wishes to thank Professor George Carrier for suggesting this problem and for his assistance in preparing this article. The paper is part of a thesis submitted in partial fulfillment of the requirements for the degree of Doctor of Philosophy in Applied Mathematics at Harvard University. The work was sponsored by the Scripps Institution of Oceanography under contract from the Office of Naval Research.

References

Courant, R. & Hilbert, D. 1953 *Methods of Mathematical Physics.* New York: Interscience.

Erdelyi, A. 1954 *Higher Transcendental Functions*, Vol. I. New York: McGraw-Hill.

Foster, P. & Campbell, G. 1954 *Fourier Integrals for Practical Applications.* New York: McGraw-Hill.

Lamb, H. 1945 *Hydrodynamics.* New York: Dover.

Morse, P. & Feshbach, H. 1953 *Methods of Theoretical Physics.* New York: McGraw-Hill.

Munk, W., Snodgrass, F. & Carrier, G. 1956 *Science* **123,** 127.

Irrotational motion associated with free turbulent flows

By R. W. STEWART

Department of Physics and Institute of Oceanography, University of British Columbia

(*Received* 11 *June* 1956)

SUMMARY

The irrotational motions induced by, but outside of, the self-preserving turbulent wake and jet are examined. It is found that there is a mean flow towards the centre of the jet, although there is no such flow in the case of the wake. Phillips's (1955) results on the nature of fluctuating irrotational flows are found to be largely unaffected by the introduction of simple inhomogeneities into the boundary conditions, but another mode of fluctuation with movement along the lines of mean flow is also shown to be likely. It is pointed out that, contrary to a statement of Corrsin & Kistler (1954), it is possible for the vorticity-free fluid between bulges of turbulent fluid to partake of the mean velocity of the turbulent fluid.

1. INTRODUCTION

Experimental researches in recent years have established beyond doubt that in all those flows, such as wakes, jets and boundary layers, where turbulence is expanding into non-turbulent regions of fluid, there exists a relatively sharp, although violently contorted, boundary separating the fully turbulent region and an external region. This external region, although not stationary, is characterized by very much smaller velocity gradients than is the turbulent region. Corrsin & Kistler (1954) and Townsend (1956) have pointed out that since vorticity can be introduced into non-vortical fluid only by viscosity, which is a very short range force, the motion in this external region is probably irrotational, and therefore can be derived from a scalar potential.

Phillips (1955) has considered a simple case of such irrotational motion, taking boundary conditions such that the velocity component u_2 is a stationary random function of the cartesian coordinates x_1, and x_3 on the plane $x_2 = 0$* and that the velocity $\mathbf{u}$ vanishes as $x_2 \to \infty$. It is the purpose of this paper to extend Phillips's results to some situations in which the statistical properties of u_2 are not independent of both x_1 and x_3, and to offer some comments and speculations on the phenomena.

* We have changed the order of the indices from that used by Phillips in order to conform to customary usage in wakes and jets. x_1 is the principal direction of flow and x_3 is parallel to any direction of symmetry.

We begin with a review of Phillips's analysis. Given that

$$(u_2)_{x_3=0} = \int e^{i\mathbf{k}\cdot\mathbf{x}}\, dA(\mathbf{k}),$$

where $\mathbf{k}$ is a (two-dimensional) vector wave-number with components $(k_1, 0, k_3)$ and magnitude k, $\mathbf{x}$ is the position vector with components (x_1, x_2, x_3) and the integration is over all $\mathbf{k}$-space (two-dimensional); and defining

$$\theta(\mathbf{k}) = \lim_{d\mathbf{k}\to 0} \frac{\overline{dA(\mathbf{k})\, dA^*(\mathbf{k})}}{dk_1\, dk_3},$$

where the bar indicates an average over the plane $x_2 = 0$ and the asterisk denotes the complex conjugate; he finds that, for all $x_2 > 0$,

$$\left.\begin{aligned} \overline{u_2^2} &= \int \theta(\mathbf{k}) e^{-2kx_2}\, d\mathbf{k}, \\ \overline{u_i^2} &= \int \frac{k_i^2}{k^2}\theta(\mathbf{k}) e^{-2kx_2}\, d\mathbf{k} \qquad (i = 1, 3). \end{aligned}\right\} \tag{1.1}$$

It is shown that, since $\theta(\mathbf{k})$ is an even function,

$$\overline{u_1 u_2} = \int \frac{k_1}{k}\theta(\mathbf{k}) e^{-2kx_2}\, d\mathbf{k} = 0 = \overline{u_2 u_3}. \tag{1.2}$$

He also states that $\overline{u_1 u_3} = 0$, and indicates that a similar proof would establish this relation. This is not the most general case, however, for in fact

$$\overline{u_1 u_3} = \int \frac{k_1 k_3}{k^2}\theta(\mathbf{k}) e^{-2kx_2}\, d\mathbf{k}, \tag{1.3}$$

which is not generally zero. Since $\overline{u_i u_j}$ is a symmetric tensor there will always, of course, be a possible choice of the x_1 and x_3-coordinate directions for which $\overline{u_1 u_3} = 0$. In the ordinary cases of the two-dimensional wake, jet or boundary layer, this choice corresponds to the 'natural' one of x_1 as the downstream direction. For the wake of a yawed cylinder or the boundary layer over a plate whose leading edge is not perpendicular to the flow, however, $\overline{u_1 u_3} \neq 0$ if the x_1-direction is chosen to be the principal direction of flow. There is no need to exclude such examples, and we may continue the analysis in the manner of Phillips.

Assuming that $\theta(\mathbf{k})$ may be expanded near $\mathbf{k} = 0$ in the form

$$\theta(\mathbf{k}) = \theta + k_i\theta_i + k_i k_j \theta_{ij} + k_i k_j k_i \theta_{ijl} + \ldots,$$

where θ, θ_i, θ_{ij}, etc. are cartesian tensors of the indicated order and are independent of the k_i, Phillips shows that $\theta = \theta_i = 0$. At large values of x_2 the values of $\theta(\mathbf{k})$ contributing significantly to the integrals in equations (1.1) to (1.3) are given approximately by

$$\theta(\mathbf{k}) \sim k_i k_j \theta_{ij}. \tag{1.4}$$

Putting (1.4) in (1.3) we get

$$\begin{aligned} \overline{u_1 u_3} &\sim \int \frac{k_1 k_3}{k^2} k_i k_j \theta_{ij} e^{-2kx_2}\, d\mathbf{k} \\ &= \int \frac{k_1^2 k_3^2}{k^2}(\theta_{13} + \theta_{31}) e^{-2kx_2}\, d\mathbf{k} \end{aligned} \tag{1.5}$$

since terms in θ_{11} and θ_{33} evidently vanish for reasons of symmetry. There is no loss of generality if we take θ_{ij} to be symmetric, so

$$\overline{u_1 u_3} \sim 2 \int \frac{k_1^2 k_3^2}{k^2} \theta_{13} e^{-2kx_2} d\mathbf{k}$$

$$= \tfrac{3}{16}\pi\theta_{13} x_2^{-4}. \tag{1.6}$$

We also write down for reference relations derived by Phillips:

$$\left.\begin{aligned} \overline{u_2^2} &\sim \tfrac{3}{8}\pi(\theta_{11}+\theta_{33})x_2^{-4}, \\ \overline{u_1^2} &\sim \tfrac{3}{32}\pi(3\theta_{11}+\theta_{33})x_2^{-4}, \\ \overline{u_3^2} &\sim \tfrac{3}{32}\pi(\theta_{11}+3\theta_{33})x_2^{-4}. \end{aligned}\right\} \tag{1.7}$$

Thus we see that in general there *is* a Reynolds shear stress due to the irrotational motion, with its direction parallel to the plane $x_2 = 0$.

It is evident from (1.1) that

$$\overline{u_2^2} = \overline{u_1^2} + \overline{u_3^2}, \tag{1.8}$$

so that the velocity fluctuations are not isotropic. This is of some consequence, for in the following sections we shall consider situations where u_2 is not statistically stationary on the plane $x_2 = 0$, and it can be shown that this lack of istropy then gives rise to stress gradients. Thus, in the absence of viscosity the total cartesian stress tensor in an incompressible fluid is

$$\tau_{ij} = P\delta_{ij} + \overline{u_i u_j} \tag{1.9}$$

where P is the pressure, δ_{ij} is the Kronecker delta, and $\overline{u_i u_j}$ is the Reynolds stress. If the fluctuating velocities are distributed isotropically, this becomes

$$\tau_{ij} = (P + \overline{u^2})\delta_{ij}, \tag{1.10}$$

and it is possible for gradients in $\overline{u^2}$ to be compensated by gradients in P, so that no net stress gradients (or accelerations) need result. In the absence of istropy this compensation becomes impossible and variations in turbulent intensity are necessarily accompanied by stress gradients.

In addition, Corrsin & Kistler (1954) have shown that in the special case of irrotational flow the relation

$$\frac{\partial u_i}{\partial x_j} = \frac{\partial u_j}{\partial x_i} \tag{1.11}$$

imposes conditions on the Reynolds stresses which have some interesting implications. For example, expression (1.8) can be derived very simply from the boundary conditions and the relation (1.11). Thus the Reynolds stress gradients must satisfy the relations

$$\frac{\partial}{\partial x_j}\overline{u_2 u_j} = \overline{u_j \frac{\partial u_2}{\partial x_j}} = \overline{u_j \frac{\partial u_j}{\partial x_2}} = \frac{1}{2}\frac{\partial}{\partial x_2}\overline{u_j u_j}.$$

But the fluctuations are stationary in the x_1- and x_3-directions. Hence

$$\frac{\partial \overline{u_1 u_2}}{\partial x_1} = \frac{\partial \overline{u_2 u_3}}{\partial x_3} = 0,$$

and so
$$\frac{\partial \overline{u_2^2}}{\partial x_2} = \frac{1}{2}\frac{\partial}{\partial x_2}\overline{u_j u_j}.$$

Then, since $\mathbf{u}$ vanishes as $x_2 \to \infty$,
$$\overline{u_2^2} = \tfrac{1}{2}\overline{u_j u_j} = \overline{u_1^2} + \overline{u_3^2}.$$

2. Cylinder wake

The predictions of Phillips's theory have been remarkably confirmed by comparison with measurements, made by A. A. Townsend in the wake of a circular cylinder. It is probably worth examining the potential flow associated with such a wake in more detail.

We shall consider only a self-preserving flow which Townsend (1956) has shown to be possible only if the turbulent velocities are small compared with the mean flow velocity U_∞. In this case the characteristic scale L varies as $x_1^{1/2}$ when the x_1-direction is the principal direction of flow and the origin of x_1 is some virtual origin not too far from the actual location of the cylinder. It is also shown that, for the transport of momentum to be independent of x_1, $U_0 \propto x_1^{-1/2}$, where U_0 is some characteristic velocity which may be taken as $U_0 = U_\infty - (U_1)_{\min}$ for any given x_1. Root-mean-square turbulent velocities vary as U_0.

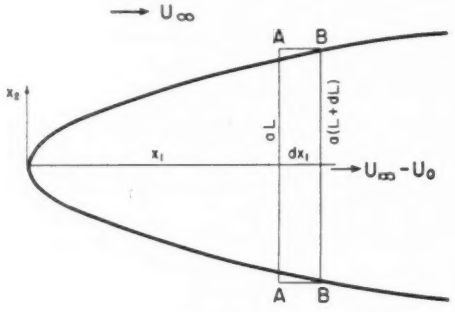

Figure 1. The self-preserving wake.
The scale in the x_2-direction is greatly expanded.

In figure 1 the total mean transport of fluid across the section AA per unit length in the x_3-direction is
$$aL(U_\infty - KU_0) + a\,dL\,U_\infty,$$
where KU_0 is the average value of $U_\infty - U_1$ across the wake, the total extent of which is aL, and K and a are constant. The total mean transport of fluid across the section BB is
$$a(L+dL)\{U_\infty - K(U_0 + dU_0)\}.$$

Neglecting second order differentials, the transport across AB in the x_2-direction is therefore

$$\tfrac{1}{2}aK(L\,dU_0 + U_0\,dL) = \tfrac{1}{2}aK\,d(U_0\,L).$$

Hence

$$U_2 \propto \frac{d}{dx_1}(U_0\,L) = 0. \tag{2.1}$$

Thus we find that there is no mean flow from the x_2-direction into a self-preserving two dimensional wake. We shall see later that this is not true of a jet.

3. Fluctuating motions outside a turbulent wake

Returning to the case considered by Phillips, let us assume that it is possible to define $\theta(\mathbf{k}, x_1)$ for every value of x_1 on some plane* $x_2 = 0$ outside, but close to, the main body of the wake. We assume that, although $\theta(\mathbf{k}, x_1)$ is inhomogeneous in x_1, Phillips' main conclusions are not materially altered.

Our similarity conditions require that

$$\theta(\mathbf{k}, x_1) = \chi(\mathbf{k}x_1^{1/2}) = \chi(\boldsymbol{\epsilon}), \tag{3.1}$$

where χ is a function of $\boldsymbol{\epsilon} = \mathbf{k}x_1^{1/2}$ only, in order that the characteristic scales should vary as $x_1^{1/2}$, and that the energy per unit mass in the fluctuations,

$$\int \theta(\mathbf{k}, x_1)\,d\mathbf{k} = x_1^{-1}\int \chi(\boldsymbol{\epsilon})\,d\boldsymbol{\epsilon},$$

should vary as x_1^{-1}. The expansion

$$\theta(\mathbf{k}, x_1) = k_i k_j \theta_{ij}(x_1) + k_i k_j k_l k_m \theta_{ijlm}(x_1) + \ldots$$

may then be written

$$\theta(\mathbf{k}, x_1) = x_1\, k_i k_j \chi_{ij} + x_1^2 k_i k_j k_l k_m \chi_{ijlm} + \ldots, \tag{3.2}$$

where χ_{ij}, etc. are absolute constants for the particular flow.

At sufficiently large values of x_2, we find from (1.7), (1.8) and (3.2) that

$$\left.\begin{aligned} \overline{u_2^2} &\sim \tfrac{3}{8}\pi(\chi_{11}+\chi_{33})x_1 x_2^{-4}, \\ \overline{u_1^2} &\sim \tfrac{3}{32}\pi(3\chi_{11}+\chi_{33})x_1 x_2^{-4}, \\ \overline{u_3^2} &\sim \tfrac{3}{32}\pi(\chi_{11}+3\chi_{33})x_1 x_2^{-4}. \end{aligned}\right\} \tag{3.3}$$

By symmetry

$$\overline{u_1 u_3} = \overline{u_2 u_3} = 0.$$

It is interesting to note that these fluctuation intensities *increase* as x_1 increases. The reason for this, of course, is that the increase in the scale of the primary causative turbulence more than compensates for the decrease in intensity. If we consider the variation on similarity surfaces $x_2 \propto x_1^{1/2}$, instead of on planes $x_2 =$ constant, we find that the fluctuation intensities are all proportional to x_1^{-1}, as they should be.

The equations for incompressible mean flow in the steady state are

$$U_k \frac{\partial U_i}{\partial x_k} + \frac{1}{\rho}\frac{\partial P}{\partial x_i} + \frac{\partial}{\partial x_k}\overline{u_i u_k} - \nu\frac{\partial^2 U_i}{\partial x_k \partial x_k} = 0. \tag{3.4}$$

* The actual surface should be parabolic, but this introduces considerable complication into the analysis and at large values of x_1 the difference should be slight.

If we have Reynolds number similarity (Townsend 1956) which we shall assume, the viscous term will be negligible. In the particular region of the flow in which we are interested we have seen that

$$U_2 \sim U_3 = \overline{u_1 u_3} = \overline{u_2 u_3} = 0,$$

and we shall see later (3.9) that $(\partial/\partial x_1)\overline{u_1 u_2} = 0$; so it would appear reasonable to write for the x_2-component

$$\frac{1}{\rho}\frac{\partial P}{\partial x_2} + \frac{\partial \overline{u_2^2}}{\partial x_2} = 0,$$

or

$$P + \rho \overline{u_2^2} = P_\infty, \tag{3.5}$$

P_∞ being the value of P at large values of x_2, where $\overline{u_2^2}$ is very small.

For the x_1-component, the ony terms of any consequence will be

$$U_2 \frac{\partial U_1}{\partial x_2} + U_1 \frac{\partial U_1}{\partial x_1} + \frac{1}{\rho}\frac{\partial P}{\partial x_1} + \frac{\partial}{\partial x_2}\overline{u_1 u_2} + \frac{\partial \overline{u_1^2}}{\partial x_1} = 0. \tag{3.6}$$

Corrsin & Kistler (1954) have shown that, for irrotational flow

$$\frac{\partial \overline{u_i u_j}}{\partial x_j} = \frac{1}{2}\frac{\partial q^2}{\partial x_i}, \tag{3.7}$$

where

$$q^2 = \overline{u_j u_j}.$$

If mean quantities are independent of x_3, (3.7) gives

$$\left.\begin{aligned} \frac{\partial \overline{u_1 u_2}}{\partial x_1} &= \frac{1}{2}\frac{\partial}{\partial x_2}(q^2 - 2\overline{u_2^2}), \\ \frac{\partial \overline{u_1 u_2}}{\partial x_2} &= \frac{1}{2}\frac{\partial}{\partial x_1}(q^2 - 2\overline{u_1^2}). \end{aligned}\right\} \tag{3.8}$$

In our case, where $\overline{u_2^2} = \overline{u_1^2} + \overline{u_3^2} = \frac{1}{2}q^2$, this yields

$$\frac{\partial \overline{u_1 u_2}}{\partial x_1} = 0, \tag{3.9}$$

$$\frac{\partial \overline{u_1 u_2}}{\partial x_2} = \frac{\partial}{\partial x_1}(\overline{u_2^2} - \overline{u_1^2}), \tag{3.10}$$

and introducing (3.5) into (3.10) we obtain

$$\frac{\partial \overline{u_1 u_2}}{\partial x_2} = -\frac{\partial}{\partial x_1}\left(\frac{P}{\rho} + \overline{u_1^2}\right). \tag{3.11}$$

Combining (3.6) and (3.11) we find that

$$U_2 \frac{\partial U_1}{\partial x_2} + U_1 \frac{\partial U_1}{\partial x_1} = 0. \tag{3.12}$$

We therefore see that the mean flow is unaffected by the irrotational fluctuations, not because the Reynolds stresses are zero, but because the gradient of the shear stress $(\partial/\partial x_2)\overline{u_1 u_2}$ is exactly balanced by the gradient of the total normal stress $(\partial/\partial x_1)(P/\rho + \overline{u_1^2})$. It would appear that such a balance is the rule rather than the exception in irrotational fluctuating flows.

The normal stress gradient tends to accelerate fluid in the direction of the mean flow. However, the shear stress transfers this acceleration to the retarded flow in the main body of the wake. The whole process must be considered as a part of the mechanism by which this retarded fluid is accelerated towards U_∞ as the wake decays.

4. Motion between bulges of turbulent fluid

There is a difference of opinion expressed in the literature as to the nature of the mean flow in that portion of the external, irrotational flow region which lies between out-thrusts or bulges of the turbulent fluid. Townsend (1949) states that "the non-turbulent fluid between successive jets is constrained by pressure gradients to move at the same mean velocity as the fluid in the adjacent jets", and shows measurements (Townsend 1956, p. 163) to support this view. Corrsin & Kistler (1954), arguing that the mean flow in these regions is irrotational and therefore gradient free, say "the mean velocity everywhere in the potential field must be constant and equal to that at infinity" and publish measurements qualitatively substantiating this statement.

An examination of Phillips's results may cast some light on this controversy. It is noteworthy that equations (1.1) exactly correspond to the classical theory of flow in gravity water waves (Lamb 1932, ch. 9) if we consider a situation where there is a continuous spectrum of wave frequencies and waves may be oriented in all possible directions. Now it is well known (Lamb 1932, p. 418) that, although such waves are purely irrotational flows, if they have finite amplitude they are accompanied by a mean transport of fluid, and a resulting mean shear. The reason for this apparent contradiction is that they are bounded by a non-planar surface, and any plane passing between the level of maximum elevation and the level of maximum depression includes regions in which the equations of irrotational flow do not apply. The simple case of a single wave train with a single frequency is sketched in figure 2(*a*), which clearly illustrates the phenomenon. Everywhere below the boundary the flow is irrotational. The velocity potential is

$$\phi = -B\cos kx_1 e^{-kx_2}, \tag{4.1}$$

where B is a constant, and the velocity components are

$$u_1 = Bk\sin kx_1 e^{-kx_2},$$

$$u_2 = Bk\cos kx_1 e^{-kx_2}.$$

For any $x_2 > 0$,

$$\overline{u_1} = \frac{Bk}{2\pi}\int_{-\pi/k}^{\pi/k} \sin kx_1 e^{-kx_2}\,dx_1 = 0, \tag{4.2}$$

but, if the boundary* is described by

$$x_2 = -h(1+\sin kx_1), \tag{4.3}$$

* The fact that the actual boundary of a theoretical water wave is trochoidal does not concern us here.

for $0 > x_2 > -2h$, we find that,

$$\overline{u_1} = \frac{Bke^{-kx_2}}{\cos^{-1}(-1-x_2/h)} \int_{\pi/2k}^{\{\sin^{-1}(-1-x_2/h)\}/k} \sin kx_1 \, dx_1$$

$$= \frac{Be^{-kx_2}}{\cos^{-1}(-1-x_2/h)} \sqrt{\left(\frac{2x_2}{h} - \frac{x_2^2}{h^2}\right)}. \tag{4.4}$$

This function is plotted in figure 2(*b*) for $B = k = h = 1$.

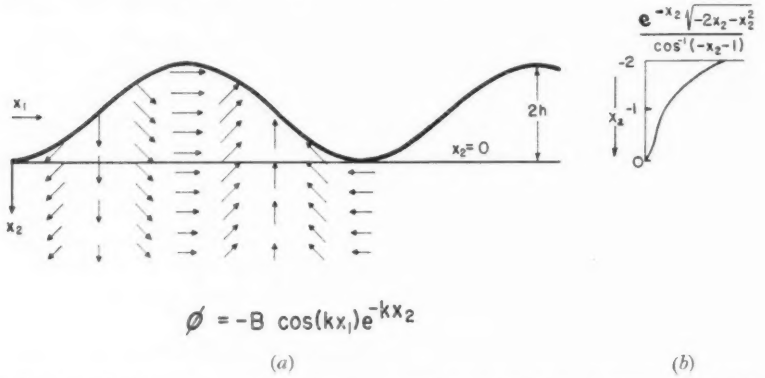

(*a*) (*b*)

Figure 2. (*a*) Flow in a simple gravity wave advancing from left to right. The length of the arrows is proportional to the logarithm of the velocity at their centres ; (*b*) the mean horizontal velocity within the wave.

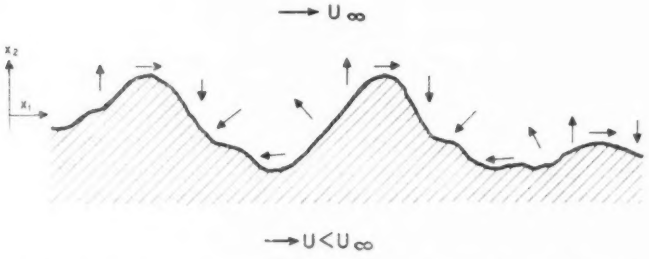

Figure 3. Probable directions of potential flow near the boundary of turbulent fluid in a wake.

The irrotational flow induced by free turbulence is another example of potential flow with an irregular boundary beyond which Laplace's equation does not hold. It is quite probable that a similar phenomenon occurs, for the pressure forces are likely to make the mean direction of the potential flow between bulges the same as that of the bulges themselves. The example of gravity waves shows that such a motion is *not* inconsistent with the equations of irrotational flow. If the flow is of this type, we can make some predictions concerning the direction of u_2 in the non-turbulent region (figure 3). In a wake this component should consistently be negative

just before the arrival of a bulge and positive just after its passage. Perhaps the similarity in appearance between the boundary of the turbulent fluid and the surface of a tumultuous sea is more than merely superficial.

5. Jets

In considering the two-dimensional wake we passed rather lightly over the fact that our similarity surfaces were not planes x_2 = constant but were parabolic. This was justified at sufficiently large values of x_1, since these surfaces there approach closely to such planes. For jets, however, such an assumption becomes very questionable. It is found (Corrsin & Kistler 1954) that in jets characteristic scales vary as x_1, and characteristic velocities vary as x_1^{-1} for circular jets and as $x_1^{-1/2}$ for two-dimensional jets. In these flows it is obviously not possible to choose suitably a unique direction for x_2 in cartesian coordinates in order to apply Phillips's theory. The appropriate coordinate system will be spherical for the circular jet and cylindrical for the two-dimensional jet.

For the circular jet we have boundary conditions defined on a cone, with vertex at a virtual origin close to the source of the jet and angle such that it just contains all the turbulent fluid (about 25° included angle according to experimental results). In spherical coordinates (r, α, β) this cone is defined by $\alpha = \alpha_0$, and following Phillips's general line of argument we define a potential $\phi(r, \alpha, \beta)$ such that $u_\alpha = (1/r)(\partial\phi/\partial\alpha)$ is a statistically prescribed function of r and β on $\alpha = \alpha_0$. $(u_\alpha)_{\alpha=\alpha_0}$ will be characterized by a typical scale which varies as r and a typical magnitude which varies as r^{-1}. Such a function can be accurately and conveniently described by

$$(u_\alpha)_{\alpha=\alpha_0} = \sum_{-\infty}^{\infty} \int_{-\infty}^{\infty} ik_r A(k_r, k_\beta) r^{ik_r} r^{-1} \exp(ik_\beta \beta)\, dk_r, \tag{5.1}$$

where k_r and k_β are dimensionless wave-numbers, the summation is over k_β which takes only integral values, and A is complex. The potential function everywhere outside the cone will then be

$$\phi = \sum \int A(k_r, k_\beta) r^{ik_r} \exp(ik_\beta S) \psi(\alpha, k_r, k_\beta)\, dk_r \tag{5.2}$$

where ψ will be expressible in terms of Associated Legendre Functions of integral order k_β, pure imaginary degree ik_r, and real argument $\cos\alpha$. The function ψ may be analytically different for the various combinations of positive and negative values of k_r and k_β and will depend to some extent on other boundary conditions such as those that are imposed, for example, if the jet issues from a hole in an infinite wall.

Unfortunately there appears to be no published study of such functions, and it hardly seems worth conducting a detailed study for the present application.

6. Mean flow outside a circular jet

A similar argument to that used to derive (2.1) shows that the mean flow component U_α is given by

$$U_\alpha = Cr^{-1}, \tag{6.1}$$

where C is a negative constant on the boundary of the turbulent region $\alpha = \alpha_0$.

A solution of Laplace's equation for the mean velocity potential Φ, with (6.1) as a boundary condition and symmetry in β, is

$$\Phi = A_1 \log(r \sin\alpha) + A_2 \log(\tan \tfrac{1}{2}\alpha), \tag{6.2}$$
$$A_1 \cos\alpha_0 + A_2 = C \sin\alpha_0.$$

Expression (6.2) leaves one arbitrary constant to be determined by other boundary conditions.

If the jet issues from a hole in an infinite wall at $\alpha = \frac{1}{2}\pi$, then $A_2 = 0$ and

$$\Phi = C \tan\alpha_0 \log(r \sin\alpha), \tag{6.3}$$

which corresponds to a very simple uniform radial flow directed everywhere towards the axis of the jet, with speed inversely proportional to the distance from this axis.

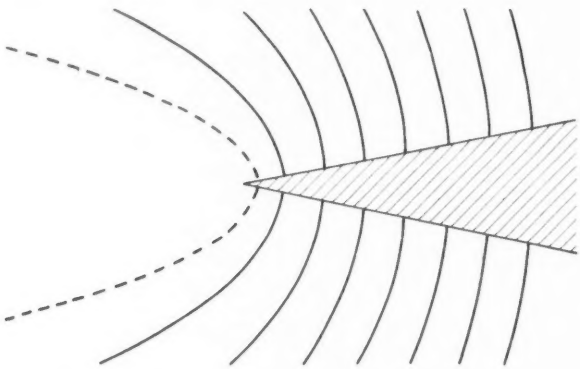

Figure 4. Flow lines into a self-preserving circular jet issuing from a nozzle.

If, as in Corrsin & Kistler's (1954) experiments, the jet issues from a nozzle, the boundary condition may be approximated by

$$\frac{\partial \Phi}{\partial \alpha} = 0 \quad \text{at} \quad \alpha = \pi$$

and we have

$$\Phi = \frac{C \sin\alpha_0}{\cos\alpha_0 + 1} \log(r \sin\alpha \tan \tfrac{1}{2}\alpha). \tag{6.4}$$

In this case the flow lines are given by

$$r(\cos\alpha + 1) = \text{constant} \tag{6.5}$$

and are sketched in figure 4. It will be noted that, even here, when close to the jet, the mean flow is directed essentially perpendicular to the axis of the jet.

7. Two-dimensional jet—mean flow

By a 'two-dimensional jet' we refer to the type of flow produced when fluid issues from a long uniform slot. The mean flow is two-dimensional, but fluctuating motions occur in all three dimensions. In this type of

flow the similarity conditions require that the scales vary as r and the characteristic velocities as $r^{-1/2}$. In cylindrical coordinates (r, α, z) this requires that

$$U_\alpha = Dr^{-1/2} \tag{7.1}$$

on the edge of the turbulent region, $\alpha = \alpha_0$. D is a negative constant if α_0 is positive.

The velocity potential satisfying (7.1) and also the condition $U_\alpha = 0$ at $\alpha = \frac{1}{2}\pi$ (corresponding to a slot in an infinite wall) is

$$\Phi = Dr^{1/2}\{\cos(\tfrac{1}{2}\alpha_0 + \tfrac{1}{4}\pi)\}^{-1} \sin(\tfrac{1}{2}\alpha + \tfrac{1}{4}\pi). \tag{7.2}$$

The corresponding flow lines, which are given by

$$r^{1/2}\cos(\tfrac{1}{2}\alpha + \tfrac{1}{4}\pi) = \text{constant}, \tag{7.3}$$

are sketched in figure 5.

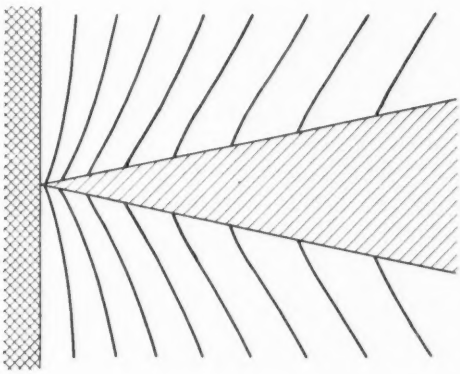

Figure 5. Flow lines into a self-preserving two-dimensional jet issuing from an infinite wall.

8. Fluctuating potential flow outside a two-dimensional jet

I have been unable to find, in three dimensions, a suitable function to describe the boundary condition for flow outside a two-dimensional jet. However, if we can imagine a flow in which the fluctuating motions are also two-dimensional the problem becomes rather simple, and the conclusions derived from a study of this hypothetical flow may, with some caution, be applied to the more complex real flows.

A velocity potential in polar coordinates (r, α), for which $\overline{u_i^2}$ varies as r^{-1} and typical scales vary as r, and which satisfies the boundary condition $u_\alpha = 0$, at $\alpha = \frac{1}{2}\pi$ (corresponding to a slot in an infinite wall), can be constructed thus:

$$\phi = r^{1/2} \int_0^\infty A\{e^{-k\alpha}\cos(B + k\log r + \tfrac{1}{2}\alpha) + e^{-k(\pi-\alpha)}\cos(B + k\log r + \tfrac{1}{2}\pi - \tfrac{1}{2}\alpha)\}\, dk, \tag{8.1}$$

where A and B are real functions of k.

Now in the region of greatest interest, $\pi - \alpha \doteqdot 3$, which is of the order of ten times as great as α. Therefore, for k greater than about one, the second term in this integral is negligible compared with the first. For small k, however, the two terms approach equality in magnitude.

For $k \ll 1$, then, the velocity components reduce to

$$\left.\begin{aligned} u_r &= \frac{\partial \phi}{\partial r} \doteqdot r^{-1/2} \sin(\tfrac{1}{2}\alpha + \tfrac{1}{4}\pi) \int_0^\infty A \cos(B + k \log r + \tfrac{1}{4}\pi)\, dk, \\ u_\alpha &= \frac{1}{r}\frac{\partial \phi}{\partial r} \doteqdot r^{-1/2} \cos(\tfrac{1}{2}\alpha + \tfrac{1}{4}\pi) \int_0^\infty A \cos(B + k \log r + \tfrac{1}{4}\pi)\, dk. \end{aligned}\right\} \tag{8.2}$$

u_r and u_α are therefore fully correlated, and the only motions at these very small wave-numbers are along streamlines given by

$$r^{1/2} \cos(\tfrac{1}{2}\alpha + \tfrac{1}{4}\pi) = \text{constant}. \tag{8.3}$$

It will be observed that (8.3) is identical with (7.3), the expression for the streamlines of the mean flow into a two-dimensional jet. We have therefore come to the interesting, if not particularly surprising, conclusion that the very small wave-number fluctuations follow the same streamlines as the mean flow, shown in figure 5. This result is expected to be valid much more generally than just in this two-dimensional case, for temporal variations in the rate of flow from the jet will be described in just this way. It should be noted that although these fluctuations are characterized by very small wave-numbers, their frequency (in time) may be quite high.

For $k > 1$, the second term in (8.1) becomes negligible, and we have

$$\left.\begin{aligned} u_r &\doteqdot r^{-1/2} \int_0^\infty A e^{-k\alpha} \{\tfrac{1}{2} \cos(B + k \log r + \tfrac{1}{2}\alpha) - \\ &\qquad - k \sin(B + \log r + \tfrac{1}{2}\alpha)\}\, dk, \\ u_\alpha &\doteqdot -r^{-1/2} \int_0^\infty A e^{-k\alpha} \{\tfrac{1}{2} \sin(B + k \log r + \tfrac{1}{2}\alpha) + \\ &\qquad + k \cos(B + k \log r + \tfrac{1}{2}\alpha)\}\, dk. \end{aligned}\right\} \tag{8.4}$$

$B(k)$ is a rapidly changing function of k satisfying the inequality

$$-\pi < B < \pi,$$

and if we average over different flow realizations we would expect that

$$\overline{\sin\{B(k_1) \pm B(k_2)\}} = \overline{\cos\{B(k_1) \pm B(k_2)\}} = 0,$$

unless $k_1 = k_2$. B will take all values equally probably in different flow realizations, so

$$\left.\begin{aligned} \overline{u_r^2} = \overline{u_\alpha^2} &= \tfrac{1}{2} r^{-1} \int_0^\infty A^2 (\tfrac{1}{4} + k^2) e^{-2k\alpha}\, dk, \\ \overline{u_r u_\alpha} &= 0. \end{aligned}\right\} \tag{8.5}$$

Thus $\overline{u_r^2} = \overline{u_\alpha^2}$, and u_r and u_α are uncorrelated, and (8.5) is obviously the two-dimensional analogue in polar coordinates of Phillips's results (1.1) and (1.2).

The scale of a motion characterized by $k = 1$ will be such that $\log r$ changes by about $\frac{1}{2}\pi$, that is r changes by a factor of the order of 5. Thus

$k = \frac{1}{4}1$ is a very small wave-number indeed, and virtually all the energy of the velocity fluctuations may be in the range of wave-numbers for which (8.5) is applicable.

Although a detailed analysis of the actual case of three-dimensional fluctuations in the two-dimensional jet has not been found possible, some of its probable characteristics can be shown.

It can readily be demonstrated that for irrotational flow in which mean quantities are invariant in the z-direction the cylindrical coordinate equivalents to equations (3.8) are

$$\left.\begin{aligned} \frac{\partial}{\partial r}(\tfrac{1}{2}q^2-\overline{u_r^2}) &= \frac{1}{r}\frac{\partial}{\partial \alpha}\overline{u_r u_\alpha}+\frac{\overline{u_r^2}-\overline{u_\alpha^2}}{r}, \\ \frac{\partial}{\partial \alpha}(\tfrac{1}{2}q^2-\overline{u_\alpha^2}) &= 2\overline{u_r u_\alpha}+r\frac{\partial}{\partial r}\overline{u_r u_\alpha}. \end{aligned}\right\} \tag{8.6}$$

Our similarity conditions permit us to write

$$q^2 = r^{-1}p^2, \qquad u_i^2 = r^{-1}v_i^2, \tag{8.7}$$

where p and $\overline{v_i v_j}$ are independent of r. Equations (8.6) then become

$$\left.\begin{aligned} \overline{v_\alpha^2}-\tfrac{1}{2}p^2 &= \frac{\partial \overline{v_r v_\alpha}}{\partial \alpha}, \\ \overline{v_r v_\alpha} &= \frac{\partial}{\partial \alpha}(\tfrac{1}{2}p^2-\overline{v_\alpha^2}). \end{aligned}\right\} \tag{8.8}$$

In view of (1.8) and (8.5), the most likely solution to these equations is

$$\overline{v_\alpha^2} = \tfrac{1}{2}p^2, \qquad \overline{v_r v_\alpha} = 0. \tag{8.9}$$

It would seem probable then that there is no Reynolds shear stress across surfaces α = constant in the two-dimensional jet. This is a result of the behaviour $q^2 \propto r^{-1}$ and would not be possible with any other dependence on r, unless $u_z \equiv 0$. It is in contrast to the situation in the wake, where we saw that a shear stress does occur.

9. Concluding note

This study, as far as it has gone, has shown that the results of Phillips's simple model of irrotational flow outside a turbulent region are not greatly affected by introducing simple inhomogeneities into the boundary conditions. It has been demonstrated that these irrotational fluctuations are capable in some circumstances of producing a Reynolds shear stress, but the basic conclusion that the velocity component directed away from the boundary of the turbulence contains about half the total energy in the fluctuations seems to be firmly established. Still unresolved then, is the contradiction pointed out by Townsend (1956, p. 191) between this kind of theory and the experimental results which indicate that in jets the downstream component is larger than this cross-stream component. Although it is not altogether satisfactory to rely on the extensibility of the results of the two-dimensional analysis of § 8 to real three-dimensional cases, flow similar to that described by (8.2) is intuitively likely and (8.5) is very similar to the three-dimensional

result (1.1). It seems reasonable to infer that in three-dimensional cases there will also be two basic modes to the irrotational fluctuations: very low wave-number motions along the mean flow lines, and higher wave-number motions similar in structure to those in gravity waves. Figures 4 and 5 and equations (1.1) and (8.9) show that both modes give greater contributions to the cross-stream than to the down-stream motions.

This paper describes work done for the Defence Research Board of Canada.

References

Corrsin, S. & Kistler, A. 1954 *Nat. Adv. Comm. Aero., Wash., Tech. Note* no. 3133.

Lamb, H. 1932 *Hydrodynamics*, 6th Ed. Cambridge University Press.

Phillips, O. M. 1955 *Proc. Camb. Phil. Soc.* **51**, 220.

Townsend, A. A. 1949 *Aust. J. Sci. Res.* **2**, 45.

Townsend, A. A. 1956 *The Structure of Turbulent Shear Flow*. Cambridge University Press.

The intensity of Aeolian tones

By O. M. PHILLIPS
Trinity College, Cambridge

(*Received* 22 *August* 1956)

SUMMARY

The generation of Aeolian tones is interpreted in terms of the theory of aerodynamic sound. To do this, the intensity of the radiated sound is expressed in terms of the fluctuations in force upon a moving rigid body using the approximation that, at low Mach numbers, these forces can be calculated assuming incompressibility of the flow. The fluctuations in lift and drag upon a circular cylinder at Reynolds numbers between 40 and 160 are calculated by integrating the fluctuations in momentum in the eddying wake, using the experimental data of Kovasznay (1949). It is found that the fluctuating lift per unit length is approximately

$$f_l = 0{\cdot}38\rho U^2 d \cos 2\pi n t,$$

where ρ is the density of the fluid and t the time, and that the magnitude of the fluctuations in drag is about 10% of this.

The axial length scale of these force fluctuations was found by an auxiliary experiment to be very large for Reynolds numbers below 100. When $100 < R < 160$, the length scale is approximately $17d$, the transition apparently occurring as a result of the instability to three-dimensional disturbances of the laminar eddying wake. Using this datum, the mean square acoustic pressure generated by the motion about the cylinder at these Reynolds numbers is found to be

$$\overline{p^2}(r) \sim 0{\cdot}27 \cos^2\theta \frac{\rho^2 l d U^6 S^2}{a^2 r^2},$$

where θ is the angle between the direction of observation and the incident stream, l the length of the cylinder and a the velocity of sound in the medium. Experiments undertaken to test this result directly, using sound intensity measurements from a whirling arm apparatus in an accoustically quiet room, gave very good agreement.

At higher Reynolds numbers, when the cylinder wake is turbulent, the theory leads to a similar expression for $\overline{p^2}$ but with a smaller numerical factor. Analysis of previous experimental data on this basis gives good agreement, with a value of about 0·037 for the numerical constant. In view of this, it is likely that some of the earlier data which had appeared to give a Mach number dependence of M^4, not M^6, have been misinterpreted.

Finally, mention is made of the conditions when the frequency of vortex generation is the same as the natural frequency of the wire, and the greatly increased intensity of the sound is seen to be the result of the greatly increased axial length scale of the force fluctuations.

The relative simplicity of this phenomenon makes possible perhaps the least ambiguous confirmation yet found of some of the essential ideas in the theory of aerodynamic sound.

1. Introduction

Aeolian tones were known in antiquity. The Aeolian harp is an old musical toy which, when placed in the wind, produces these sounds in strange successions and combinations. They are heard in the singing of the wind through telegraph wires and its sighing through the twigs and branches of a leafless tree. It was not until 1878 that the first scientific study of them was made by Strouhal, whose apparatus consisted of a cylinder mounted upon a whirling arm so that it moved through the air at constant speed. Already by 1896, Rayleigh had recognized that the production of Aeolian tones is connected with the instability of the vortex sheets in the cylinder wake, and most significantly, that it is *not* essential that the cylinder should partake of the vibration to generate these tones, although the intensity is greatly enhanced by resonance between the natural frequency of the wire and the frequency of the vortex instability. He further perceived that the frequency of the note (expressed non-dimensionally as the Strouhal number S) depends upon the Reynolds number of the flow past the cylinder, and until recently, much of the later work on this phenomenon was connected with the determination of this dependence, and with the relation between the frequency of the note and that of the vortex instability in the wake. Relf (1921) showed that the fundamental frequency of the note and the vortex frequency on each side of the cylinder wake are equal over a range of Reynolds numbers which has since been extended to values between 50 and 10^4 by the work of Kovasznay (1949), Roshko (1953) and Gerrard (1955). Measurements of the intensity of the sound under various conditions were made by Holle (1938) and Gerrard, who measured its directional distribution also. Comparison will later be made between the results of these intensity determinations and the theoretical predictions of this paper. In 1896, Rayleigh wrote concerning this problem that "a dynamical theory has yet to be given", and to some extent this statement remains true. The purpose of this paper is to interpret the properties of these tones in terms of our empirical knowledge of the flow pattern; the prediction of the latter still lies beyond the attainments of present theory.

Rayleigh's important observation that Aeolian tones can be produced without vibration of the cylinder suggests that the phenomenon can be interpreted within the framework of the theory of aerodynamic sound.

However, to include the resonant case also in our considerations, the definition of this term can be extended slightly. It has previously been restricted to sound generated by the action of aerodynamic forces upon fixed surfaces, but since in many instances, these forces will themselves produce vibrations of the surfaces, the term can conveniently be extended to include those cases in which oscillations of the surface may occur as a result of the instability of the basic flow. A distinction is therefore drawn in what seems the natural place, between such situations and those in which the vibrations are caused by some external mechanism unrelated to the flow (a violin bow, perhaps). In the latter class, it is the vibrations themselves that set up the fluctuating force in the medium, whereas in aerodynamic sound the vibrations may occur as a result of the force fluctuations from the flow.

2. The sound field

The two well-known papers by Lighthill (1952, 1954) which laid the foundations of the subject of aerodynamic sound, were concerned with the sound field generated by the unsteady motion of an unbounded fluid. More recently, Curle (1955), using the same technique as Lighthill, was able to account for the effect of solid boundaries to the flow and showed that the sound can be considered to be produced by three separate mechanisms. The first is due to the unsteadiness in the fluid itself, and as Lighthill showed, is equivalent acoustically to a distribution of quadrupoles throughout the fluid. Curle pointed out that, in general, the presence of boundaries introduces additional dipole contributions to the sound field from the fluctuating stresses acting upon the fluid at the boundary and also perhaps source contributions from dilatation of the boundaries. The general expression for the density field $\rho(\mathbf{x})$ involves terms which represent these three effects separately, and can be written as

$$\rho(\mathbf{x})-\rho_0 = \frac{1}{4\pi a_0^2}\frac{\partial^2}{\partial x_i \partial x_j}\int \frac{1}{r}\,T_{ij}(\mathbf{y})\,dV(\mathbf{y}) + \\ + \frac{1}{4\pi a_0^2}\frac{\partial}{\partial x_i}\int \frac{1}{r}\,(\rho v_i v_j + p_{ij})\,dS_j(\mathbf{y}) - \frac{1}{4\pi a_0^2}\int \frac{1}{r}\,\frac{\partial(\rho v_i)}{\partial t}\,dS_i(\mathbf{y}), \quad (2.1)$$

where ρ_0 and a_0 are the density and velocity of sound in the undisturbed medium, v_i and p_{ij} are the velocity and stress tensor at a point $\mathbf{y}$ in the fluid and $r = |\mathbf{x}-\mathbf{y}|$. The tensor T_{ij} is given by

$$T_{ij} = \rho v_i v_j + p_{ij} - a_0^2 \rho\,\delta_{ij}, \quad (2.2)$$

and the integrands in (2.1) are taken at the retarded time $t - r/a_0$.

This gives the fluctuations in density in the medium in terms of the properties of the flow, which are assumed to be specified *a priori*. In general, of course, the density field itself must be included in the specification of the flow, and in practice (2.1) is meaningful only to the first order in the Mach number in which the direct dynamical interaction between the sound field and the velocity field can be ignored. To obtain this first order term,

it is legitimate to substitute into the right-hand side of (2.1) the values that would obtain if the fluid were incompressible, and this, incompressibility approximation' has invariably been made in the applications of the theory up to the present time. With its aid, retaining the leading term in each of the integrals, it is found that the radiated part of the sound field from the motion in the neighbourhood of a finite closed body is given by

$$\rho(\mathbf{x})-\rho_0 \sim \frac{1}{4\pi a_0^4}\frac{x_i x_j}{x^3}\int \frac{\partial}{\partial t^2} T_{ij}\, dV(\mathbf{y}) + \frac{1}{4\pi a_0^3}\frac{x_i}{x^2}\int \frac{\partial}{\partial t}(\rho_0 v_i v_j + p_{ij})\, dS_j(\mathbf{y}) - \\ - \frac{1}{4\pi a_0^2}\frac{\rho_0}{x}\int \frac{\partial v_i}{\partial t}\, dS_i(\mathbf{y}). \quad (2.3)$$

Curle (1955) simplifies this expression when the boundaries are perfectly rigid—perfect acoustic reflectors—and at rest, so that $v_i = 0$ over $S_i(\mathbf{y})$, but it will be shown here that the same simplification is possible in rather less restrictive circumstances. A sufficient condition for the vanishing of the source contribution is simply that the body be incompressible, so that its dilatation is zero. The Reynolds stress term in the dipole contribution also vanishes if the surface moves uniformly as that of a rigid body. For then $v_i(\mathbf{y}) = u_i + \epsilon_{ijk}\omega_j y_k$ on $S_i(\mathbf{y})$, where u_i is the velocity of, and ω_i the angular velocity about, the centre of mass, and on substitution into this term of the integral and application of Gauss's theorem, it is found to vanish. This second condition clearly embraces the first and (2.3) reduces to

$$\rho(\mathbf{x})-\rho_0 \sim \frac{1}{4\pi a_0^4}\frac{x_i x_j}{x^3}\int \frac{\partial^2 T_{ij}}{\partial t^2}\, dV(\mathbf{y}) - \frac{1}{4\pi a_0^3}\frac{x_i}{x^2}\frac{dF_i}{dt}, \quad (2.4)$$

where $F_i = -\int p_{ij}\, dS_j$ is the total force with which the body acts upon the fluid. Finally, when the orders in the Mach number M of the two terms on the right of this equation are examined, it is found that the dipole contribution is of order M^3 whereas the quadrupole term is of order M^4, that is, of the same order as the quantities already neglected in the incompressible approximation to the dipole term. So the quadrupole term too can be neglected and, when M is small,

$$\rho(\mathbf{x})-\rho_0 \sim -\frac{1}{4\pi a_0^3}\frac{x_i}{x^2}\frac{dF_i}{dt}. \quad (2.5)$$

In the generation of Aeolian tones, the fluctuating force is distributed along the length of the cylinder, and at low Reynolds numbers, if the flow were accurately two-dimensional, the force fluctuations would be in phase at all points. However, there are many reasons for believing that in a practical situation with a long cylinder (say, a long, thin wire) this will not be so, but that the phase of the force fluctuations will vary slowly, probably randomly, along its length. One reason is that the inherent small variations in the cylinder diameter will result in small changes in the frequency of vortex generation at different points which, in a large number of cycles, produce finite variations in phase. The coupling between the motions in

planes separated by a large number of diameters cannot be presumed to be so tight that such phase differences will not occur. Again, even with a perfectly uniform cylinder, if there is a three-dimensional instability of any kind, phase differences assuredly will be found, the extreme case being given when the flow behind the cylinder is turbulent. This question will be considered later in some detail, but if, for whatever reason, a random phase variation is present, then the sound intensity radiated from a cylinder of length l is approximately

$$I(\mathbf{x}) \sim \frac{x_i x_j}{16\pi^2\rho a^3 x^4} l \int_{-\infty}^{\infty} \overline{\frac{\partial f_i(z_0)}{\partial t} \frac{\partial f_j(z_0+z)}{\partial t}}\, dz,$$

$$\sim \frac{1}{16\pi^2\rho a^3 x^4} \overline{\left(x_i \frac{\partial f_i}{\partial t}\right)^2} sdl, \tag{2.6}$$

where $f_i(z)$ is the fluctuation in force per unit length at the axial position z, s is the dimensionless correlation distance along the axis (so that the actual distance is sd) and the subscripts to ρ and a have been omitted. In (2.6) it is further assumed that $l \ll sd$, as seems likely in many practical cases, so that end effects can be neglected. The two principal quantities to be determined on the right of this expression are first the mean square value of $\partial f_i/\partial t$ and second the axial scale s. The first is to be found from the experimental results of Kovasznay (1949) for the eddying motion in the wake at a Reynolds number in the regime of two-dimensional flow. This restricts our consideration initially to Reynolds numbers below those for which the motion is turbulent, although the theory is extended in a later section to conditions beyond this range. The second quantity, the correlation distance s, is the subject of a subsidiary experiment described in § 5.

3. The fluctuations in lift and drag upon a circular cylinder

The fluctuations in lift and drag have been calculated by integration of the acceleration field of the eddying wake in the directions normal and parallel to the direction of the oncoming stream, using the very extensive experimental data given by Kovasznay (1949) for a Reynolds number of 50. He expressed the velocity fluctuations in the direction of the oncoming stream, in the two-dimensional motion, as

$$u(x,y,t) = \phi_1(x,y)\cos 2\pi[\zeta_1(x)+nt] + \phi_2(x,y)\cos 4\pi[\zeta_2(x)+nt], \tag{3.1}$$

where the amplitude functions ϕ_1 and ϕ_2 vary slowly with x (the downstream coordinate), but rapidly with y, i.e. across the stream. ϕ_1 is an odd function of y, and ϕ_2 an even function. Here $\zeta_1(x)$ and $\zeta_2(x)$ are not quite linear functions of x, in order to account for the slightly non-uniform spacing of the vortices, and the frequency n is constant in time. Kovasznay measured $\phi_1(x,y)$ and $\phi_2(x,y)$ across the wake at various stations downstream as far as $x/d = 40$, and, by smoothing and interpolating between his points, these functions have been found for values of y within the wake and for values of x between 0 and $40d$. Interpolated values of the functions $\zeta_1(x)$ and $\zeta_2(x)$ have also been obtained from his measurements.

The fluctuations in drag per unit length can be found directly by integration of (3.1) and use of the equation

$$f_d = \rho \frac{d}{dt} \iint u \, dxdy,$$

where the integration is over a plane normal to the cylinder axis. The calculation presents no difficulties concerning convergence, since $\phi_2(x, y)$ is negligibly small for values of y beyond the centres of the vortices. The function $\phi_1(x, y)$ is odd in y, so that the integral of the first term in (3.1) vanishes, and the fluctuations in drag have a frequency just twice the fundamental n. However, the calculation of the fluctuations in lift per unit length f_l is not so straightforward, since the velocity fluctuations normal to the oncoming stream were not measured. They could perhaps be calculated from the continuity condition

$$\frac{\partial u}{\partial x} + \frac{\partial v}{\partial y} = 0,$$

which gives

$$v = \int_{\infty}^{y} \frac{\partial u}{\partial x} \, dy.$$

The difficulty with this method is that measurements of u were not made beyond the vortical region of the wake, and to make a correct allowance for the virtual mass of the irrotationally moving fluid would indeed be complicated. An alternative method was used which required information about the vorticity field alone.

It is shown in the Appendix that

$$\iint v \, dxdy = - \iint \omega x \, dxdy, \tag{3.2}$$

where the vorticity ω, which vanishes outside the wake, is given by

$$\omega = \frac{\partial v}{\partial x} - \frac{\partial u}{\partial y},$$

so that, using the continuity condition,

$$\frac{\partial \omega}{\partial y} = - \frac{\partial^2 u}{\partial x^2} - \frac{\partial^2 u}{\partial y^2}.$$

Hence

$$\omega = \int^{y} \left(\frac{\partial^2 u}{\partial x^2} + \frac{\partial^2 u}{\partial y^2} \right) dy, \tag{3.3}$$

the integration being commenced at the edge of the wake. The integral $\iint v \, dxdy$ is calculated from (3.2), (3.3) and (3.1), and some of the details of this, including the devices used to ensure more rapid convergence, are described in the Appendix.

The result is found to be

$$M = \rho \iint v \, dxdy = 0{\cdot}48 \rho U d^2 \cos 2\pi nt, \tag{3.4}$$

where U is the mean stream velocity, and thus the fluctuating lift per unit length is

$$f_l = \frac{dM}{dt} = 0{\cdot}38\rho U^2 d \cos 2\pi nt, \tag{3.5}$$

(taking a new time origin), since $n = 0{\cdot}13U/d$ at $R = 50$. The fluctuation in drag per unit length is found by direct integration, and its magnitude is very much smaller. In fact,

$$f_d = 0{\cdot}04\rho U^2 d \cos 4\pi nt. \tag{3.6}$$

Just as the fluctuations in drag are determined by the term in (3.1) which is an even function of y, so the fluctuating lift is determined by the odd part in y, as the result (3.5) implies. For, from (3.2), only the even part of ω is relevant, or, from (3.3), only the odd part of u.

The mean drag per unit length at a Reynolds number of 50 is about $0{\cdot}75\rho U^2 d$, so that our calculation shows that the magnitude of the maximum lift is about 50% of the mean drag.

The value 0·38 for the coefficient in (3.5) can be shown to be a not unreasonable figure by constructing a very crude upper limit to the amplitude of the fluctuating lift in the following way. Suppose that vortex sheets of strength U are generated at each side of the cylinder which, because of their instability, curl up into discrete vortices like a Karman street. Suppose further that all the vorticity is gathered into these vortices, none being lost by diffusion. The separation of the vortices is approximately $\frac{1}{2}U/n$, which, at a Reynolds number of 50 and Strouhal number of 0·13, is equal to nearly $4d$. The strength of the discrete vortices is therefore $4Ud$, and the amplitude of the fluctuating circulation about a fixed contour in the irrotational fluid is $2Ud$, so that the amplitude of the fluctuating lift is $\rho U . 2Ud = 2\rho U^2 d$. That this is so much greater than the actual value can presumably be ascribed to the fact that the process of viscous diffusion would lead to a reduction of the coefficient.

The accuracy of the calculated value (3.5) is admittedly not very high. The numerical differentiations reduce the accuracy, only partial compensation being provided by the subsequent integrations, and inspection of the working suggests that an accuracy of 40% is probably the best that can be claimed. However, this is ample for the present purpose in view of the uncertainties of the acoustical measurements themselves.

4. The effect of Reynolds number

The estimate (3.5) was obtained from consideration of the flow pattern at $R = 50$, and it would be very satisfying if similarly detailed measurements were available at other Reynolds numbers in the range of two-dimensional eddying motion. Unfortunately, they are not, and some general argument will have to be invoked concerning the effect of viscosity upon the flow pattern. Such an argument would not be required to give results that are

accurate in detail, but only to give a good indication of the variation of the amplitude of the lift fluctuations with Reynolds number.

Let us consider the mechanism of the development of the vortices in the wake. The initial instability introduces small fluctuations in the y-position of the vortex layer on each side of the wake, and these result in differential convection velocities of the vorticity and the eventual rolling up of the layer. The development of the vortices is opposed by the diffusive action of viscosity, and the maximum concentration is reached when the two effects balance. Thereafter the vortices decay by viscous diffusion between those of opposite sign, but it is not difficult to show that, at $R = 50$, this process hardly commences within the first 50 diameters (this being the part of the wake upon which the lift and drag calculations of § 3 depend). For, in time t, the vorticity diffuses over a distance of order $(\nu t)^{1/2}$, so that at a point k diameters downstream it has diffused a distance of order $(\nu kd/U)^{1/2} = (k/R)^{1/2}d$. When $R = 50$, this is of order d (still much less than the vortex spacing) at 50 diameters from the cylinder; the details of the motion in the wake beyond such points having little influence upon the fluctuating forces on the cylinder. For the present purposes, then, a decrease in the viscosity of the fluid (or an increase in R) has two consequences; it modifies the frequency of the initial instability and also postpones the attainment of the balance between viscous and convective vorticity transfer, so that the vortices become more concentrated.

Regarding the second effect, (3.2) shows that, in discussing the fluctuating lift, we are concerned not so much with the concentration of the fluctuations in vorticity as with their integrated magnitude or with the total strength of the vortices. If we assume as an approximation that the lateral spacing of the vortices is materially unaltered by a decrease in viscosity, the Reynolds number effect must lie in the variation of the strength of the vortices. This is indeed a consequence of the first effect, the modification of the frequency of the initial instability and so of the spacing of the vortices. The strength of the vortices can be assumed to be proportional to their spacing, U/n approximately, so that as the viscosity varies, the vortex strength varies as S^{-1}, since $S = nd/U$. Therefore the momentum fluctuations normal to the direction of the oncoming stream are proportional to S^{-1}, and on differentiation f_l is independent of S and so of R; consequently

$$f_l \simeq 0{\cdot}38\rho U^2 d \cos 2\pi nt, \tag{4.1}$$

for $40 < R < 160$. It follows immediately that

$$\frac{\partial f_l}{\partial t} = 2{\cdot}4\rho U^3 S \cos 2\pi nt. \tag{4.2}$$

The Strouhal number S is well defined empirically as a function of Reynolds number (Kovasznay 1949, Gerrard 1955) so that this equation gives approximately the dependence on Reynolds number of the term $\partial f_l/\partial t$ in the expression (2.6).

5. The correlation distance s

Very little published information is available concerning the scale of the variations in phase of the fluctuations along the axis of the cylinder. Both Roshko (1953) and Gerrard (1955), making observations at Reynolds numbers greater than about 150, found slow spanwise variation in phase along the cylinder, but insufficient data were available to estimate its length scale. On the other hand, Kovasznay (1949) found no measurable differences at $R = 50$ over distances of the order of 20 diameters, so that presumably the length scale is very much greater than this. An estimate of s is necessary for the application of (2.6), and so to obtain this, and to clarify the situation if possible, a supplementary experiment was made in a water tank.

A hollow tube of outside diameter $\frac{1}{4}$ in. was stopped up at one end and a row of small holes drilled down one side at $\frac{1}{4}$ in. centres. These holes were then filled with plasticine which could be removed easily from two of them to give open holes separated by any desired number of diameters from 1 to 30. The tube was filled with dye and lowered vertically into a tank of still water. The tube was drawn through the water with a given velocity, and the vortex patterns were observed at two different axial positions by the dye traces at the two free holes. End effects were avoided by making no observations within 10 diameters of the stopped end of the tube or within 4 diameters of the free surface. The differences in phase were measured by looking vertically downwards at the dye patterns behind the cylinder, and, by repeating the experiment a large number of times for points at a given separation, the correlation coefficient of the fluctuations in lift was estimated. By repeating this procedure with holes at different separations, the length scale of the lift fluctuations was determined approximately.

The results of these observations can be summarized as follows. For Reynolds numbers below about 80, very little phase difference was observed even for the largest available separation of 30 diameters, so that under these conditions the axial scale is certainly much greater than this. However, when the Reynolds number was between 100 and 160, the phase differences were clearly observed. At a separation of about 30 diameters, the phases appeared to be almost uncorrelated. The scale s was estimated to be between 15 and 20 diameters, and did not appear to depend critically upon Reynolds number or upon the presence or absence of small disturbances in the water before the passage of the cylinder. At Reynolds numbers between these two ranges, i.e. between 80 and 100, it was noticed that there was little difference in phase if the tank was allowed to settle for a minute or two between successive trials, but that random variations were set up with about the same scale as at higher Reynolds numbers if two trials were carried out in rapid succession or if the water was disturbed slightly prior to an attempt.

These observations suggest that, at Reynolds numbers between about 40 and 80, the eddying motion is truly two-dimensional, and apparently stable to small disturbances in the oncoming stream. As the Reynolds

number increases to a value between 80 and 100, however, the laminar motion becomes unstable to three-dimensional disturbances with a length scale along the axis of about $17d$, and the flow becomes only approximately two-dimensional. This new type of motion persists until about $R = 160$, when yet further modes are excited and the flow eventually becomes turbulent. These observations are consistent with those already mentioned for Reynolds numbers of 50 and 150.

Returning to our basic problem, it seems that a reasonable value for s in (2.6) is about 17 for Reynolds numbers between 100 and 160. Below this range, a much larger value can be expected, and its magnitude would be determined, not by the flow conditions, but by the small imperfections and irregularities in the diameter of the wire, as has been explained in § 2. These can hardly be considered to be under the control of the experimenter, and reasonable *a priori* estimates of the magnitude of the radiated sound are difficult without detailed examination of each particular wire. One further point arises from these observations. The fluctuating lift and drag were calculated on the assumption of a two-dimensional flow, and some error will be introduced into (4.1) by the lack of two-dimensionality at values of R between 100 and 160. However, since the scale of the variations along the axis of the cylinder is very much greater than that in the plane normal to the axis, such errors are expected to be quite small.

6. Comparison with experiment

The radiated intensity can be found immediately from (2.6) and (4.1). Neglecting the relatively small fluctuations in drag, the radiated sound is generated by the fluctuating lift, and so consists of a dipole field with its axis normal to the direction of the oncoming stream. From (4.2),

$$\overline{\left(\frac{df_l}{dt}\right)^2} = 2{\cdot}4\rho^2 U^6 S^2,$$

so that the total radiated intensity at points distant r from a cylinder of length l is

$$I(r) \sim 0{\cdot}27\cos^2\theta \frac{\rho l d U^6 S^2}{a^3 r^2}, \tag{6.1}$$

where θ is the angle between the oncoming stream and the direction of the line joining the point of observation to the cylinder, and s has been taken as 17. The mean square acoustic pressure is

$$\overline{p^2}(r) = \rho a I(r),$$

$$\sim 0{\cdot}27\cos^2\theta \frac{\rho^2 l d U^6 S^2}{a^2 r^2}. \tag{6.2}$$

Some experiments were undertaken to test this result, particularly the variation of $\overline{p^2}$ as the sixth power of the Mach number. The measurements of sound intensity, which were made at the Acoustics Laboratory of the

National Physical Laboratory, Teddington, by the kind permission of the Superintendent of the Physics Division and Mr N. Fleming, were executed by Mr W. C. Copeland. I am greatly indebted to them for their generous and able assistance. The apparatus consisted of two thin wires, 60 cm in length and 0·0123 cm in diameter, held vertically with just sufficient tension to prevent sagging, between two arms mounted on a spinning shaft of diameter $\frac{5}{8}$ in.—the same type of arrangement as that used by Strouhal and Gerrard. The supporting arms were made of $\frac{3}{16}$ in. dural sheet tapered and streamlined to reduce disturbances. The shaft was belt-driven from an electric motor, and, to reduce the background noise level, the motor and all the ball-bearings were enclosed in felt-lined boxes. The apparatus was mounted on an open steel frame and, when in position for the measurements, was placed in the acoustically quiet room at the N.P.L. with a microphone 115 cm from the axis of the shaft in the plane bisecting the wires. The apparatus was tested by running it with the wires removed, and the noise level was found to be negligible in the frequency range at which the measurements were made.

The microphone signal was amplified and passed through a variable frequency narrow-band analyser, and displayed on the screen of a cathode-ray oscillograph. The modulation with time, corresponding in the whirling arm apparatus to the variation with θ, followed closely that indicated by the $\cos^2\theta$ factor in (6.2). For the intensity measurements, the peak values of $\overline{p^2}$, corresponding to orientations $\theta = 0$, were observed at a number of frequencies within the narrow spectrum of the sound generated, from which the total radiation was calculated. The speed of the wires was altered by variation of their radial position and of the speed of the motor. The results of these measurements are shown as the solid points in figure 1, together with the predicted relation (6.2), and the agreement is seen to be remarkably good. However, the constant in (6.2) is reliable only to within a factor of two, this range of uncertainty being approximately the same as the experimental uncertainty shown by the scatter of the points. For values of $U(ldS^2/r^2)^{1\cdot6}$ less than about 140, corresponding in these measurements to Reynolds numbers less than about 100, an intermittent signal of very much higher intensity was sometimes recorded, which was consistent with the establishment of the regime of truly two-dimensional flow over most of the length of the wires and the consequent enormous increase in the value of s. However, under the experimental conditions, it was not possible to produce a sufficiently stable signal to make systematic observations, and indeed, even had this been possible, there remains the strong suspicion that the results would not be generally applicable, but would depend upon the imperfections of the particular wire used.

These results offer good evidence for the validity of the expression (6.2) in the Reynolds number range from 100 to 160. The variation of the sound intensity as the sixth power of the velocity seems to be confirmed well, and in the next section it will be shown that this remains true when the flow is turbulent at higher Reynolds numbers.

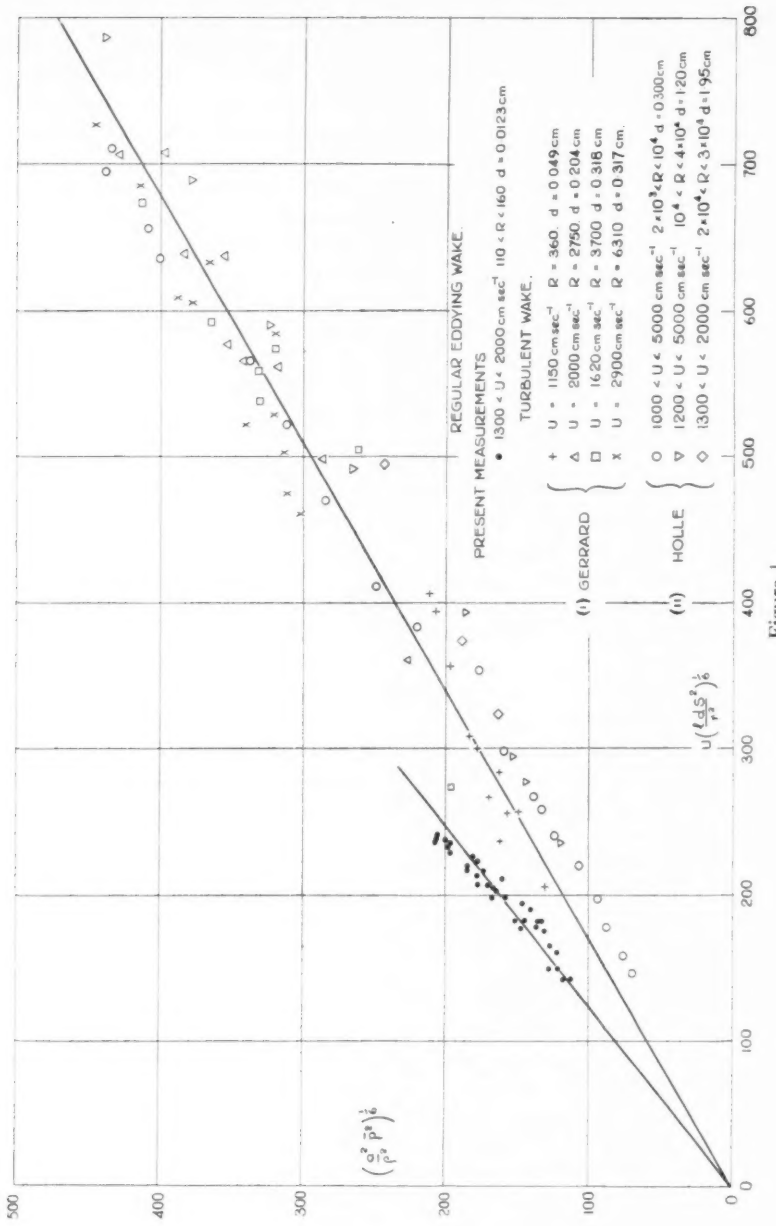
REGULAR EDDYING WAKE.
PRESENT MEASUREMENTS
• 1300 < U < 2000 cm sec⁻¹ 110 < R < 160 d = 0·0123 cm
TURBULENT WAKE.
(i) GERRARD
+ U = 1150 cm sec⁻¹ R = 360. d = 0·049 cm
△ U = 2000 cm sec⁻¹ R = 2750. d = 0·204 cm
□ U = 1620 cm sec⁻¹ R = 3700 d = 0·318 cm
× U = 2900 cm sec⁻¹ R = 6310 d = 0·317 cm.
(ii) HOLLE
○ 1000 < U < 5000 cm sec⁻¹ 2×10³ < R < 10⁴ d = 0·300 cm
▽ 1200 < U < 5000 cm sec⁻¹ 10⁴ < R < 4×10⁴ d = 120 cm
◇ 1300 < U < 2000 cm sec⁻¹ 2×10⁴ < R < 3×10⁴ d = 195 cm
$\left(\frac{\alpha^2 \bar{T}^2}{\rho^2}\right)^{\frac{1}{6}}$
$U\left(\frac{\ell S^2}{\rho^2}\right)^{\frac{1}{6}}$
0
100
200
300
400
500
600
700
800

Figure 1.

7. Turbulent flow

Hitherto attention has been concentrated upon conditions at Reynolds numbers below that for the onset of turbulent flow. As R increases beyond this range, intermittent bursts of turbulence occur in the flow, as described by Roshko (1953), until at about $R = 300$ the wake behind the cylinder is fully turbulent. The expressions given for the fluctuating lift and axial length scale are no longer relevant but we can still predict their order of magnitude and dependence on Reynolds number and obtain, for these new conditions, an expression for the intensity of the radiated sound which is arbitrary only to the extent of an unknown constant factor.

It is clear that the presence of a fluctuating lift depends upon the existence of large-scale axial eddies of alternating sign near the cylinder. Some measurements have recently been made by Mr I. C. T. Nisbett at the Cavendish Laboratory in the turbulent flow near the cylinder at Reynolds numbers of order 5×10^3. He has established the presence of a surprisingly distinct large-scale structure, similar in many ways to that observed in the two-dimensional eddying flow at lower Reynolds numbers. These large eddies are approximately parallel to the cylinder axis, and contain an appreciable amount (about half) of the turbulent energy, the remainder being in the irregular smaller-scale fluctuations. They appear to be somewhat contorted in the axial direction, since simultaneous velocity correlations between similar points in planes normal to the axis are alternately positive and negative as the axial separation increases up to about 20 diameters. The integral length scale of these eddies along the axis is about three diameters. These observations, in the light of our previous discussion and of such formal expressions as (3.2), suggest that the fluctuations in lift are still dominant even at these Reynolds numbers, and that their length scale is about $3d$, although we can make no *a priori* statement about their magnitude.

What of the variation of the magnitude of the fluctuating lift with Reynolds number? Here, again, the general arguments of § 4 still apply with equal force, and we have

$$(\overline{f_l^2})^{1/2} = \text{constant } \rho U^2 d. \tag{7.1}$$

Some further support to this relation is afforded by the principle of Reynolds number similarity (Townsend 1956). This principle expresses the fact that the large-scale components of the motion are not influenced by the fluid viscosity if it is sufficiently small, i.e. by the Reynolds number provided it is sufficiently large. We have seen that the fluctuating lift is a consequence of the large eddy motion in the wake, so that (7.1), which is correct dimensionally, is also independent of the (large) Reynolds number. Whether or not the principle of Reynolds number similarity holds in this situation for values of R as low as 300 is perhaps open to question, but for higher values it can certainly be invoked to support (7.1). Using this

relation, then, we have from (2.6) that the radiated intensity from a cylinder of length l is

$$I(r) = \alpha \cos^2\theta \frac{\rho l d U^6 S^2}{a^3 r^2}, \tag{7.2}$$

which differs from (6.1) only in the constant factor which is now represented by α. Again, as in (6.2), the mean square acoustic pressure is given by

$$\overline{p^2}(r) = \alpha \cos^2\theta \frac{\rho^2 l d U^6 S^2}{a^2 r^2}, \tag{7.3}$$

where the Strouhal number S involves the frequency of 'shedding' of the large eddies, or the fundamental frequency of the sound generated. The constant α can be expected to be considerably smaller than 0·27, because of the reduced length scale of the fluctuations in lift per unit length and also possibly a reduced intensity arising from the decreased coherence in the turbulent flow.

Detailed measurements of the sound intensity radiated at Reynolds numbers for which the flow is turbulent have been made by Holle (1938) and by Gerrard (1955). Now, Gerrard's curves of intensity as a function of velocity at constant Reynolds number (obtained by keeping the product Ud fixed) appear to show that $\overline{p^2} \propto U^4$, but this behaviour is inconsistent with the U^6 variation suggested by a rough application of the theory (as he himself points out) and his results have hitherto presented something of an anomaly. However, (7.3) shows that, with Ud fixed, we should expect that $\overline{p^2} \propto U^5$, so that the anomaly is not as serious as might appear at first. A possible cause of the discrepancy lies in Gerrard's having taken $\overline{p^2} \propto l^2/r^2$ when $l \gg d$ in the analysis of his data, which implies that the fluctuations in lift are in phase along the entire length of the cylinder, over many hundreds of diameters. In turbulent flow, the case for assuming a random phase variation along the cylinder (leading to intensities proportional to the *first* power of the length as in (7.2)) is even stronger than at the lower Reynolds numbers discussed in the previous sections, yet independent confirmation that this is so even under these latter conditions has been given by the agreement between the absolute values of the measured and predicted sound intensities shown in the upper curve of figure 1*. Nisbett's observations on the flow at high Reynolds numbers provide yet further strong evidence for random phase variations, so that it seems inevitable that, in fact, $\overline{p^2} \propto l/r^2$ in the radiated field under the circumstances of Gerrard's measurements.

In his figure 4, some of Gerrard's measured values of $\overline{p^2}$ under a variety of conditions are plotted as a series of curves together with the relevant experimental parameters. Assuming that in fact $\overline{p^2} \propto l/r^2$, these points have been replotted as a function of velocity and Reynolds number in the lower curve of figure 1 of this paper. This diagram also shows a

* If, in (6.2), sd is replaced by the length l, the expression would give values of $\overline{p^2}$ about 250 times those measured in the experiments of § 5.

representative sample of Holle's (1938) measurements*, and these agree well with Gerrard's replotted points. They all lie about a single straight line passing through the origin, as predicted by equation (7.3), and cover a fairly wide range of conditions. The slope of the line is less than under conditions of non-turbulent flow and corresponds to a value of α of approximately 0·037. The scatter of the points is not inconsiderable, but the linearity of the relation seems to be confirmed well, and provides good support for the result (7.3) which is based upon the ideas of the theory of aerodynamic sound.

8. Some final remarks

The satisfactory agreement between these various experimental results and the theory gives confidence that the latter is firmly founded. One factor ignored in our considerations, however, is the possibility of vibration of the wire. However it is not difficult to show that the amplitude of the vibrations is indeed small compared with the wire diameter provided the tension is such that the natural frequency of the wire is very far from the vortex frequency, and the density of the medium is much less than that of the wire. Under these conditions, which have been satisfied in the experiments mentioned here, the vibrations of the wire can reasonably be neglected. On the other hand, if the frequency of vortex shedding coincides with the fundamental frequency of the wire, or with one of its low harmonics, then resonance will lead to vibrations of finite amplitude. Rayleigh's observation that the acoustic intensity is greatly enhanced under these conditions was mentioned earlier in this paper, and there arises the question of accounting for this within the framework of the present theory.

Now, the two basic variables which determine the intensity of the radiated sound are the magnitude of the fluctuations in lift, and the correlation distance s. The first quantity will clearly be modified by the presence of vibrations, both through the introduction into equations such as (3.2) of an additional term describing the motion of the boundary and through the modification of the flow pattern, but since the maximum velocity of the vibrating wire could not be expected to be much greater than the wind velocity, these could not reasonably be expected to contribute a factor of more than about 5 to the intensity of the sound radiation. A much more powerful contribution will be given by the increase in the value of s brought about by the equalization of the phase of the fluctuating lift along the wire. The vibrations, which may be in phase over the whole length and are at the same frequency as the vortex 'shedding', clearly provide a coupling between the motions in the fluid at different axial positions that is far more effective than any hydrodynamic coupling. The phase of the large eddies loses its randomness along the cylinder, and is determined by the phase of the vibrations, so that for the fundamental the correlation distance sd now becomes the length l, which can represent an increase of

* Incidentally, Holle found experimentally that $\overline{p^2} \propto l/r^2$ approximately, as in (7.3), and that the velocity dependence was as U^7, nearly. But a reasonably fit is still obtained by plotting $(\overline{p^2})^{1/6}$ against U as in figure 1.

many hundreds of times. The explanation of Rayleigh's observation seems to lie in this effect rather than in any increase in the magnitude of f_l.

The value of this work may go beyond the interpretation and understanding of the phenomenon of Aeolian tones. The relative simplicity of the fluid motion makes possible what is perhaps the least ambiguous confirmation yet found of some of the essential ideas in the theory of aerodynamic sound, and gives even greater confidence in their application to more complex problems.

Appendix. Fluctuations in wake momentum

From the vector identity

$$\mathbf{x}\times\boldsymbol{\omega} = \nabla(\mathbf{x}.\mathbf{v}) - (\mathbf{v}.\nabla)\mathbf{x} - (\mathbf{x}.\nabla)\mathbf{v}, \tag{A.1}$$

it can readily be shown that

$$\int \mathbf{v}\,d\mathbf{x} = \tfrac{1}{2}\int (\mathbf{x}\times\boldsymbol{\omega})\,d\mathbf{x} + \tfrac{1}{2}\int \mathbf{x}\times(d\mathbf{S}\times\mathbf{v}), \tag{A.2}$$

where the integration is throughout the region bounded by the closed surface S. We apply this to the two-dimensional flow about a cylinder centred on the z-axis, considering the volume bounded by the planes $z = 0$ and $z = d$, say. The cylinder is considered to be fixed, and the surface of integration reduces to the two planes, so that (A.2) becomes

$$d\iint \mathbf{v}\,dxdy = \tfrac{1}{2}d\iint (\mathbf{x}\times\boldsymbol{\omega})\,dxdy + \tfrac{1}{2}\left[\int \mathbf{x}\times(d\mathbf{S}\times\mathbf{v})\right]_{z=d} + \\ + \tfrac{1}{2}\left[\int \mathbf{x}\times(d\mathbf{S}\times\mathbf{v})\right]_{z=0}.$$

In the two-dimensional motion the fluctuations in velocity and vorticity are $\mathbf{v} = (u, v, 0)$ and $\boldsymbol{\omega} = (0, 0, \omega)$, and on substituting these into the last expression, we obtain for the fluctuations in momentum in the y-direction normal to the oncoming stream,

$$d\iint v\,dxdy = -\tfrac{1}{2}d\iint \omega x\,dxdy + \tfrac{1}{2}d\iint v\,dxdy,$$

since $d\mathbf{S} = (0, 0, -dxdy)$ on $z = d$. Therefore

$$\iint v\,dxdy = -\iint \omega x\,dxdy, \tag{A.3}$$

and similarly

$$\iint u\,dxdy = \iint \omega y\,dxdy. \tag{A.4}$$

where the limits are understood to be taken in the sense

$$\lim_{x\to\infty}\left(\lim_{y\to\infty}\int_{-x}^{x}\int_{-y}^{y} v\,dydx\right).$$

In the eddying wake behind a cylinder (of unit diameter) we shall neglect fluctuations in the vorticity of the boundary layer, since Kovasznay's measurements indicate that the unsteady motion is small within the first few diameters of the centre of the cylinder. The fluctuations in vorticity

are found from equation (3.3), and on considering only that part of u in (3.1) that is an odd function in y,

$$\frac{\partial^2 u}{\partial x^2} = \left\{\frac{\partial^2 \phi_1}{\partial x^2} - 4\pi^2 \phi_1 [\zeta_1'(x)]^2\right\} \cos 2\pi[\zeta_1(x) + nt] -$$

$$- \left\{4\pi \frac{\partial \phi_1}{\partial x} \zeta_1'(x) + 2\pi \phi_1 \zeta_1''(x)\right\} \sin 2\pi[\zeta_1(x) + nt],$$

$$= A(x, y)\cos 2\pi[\zeta_1(x) + nt] - B(x, y)\sin 2\pi[\zeta_1(x) + nt],$$

say. Therefore

$$\omega = \left(\alpha - \frac{\partial \phi_1}{\partial y}\right)\cos 2\pi[\zeta_1(x) + nt] - \beta \sin 2\pi[\zeta_1(x) + nt],$$

where $$\alpha(x, y) = \int_y^5 A(x, y)\, dy, \qquad \beta(x, y) = \int_y^5 B(x, y)\, dy,$$

the upper limit being taken at $y = 5$ since it was found that the vorticity was zero along this line over the length of the wake to be considered. The integration over y in (A.3) is most conveniently performed first; since ϕ_1 is an odd function of y, we have

$$\int_{-\infty}^{\infty} \omega\, dy = \chi_1(x)\cos 2\pi[\zeta_1(x) + nt] - \chi_2(x)\sin 2\pi[\zeta_1(x) + nt],$$

where $$\chi_1(x) = \int_{-5}^{5} \alpha\, dy, \qquad \chi_2(x) = \int_{-5}^{5} \beta\, dy,$$

and so

$$-\iint v\, dx dy = \left\{\int_0^{\infty} x\chi_1(x)\cos 2\pi\zeta_1(x)\, dx - \int_0^{\infty} x\chi_2(x)\sin 2\pi\zeta_1(x)\, dx\right\}\cos 2\pi nt -$$

$$- \left\{\int_0^{\infty} x\chi_1(x)\sin 2\pi\zeta_1(x)\, dx + \int_0^{\infty} x\chi_2(x)\cos 2\pi\zeta_1(x)\, dx\right\}\sin 2\pi nt.$$

An integration by parts makes these integrals more rapidly convergent;

$$-\iint v\, dx dy = \cos 2\pi nt \int_0^{\infty} [\theta_1(x)\sin 2\pi\zeta_1(x) + \theta_2(x)\cos 2\pi\zeta_1(x)]\, dx +$$

$$+ \sin 2\pi nt \int_0^{\infty} [\theta_1(x)\cos 2\pi\zeta_1(x) + \theta_2(x)\sin 2\pi\zeta_1(x)]\, dx, \quad \text{(A.5)}$$

where $$\theta_1(x) = \frac{d}{dx}\left\{\frac{x\chi_1(x)}{2\pi\zeta_1'(x)}\right\},$$

with a similar expression for $\theta_2(x)$.

The expression (A.5) is that from which the fluctuations in wake momentum were calculated. Kovasznay's (1949) experimental results for $\phi_1(x, y)$ were smoothed and interpolations were made so that a map of the function was obtained for the domain $-5 < y < 5$, $0 < x < 40$. The functions $\alpha(x, y)$ and $\beta(x, y)$ were found numerically, and $\chi_1(x)$ and $\chi_2(x)$ calculated by integration. $\theta_1(x)$ and $\theta_2(x)$ were thence obtained, and the

final result emerged from the integration of (A.5). It was that

$$\iint v\,dxdy = 0{\cdot}48Ud^2\cos 2\pi nt, \tag{A.6}$$

giving the fluctuating lift as

$$f_l = 0{\cdot}38\rho U^2 d\cos 2\pi nt, \tag{A.7}$$

since at this Reynolds number $n = 0{\cdot}13U/d$. These are the results quoted in (3.4) and (3.5).

References

Curle, N. 1955 *Proc. Roy. Soc.* A, **231,** 505.

Gerrard, J. H. 1955 *Proc. Phys. Soc.* B, **68,** 453.

Holle, W. 1938 *Akust. Zeits.* **3,** 321.

Kovasznay, L. S. G. 1949 *Proc. Roy. Soc.* A, **198,** 174.

Lighthill, M. J. 1952 *Proc. Roy. Soc.* A, **211,** 564.

Lighthill, M. J. 1954 *Proc. Roy. Soc.* A, **222,** 1.

Rayleigh, Lord 1896 *The Theory of Sound*, Vol. II. London : Macmillan.

Relf, E. F. 1921 *Phil. Mag.* (6th Series), **42,** 173.

Roshko, A. 1953 *Nat. Adv. Comm. Aero., Wash., Tech. Note* no. 2913.

Strouhal, V. 1878 *Wied. Ann.* **5,** 216.

Townsend, A. A. 1956 *The Structure of Turbulent Shear Flow.* Cambridge University Press.

The wall jet

By M. B. GLAUERT
Department of Mathematics, University of Manchester

(*Received* 13 *August* 1956)

SUMMARY

This paper considers the flow due to a jet spreading out over a plane surface, either radially or in two dimensions. Solutions of the boundary layer equations are sought, according to which the form of the velocity distribution across the jet does not vary along its length. For laminar flow, such a similarity solution is obtained explicitly. For turbulent flow, an eddy viscosity is introduced, and it is eventually seen that complete similarity is not attainable, but that confident predictions can nevertheless be made about the nature of the velocity distribution and the rate of growth of the wall jet.

1. INTRODUCTION

When a jet of air strikes a surface at right angles and spreads out radially over it, it forms what will be termed a wall jet. Such a flow is produced by the downwards-directed jet from a vertical-take-off aircraft spreading out over the ground, or by a jet of water from a tap falling into a partly full sink and spreading out over the bottom. It should be noted that the flow due to a jet of water falling into an empty sink is in a quite different category, as then the condition at the free surface is that the pressure is constant; for a wall jet, as for a free jet, the corresponding condition is that the radial velocity component falls to zero at the outer edge of the jet.

Plane wall jets may also arise. If the water levels are different in two sections of a canal, separated by a sluice, and if the sluice is slightly raised, the flow into the section with the lower water level will take the form of a wall jet. Alternatively, if a plane jet impinges on a fixed plate parallel to the direction of flow, a wall jet will be produced on each side of the plate.

The theory of such wall jets, radial or plane, laminar or turbulent, forms the subject of this paper. It does not appear to have received attention previously. The appropriate boundary layer equations are set up, and a search is made for a similarity solution, in which the form of the velocity distribution across the jet does not vary along its length. This is a familiar procedure in boundary layer theory. Two similarity exponents, giving the variation with distance of the maximum velocity and the jet width, have to be determined, and one relation between them is obtained from the boundary layer equations themselves. In the corresponding problem for a free jet, a second relation is deduced from the constancy of momentum flux, and for a boundary layer the second relation is even simpler in form,

since the velocity must vary in the same manner as does the known external flow. For a wall jet, neither of the principles can be applied. It is shown in § 2 that the solution depends on an eigenvalue problem, which for laminar flow is satisfactorily solved in §§ 2 and 3. The calculation of the jet profile is carried out in § 4, and it is found possible to perform the integrations analytically. The same velocity distribution applies for both radial and plane wall jets, a fortunate circumstance which occurs in all the cases considered in this paper, and greatly shortens the work.

In most practical examples, the wall jet will be turbulent. The attempts in §§ 5–9 at predicting its form are all based on the idea of replacing the molecular viscosity by an effective eddy viscosity, and requiring this to vary in a plausible manner. The first attempt, in § 5, makes use of the hypothesis for free turbulent flow due to Prandtl (1942), according to which the eddy viscosity is constant across the breadth of the jet. The velocity profile thus derived is shown to be identical with that in the laminar case, and further implications of this result are noted. Near the wall, this solution is not in accord with preliminary experiments (Bakke 1956), and in § 6 a second attempt is made, with an eddy viscosity as required to satisfy the law due to Blasius (1913) for flow in a pipe. The solution again is calculated without difficulty, and might be expected to be accurate in the region near the wall. A more realistic procedure is to postulate an eddy viscosity based on Blasius's law near the wall and Prandtl's hypothesis further out. This implies that complete similarity is no longer possible. Also, the eigenvalue problem to determine the similarity exponents, which in the earlier attempts was solved by a simple extension of the analysis for a laminar wall jet, has to be considered afresh. In spite of these difficulties, in §§ 7–9 an analysis is carried out which results in definite predictions as to the velocity distribution and the values of the similarity exponents, as slowly varying functions of the Reynolds number. As in all problems involving Prandtl's hypothesis, the value of a single constant has to be assigned from experimental observations. The final results are put forward with some confidence in the belief that they do correctly predict the main features of an actual turbulent wall jet.

In what follows, the theory is developed for the case of a radial jet, as being of the greater practical interest. The modifications required to make the analysis applicable to a plane wall jet are only slight, and are noted at the end of each section.

2. Similarity solutions

We now consider the equations governing a radial laminar jet flowing over a plane wall. On the boundary layer approximation, the pressure is everywhere uniform, and the momentum equation is

$$u\frac{\partial u}{\partial x}+v\frac{\partial u}{\partial y}=\nu\frac{\partial^2 u}{\partial y^2}, \tag{2.1}$$

where x and y denote distances along and normal to the wall, x being measured from the jet axis, u and v the corresponding velocity components, and ν the kinematic viscosity. The equation of continuity is

$$\frac{\partial(xu)}{\partial x} + \frac{\partial(xv)}{\partial y} = 0, \tag{2.2}$$

and hence there is a Stokes stream function ψ satisfying

$$xu = \frac{\partial \psi}{\partial y}, \qquad xv = -\frac{\partial \psi}{\partial x}. \tag{2.3}$$

The boundary conditions are

$$u = v = 0 \quad \text{at } y = 0, \qquad u \to 0 \quad \text{as } y \to \infty. \tag{2.4}$$

Consider the possibility that there shall be a similarity solution of these equations, with $u \propto x^a$, and the jet thickness $\delta \propto x^b$. The two sides of (2.1) will vary with x in the same manner if

$$a + 2b = 1. \tag{2.5}$$

In other boundary layer problems, a second relation between a and b is obtained from the general nature of the flow. Thus for a boundary layer in a stream $U = cx^m$, it is at once clear that $a = m$, and for a free jet, constancy of momentum flux gives the second relation. For a wall jet, there is no help from the boundary conditions, momentum is not conserved, and there is no obvious quantity to consider instead. Indeed $\psi \equiv 0$ satisfies both equations and boundary conditions. This suggests that only for particular values of a and b will non-trivial solutions arise.

For convenience, we introduce non-dimensional variables by writing

$$u = U\bar{u}, \quad v = U\bar{v}, \quad x = \nu\bar{x}/U, \quad y = \nu\bar{y}/U, \quad \psi = \nu^2\bar{\psi}/U, \tag{2.6}$$

where U is a constant velocity. Using (2.5), we write

$$\bar{\psi} = \bar{x}^{2-b} f(\eta),$$

where $$\eta = (2-b)\bar{y}\bar{x}^{-b}.$$

Then $$\bar{u} = (2-b)\bar{x}^{1-2b} f'(\eta),$$

and equation (2.1) becomes

$$f''' + ff'' + \alpha f'^2 = 0, \tag{2.7}$$

where $$\alpha = (2b-1)/(2-b). \tag{2.8}$$

The boundary conditions (2.4) require that

$$f(0) = f'(0) = 0, \qquad f'(\infty) = 0. \tag{2.9}$$

For any α, there are solutions of (2.7) with $f'(\infty) = 0$. We now investigate the possibility that, for such a solution, f and f' shall both be zero at some finite η, so that (2.9) may be satisfied, with a suitably chosen zero of η. Integrating (2.7) between the limits η and ∞, we obtain

$$f'' + ff' - (\alpha - 1)g = 0, \tag{2.10}$$

where $$g(\eta) = \int_\eta^\infty f'^2 \, d\eta.$$

Note that g is certainly positive. Multiplying (2.10) by f' and integrating again, we have

$$\tfrac{1}{2}f'^2 - fg + (\alpha - 2)\int_\eta^\infty f'g\, d\eta = 0. \tag{2.11}$$

If, at the first zero of f' to be encountered as η decreases, f is also zero, then since the integral in (2.11) is certainly positive, this equation requires that $\alpha = 2$. Equations (2.5) and (2.8) now show that

$$a = -\tfrac{3}{2}, \qquad b = \tfrac{5}{4}. \tag{2.12}$$

Unique values have thus been found for the similarity exponents. The only assumption in the argument, that f' is nowhere negative, i.e. that there is no reversed flow, is clearly acceptable on physical grounds.

For a plane wall jet, the equation of continuity $\partial u/\partial x + \partial v/\partial y = 0$ is satisfied by introducing a stream function ψ such that $u = \partial\psi/\partial y$, $v = -\partial\psi/\partial x$. On writing $\bar{\psi} = \psi/\nu = \bar{x}^{1-b}f(\eta)$, where $\eta = (1-b)\bar{x}^{-b}$, we obtain (2.7) precisely as before, where now $\alpha = (2b-1)/(1-b)$. The proof that $\alpha = 2$ is unchanged, and hence, for a plane wall jet,

$$a = -\tfrac{1}{2}, \qquad b = \tfrac{3}{4}. \tag{2.13}$$

The equations being identical, the velocity distributions across the jet are the same in the radial and plane cases.

Before proceeding further, we may note some important implications of (2.10). If f and f'' are to vanish simultaneously, with $f' > 0$, this equation shows that $\alpha = 1$. These are precisely the conditions which hold for a free jet (where $\partial u/\partial y = 0$ on the centre line $y = 0$), and (2.7) with $\alpha = 1$ is indeed the equation for the velocity distribution in a plane free jet, found by Schlichting (1933) and Bickley (1937). The above arguments show that this same velocity distribution applies also to the similar state of a radial free jet, as would occur when a radial wall jet had passed beyond the edge of a finite circular plate. For here, too, the equation must be of the same form as (2.7). The similarity exponents are found from (2.8) to be $a = -1$, $b = 1$. These results for a radial free jet are in agreement with those of Squire (1955). A practical example of a radial free jet occurs, approximately, in the circular grilling burner of a gas cooker. The fact that, for a free jet, (2.10) leads to the same values of the similarity exponents as does a consideration of momentum flux, suggests that it may, after all, be possible to deduce the values for a wall jet by analogous considerations. This is indeed the case, as will be shown in the next section.

3. Exterior momentum flux

Our aim is to deduce an integral relation for a radial laminar wall jet, from the basic equations (2.1) to (2.4). Multiply (2.1) by x and integrate with respect to y between the limits y and ∞, using the condition that $u \to 0$ as $y \to \infty$. By (2.2),

$$\int_y^\infty xv\frac{\partial u}{\partial y}\, dy = -xvu + \int_y^\infty u\frac{\partial(xu)}{\partial x}\, dy.$$

and so we obtain

$$\frac{\partial}{\partial x}\int_y^\infty xu^2\,dy - xvu + vx\frac{\partial u}{\partial y} = 0. \tag{3.1}$$

Multiplying by xu, and integrating with respect to y between the limits 0 and ∞, we then have

$$\frac{\partial}{\partial x}\int_0^\infty xu\left\{\int_y^\infty xu^2\,dy\right\}dy - \int_0^\infty \frac{\partial(xu)}{\partial x}\left\{\int_y^\infty xu^2\,dy\right\}dy - \\ - \int_0^\infty x^2vu^2\,dy + \left[\tfrac{1}{2}vx^2u^2\right]_0^\infty = 0. \tag{3.2}$$

From the continuity equation, the second term of (3.2) is

$$\left[xv\int_y^\infty xu^2\,dy\right]_0^\infty + \int_0^\infty x^2vu^2\,dy.$$

Now at $y = 0$, $u = v = 0$, and so (3.2) reduces to

$$\frac{\partial}{\partial x}\int_0^\infty xu\left\{\int_y^\infty xu^2\,dy\right\}dy = 0,$$

or

$$F = \int_0^\infty xu\left\{\int_y^\infty xu^2\,dy\right\}dy = \text{constant}. \tag{3.3}$$

Physically, this equation may perhaps be interpreted as saying that the flux of exterior momentum flux is constant, but this is hardly a familiar concept. The close similarity between the types of expression in equations (2.11) and (3.2) may be noted. In the case of a similarity solution, (3.3) shows at once that

$$3a + 2b + 2 = 0, \tag{3.4}$$

and, taken together with (2.5), this leads to the values of a and b already given in (2.12). If there is reversed flow, it is possible that F is zero, and in this case the deduction (3.4) cannot be made. So here, as in § 2, there is the mathematical possibility of solutions with reversed flow, for some other values of the similarity exponents.

The arguments leading to the constancy of F are not dependent on the velocity profiles being similar. The similarity solution requires an infinite velocity and zero jet width at $x = 0$, so in an actual wall jet there must be a region where the velocity distribution differs from its final similar state. Equation (3.3) gives valuable information about the state of affairs in this region.

We may note that a rough estimate of the magnitude of F may be deduced from a knowledge of conditions in the impinging free jet, by writing

$$F = \int_0^\infty xu\left\{\int_y^\infty xu^2\,dy\right\}dy = u^*\int_0^\infty xu\left\{\int_y^\infty xu\,dy\right\}dy \\ = \tfrac{1}{2}u^*\int_0^\infty -\frac{\partial}{\partial y}\left\{\int_y^\infty xu\,dy\right\}^2 dy \\ = \tfrac{1}{2}u^*\left\{\int_0^\infty xu\,dy\right\}^2, \tag{3.5}$$

where u^* is a velocity typical of that in the jet. Thus

$$F = \tfrac{1}{2}(\text{typical velocity}) \times (\text{volume flow per radian})^2.$$

Neither the volume flow nor the magnitude of the fluid velocity will alter greatly when the jet is deflected on striking the wall, so that the value of (3.5), estimated from conditions in the impinging jet, provides a measure of F in the wall jet.

For plane flow, the analysis of this section is unchanged, except that the x's are omitted and the final result,

$$F = \int_0^\infty u\left\{\int_y^\infty u^2\,dy\right\}dy = \text{constant}, \tag{3.6}$$

leads to

$$3a+2b = 0, \tag{3.7}$$

again agreeing with the previously obtained result.

If the flow is turbulent, momentum flux arguments still hold for a free jet, but for a wall jet F will remain constant only under certain special assumptions about the nature of the turbulent stresses. These matters will be discussed in later sections.

4. Velocity distribution

The expression for the stream function given in §2, with the value $b = \frac{5}{4}$ found in (2.12), was $\psi = (\nu^5x^3/U)^{1/4}f(\eta)$, where $\eta = \frac{3}{4}(\nu^3/Ux^5)^{1/4}y$, and hence $u = \frac{3}{4}(\nu^3/Ux^3)^{1/2}f'(\eta)$. The equation for f was shown to be

$$f''' + ff'' + 2f'^2 = 0 \tag{4.1}$$

with boundary conditions $f(0) = f'(0) = 0$, $f'(\infty) = 0$.

Multiply the equation by f. The first term may now be integrated by parts, and the remaining two form a perfect differential. Hence

$$ff'' - \tfrac{1}{2}f'^2 + f^2f' = 0, \tag{4.2}$$

since $f'(\infty) = 0$. Multiply by $f^{-3/2}$, and integrate again. Thus

$$f^{-1/2}f' + \tfrac{2}{3}f^{3/2} = \text{constant}. \tag{4.3}$$

Now if $f_0(\eta)$ is a solution of (4.1), so also is $f_1(\eta) = Af_0(A\eta)$, for any constant A, and f_1 satisfies the boundary conditions if f_0 does. But the effect of selecting f_1 instead of f_0 as the solution for substitution into the expressions given above for ψ, η and u is precisely the same as that of changing the value of the arbitrary constant velocity U to U/A^4. Hence, without loss of generality, we may select the solution with $f(\infty) = 1$, and take the constant in (4.3) to have the value $\frac{2}{3}$. Write $f = g^2$; then $f' = 2gg'$, and (4.3) becomes

$$g' = \tfrac{1}{3}(1-g^3), \tag{4.4}$$

which gives on integration

$$\eta = \log\frac{\sqrt{(1+g+g^2)}}{1-g} + \sqrt{3}\tan^{-1}\frac{\sqrt{3}g}{2+g}. \tag{4.5}$$

The values of η, f and f' corresponding to given values of g may now be tabulated. The variations with η of f and f' are illustrated in figure 1. The main properties of the velocity distribution are easily calculated directly. Thus, the shearing stress at the wall is related to $f''(0) = \frac{2}{9}$, and the maximum value of f' is $2^{-5/3} \doteqdot 0{\cdot}315$, occurring at the point at which $f = 2^{-4/3} \doteqdot 0{\cdot}397$.

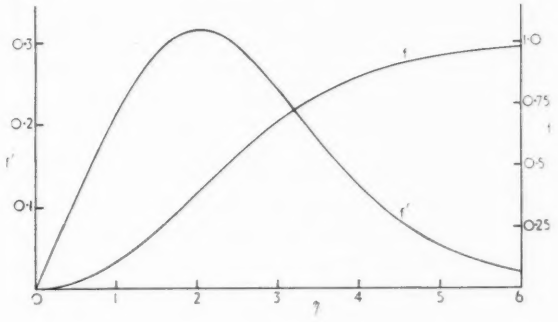

Figure 1. Laminar wall jet. Variation of mass flux (f) and velocity (f') with distance from the wall (η).

The arbitrary velocity U may be eliminated by introducing the quantity F of § 3. It is easily verified that

$$F = \frac{3\nu^4}{4U}\int_0^\infty f'\left\{\int_\eta^\infty f'^2\,d\eta\right\}d\eta = \frac{3\nu^4}{40U}. \tag{4.6}$$

Hence we may write

$$\left.\begin{aligned}\psi &= \left(\frac{40F\nu x^3}{3}\right)^{1/4} f(\eta),\\ u &= \left(\frac{15F}{2\nu x^3}\right)^{1/2} f'(\eta),\\ \eta &= \left(\frac{135F}{32\nu^3 x^5}\right)^{1/4} y.\end{aligned}\right\} \tag{4.7}$$

The skin-friction τ_0 is given by

$$\frac{\tau_0}{\rho} = \nu\left(\frac{\partial u}{\partial y}\right)_{y=0} = \left(\frac{125F^3}{216\nu x^{11}}\right)^{1/4}. \tag{4.8}$$

For a plane wall jet, the expressions corresponding to (4.6), (4.7) and (4.8) are

$$\left.\begin{aligned} F &= \frac{\nu^2 U}{40}, \\ \psi &= (40F\nu x)^{1/4} f(\eta), \\ u &= \left(\frac{5F}{2\nu x}\right)^{1/2} f'(\eta), \\ \eta &= \left(\frac{5F}{32\nu^3 x^3}\right)^{1/4} y, \\ \frac{\tau_0}{\rho} &= \frac{1}{9}\left(\frac{125F^3}{8\nu x^5}\right)^{1/4}. \end{aligned}\right\} \tag{4.9}$$

5. Prandtl's hypothesis

In most practical situations, the wall jet will be turbulent, and we now investigate how the foregoing analysis must be modified to apply in this case. If we introduce the concept of an eddy viscosity ϵ, the boundary layer equation (2.1) becomes

$$u\frac{\partial u}{\partial x} + v\frac{\partial u}{\partial y} = \frac{\partial}{\partial y}\left(\epsilon\frac{\partial u}{\partial y}\right), \tag{5.1}$$

where u and v now denote the components of the mean velocity. The continuity equation (2.2) and the boundary conditions (2.4) are unchanged.

Some assumption must be made about the behaviour of ϵ. The simplest and most convenient one, which has proved satisfactory in describing free turbulent boundary layer flows, is the hypothesis due to Prandtl (1942), that the eddy viscosity is constant across the layer, and is proportional to the product of the maximum mean velocity and the width of the layer. A wall jet would appear to be half-way between a free flow and a wall flow, so it is not unreasonable to adopt Prandtl's hypothesis as a first attempt.

If there is to be a similarity solution of (5.1), with $u \propto x^a$ and $\delta \propto x^b$, we then require that $\epsilon \propto x^{a+b}$, and the two sides of (5.1) will vary with x in the same manner if

$$b = 1. \tag{5.2}$$

In the arguments of §3 relating to exterior momentum flux, ν has to be replaced by ϵ, but since this is a function of x only, the analysis applies unchanged. Once again, F = constant, whether or not there is similarity. For a similarity solution, (3.4) holds as before, showing that

$$a = -\tfrac{4}{3}. \tag{5.3}$$

To study the velocity distribution, introduce the non-dimensional variables (2.6), and let

$$\epsilon = \lambda\bar{x}^{-1/3}\nu, \tag{5.4}$$

where λ is a constant, to be determined later. Then if we write

$$\psi = \bar{x}^{2/3} f(\eta), \qquad \eta = \frac{2\bar{y}}{3\lambda\bar{x}} = \frac{2y}{3\lambda x}, \tag{5.5}$$

(5.1) shows that f satisfies $f'''+ff''+2f'^2=0$, with boundary conditions $f(0)=f'(0)=0, f'(\infty)=0$, precisely as for the laminar case. The solution of § 4 is still applicable, and thus, on Prandtl's hypothesis, the velocity profile is identical in the laminar and turbulent cases. This result follows at once from the integral arguments of § 2, as soon as it is established that the equation is of the same basic type in the two cases, and it applies equally well to a plane turbulent wall jet.

For a plane free jet, it was shown by Görtler (1942) that, on the basis of Prandtl's hypothesis, the velocity profile of a turbulent jet is the same as that of a laminar one. This again is an immediate deduction from the arguments of § 2. Further, a radial free jet, as described in § 2, would also have this same velocity profile in either laminar or turbulent flow. For all these jets, the use of Prandtl's hypothesis is well justified.

It would indeed be satisfactory if this simple approach sufficed to describe a turbulent wall jet. However, it is found by experiment (Bakke 1956) that the velocity gradient near the wall is much greater than in the velocity distribution of figure 1. Consequently, we shall not proceed to set out further details of the solution based on Prandtl's hypothesis. We merely note that, in this method, the only undetermined quantity is the constant λ introduced in (5.4), and this would be chosen to give the best agreement with experiment, as in other problems where Prandtl's hypothesis is used.

6. Effect of the wall

Once it is conceded that there is large velocity gradient near the wall, the idea of a free turbulent flow is seen to be an inadequate one. It becomes clear that the friction at the wall is a decisive agency, and must be given a prominent place in any theory. We shall retain the concept of an eddy viscosity, but shall require it to vary in a suitable manner across the breadth of the wall jet.

We may make use of the empirical formula due to Blasius (1913), based on a study of turbulent pipe flow, in the form

$$\tau_0 = 0{\cdot}0225\rho U^2\left(\frac{\nu}{Ua}\right)^{1/4}, \tag{6.1}$$

where U is the maximum velocity and a the radius of the pipe. The formula is often written with the mean velocity and the pipe diameter in place of U and a; this merely involves a modification of the numerical coefficient. Since τ_0 is governed by conditions near the wall, it has been argued that U and a in (6.1) may be replaced by u and y, so that the equation becomes

$$\tau_0 = 0{\cdot}0225\rho u^2\left(\frac{\nu}{uy}\right)^{1/4}. \tag{6.2}$$

This may be expected to hold near the wall in any turbulent boundary layer flow, outside the viscous sublayer. A discussion of equation (6.2), first discovered by Prandtl, is given by Schlichting (1955, p. 404). He shows

that the formula is adequate at Reynolds numbers up to 10^5. This power law expression is easier to apply in our present theory than is the logarithmic relation which is theoretically more acceptable, and its accuracy should be quite adequate for our purposes. At higher Reynolds numbers a formula similar to (6.2), with a suitably modified exponent, might be used.

Equation (6.2) implies that, near the wall, $u \propto y^{1/7}$. The shearing stress $\tau = \epsilon\, \partial u/\partial y$ has a finite non-zero value at the wall and hence, for fixed x,

$$\epsilon \propto y^{6/7} \propto u^6. \tag{6.3}$$

The assumption we shall now make is that ϵ is proportional to u^6, in accordance with (6.3). At first we shall assume that this relation holds throughout the whole width of the jet, though later we shall apply it only in a limited region near the wall. Thus, we choose

$$\epsilon = m(x)u^6, \tag{6.4}$$

where m is as yet unspecified. The main reason for choosing ϵ to be a function of u rather than of y, is that in consequence η does not appear explicitly in the equations, but the behaviour is also satisfactory in that ϵ will not continue to rise beyond the velocity maximum. An additional and rather amusing point is that the exterior momentum flux arguments of § 3 still apply in this case. The last term of equation (3.1) becomes $mxu^6\,\partial u/\partial y$, and hence the last term of (3.2) is replaced by $\frac{1}{8}mx^2u^8$, which vanishes at the wall and at the outer edge of the jet. Consequently equations (3.3) and (3.4) remain true. However, it is not really plausible to consider that this form for ϵ is applicable in the outer parts of the jet, where the velocity is falling to zero again.

Consider the conditions for a similarity solution of the boundary layer equation (5.1), in which $u \propto x^a$, $\delta \propto x^b$. Blasius's formula (6.2) requires that $\tau_0 \propto u^{7/4}\delta^{-1/4}$, and hence

$$\epsilon \propto u^{3/4}\delta^{3/4} \propto x^{3(a+b)/4}. \tag{6.5}$$

The two sides of (5.1) will depend on x in the same manner if

$$a + 5b = 4. \tag{6.6}$$

Introduce the non-dimensional variables (2.6) and, in accordance with the above results, let

$$\bar{\psi} = \bar{x}^{5-4b}f(\eta), \qquad \eta = \frac{5-4b}{\lambda}\bar{y}\bar{x}^{-b}, \tag{6.7}$$

and

$$\epsilon = A\lambda\bar{x}^{3-3b}f'^6\nu, \tag{6.8}$$

where λ and A are constants. The reasons for the introduction of the second constant will appear in the next section. Equation (5.1) then gives

$$\frac{d}{d\eta}(Af'^6f'') + ff'' + \alpha f'^2 = 0, \tag{6.9}$$

where

$$\alpha = (5b-4)/(5-4b). \tag{6.10}$$

The boundary conditions are $f' \propto \eta^{1/7}$ as $\eta \to 0$, $f'(\eta_\infty) = 0$, where η_∞ is the value of η at the outer edge of the jet. As a result of the peculiar choice of ϵ, η_∞ is finite, as will be seen later. From (6.5) and (6.10), we have

$$a = -\frac{9\alpha}{5+4\alpha}, \qquad b = \frac{4+5\alpha}{5+4\alpha}. \tag{6.11}$$

The integral arguments of §2 may be applied as before to show that $\alpha = 2$, a result which also follows from the considerations of exterior momentum flux given above. With this value, (6.11) shows that

$$a = -1{\cdot}38, \qquad b = 1{\cdot}08, \tag{6.12}$$

and equation (6.9) may be integrated directly. By a suitable choice of λ, we may take $A = 1$, and the equation then becomes

$$\frac{d}{d\eta}(f'^6 f'') + ff'' + 2f'^2 = 0. \tag{6.13}$$

Multiplying by f and integrating, we obtain

$$ff'^6 f'' - \tfrac{1}{8}f'^8 + f^2 f' = 0, \tag{6.14}$$

the constant being zero in view of the required behaviour of f near $\eta = 0$. Multiply (6.14) by $7f^{-15/8}$, and integrate again,

$$f^{-7/8}f'^7 + \tfrac{56}{9}f^{9/8} = \text{constant}. \tag{6.15}$$

Choose the constant so that $f = 1$ when $f' = 0$. Solutions for other values of the constant are then expressible as $X^7 f(X^{-5}\eta)$, for some constant X. We then have

$$\tfrac{9}{56}f'^7 = f^{7/8} - f^2. \tag{6.16}$$

It is convenient to write $g(\xi) = f^{7/8}$, where $\xi = \frac{7}{8}(\frac{56}{9})^{1/7}\eta$. Equation (6.15) then shows that

$$g'^7 = 1 - g^{9/7},$$

and hence

$$\xi = \int_0^g \frac{dg}{(1-g^{9/7})^{1/7}}. \tag{6.17}$$

This integral was computed numerically, and at each stage the corresponding values for f, f' and η were calculated. The value of ξ at the edge of the jet, $g = 1$, is expressible as a beta function, and thus a useful check was made on the accuracy of the work. The variations with η of f and f' are illustrated in figure 2. The solution is satisfactory up to the velocity maximum, but the rapid fall of velocity in the outer region, a consequence of the assumption $\epsilon \propto u^6$, is quite unacceptable. A more realistic assumption is that ϵ is constant in the outer part of the jet, in accordance with Prandtl's hypothesis. We now consider how this may be achieved.

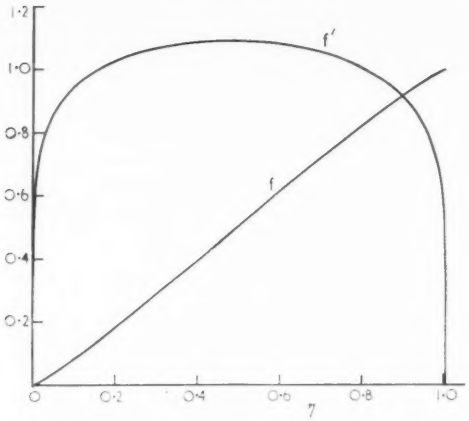

Figure 2. Turbulent wall jet, eddy viscosity proportional to u^6. Variation of mass flux (f) and velocity (f') with distance from the wall (η).

7. Matching of solutions

The first thing to realize is that, if the inner part of the wall jet is to be governed by Blasius's formula, and the outer part by Prandtl's hypothesis, complete similarity is no longer possible. For, as functions of x, $\epsilon \propto R^{3/4}$ in the inner layer, as shown in (6.5), and $\epsilon \propto R$ in the outer layer, where $R = u\delta/\nu$ is the Reynolds number. With increasing x, u decreases rather faster than δ increases, and hence R decreases slowly. Consequently the velocity profile must change gradually as the jet develops, the inner layer occupying a progressively larger part of the jet width. This is not dependent on the precise forms selected for the eddy viscosity in the parts of the jet near and far from the wall. Any method which relates the inner part to the presence of the wall, and the outer part to free turbulent flow, will give the same conclusion.

However, the ratio of the eddy viscosities in the outer and inner parts of the layer varies only as the fourth root of the slowly changing Reynolds number, and we shall ignore this relative variation in seeking to derive a solution. A process of matching inner and outer solutions will then enable us to estimate the Reynolds number to which a particular matched profile is appropriate. It is hoped by this means to predict the main features of an actual turbulent wall jet. The assumptions in regard to the eddy viscosity, on which the whole method depends, are themselves of such dubious validity that it is hardly justifiable to try to develop any more precise procedure at this stage.

We now consider the equations for the inner and outer parts of the jet. For the inner layer, equations (6.5) to (6.11) continue to apply unchanged. In the outer layer we retain the same variables, but, in place of (6.8), we write

$$\epsilon = \lambda \bar{x}^{a-3b}\nu, \tag{7.1}$$

which is proportional to $R^{3/4}$, instead of being proportional to R as indicated by Prandtl's hypothesis. This is the price that must be paid if we are still to have a solution in terms of the similarity variables. The equations are

$$\frac{d}{d\eta}(Af_1'^6 f'') + f_1 f_1'' + \alpha f_1'^2 = 0, \tag{7.2}$$

$$f_0''' + f_0 f_0'' + \alpha f_0'^2 = 0, \tag{7.3}$$

where the suffixes denote the inner and outer layers respectively. The values of a and b, the similarity exponents, are given as functions of α by (6.11). As boundary conditions, we have $f_1'\eta^{-1/7} \to$ constant as $\eta \to 0$, and $f_0'(\infty) = 0$. Clearly certain further conditions must hold at the junction of the inner and outer layers. The value $\alpha = 2$ was determined in previous cases by exterior momentum flux arguments. These are no longer helpful, so α remains arbitrary. Indeed it is the variation of α along the jet length which represents the gradual change of jet profile, as different values of α will be appropriate at different Reynolds numbers.

Details of the calculations involved in the integration of (7.2) and (7.3), for general values of α, are deferred to the next section. For the present, we merely assert that such solutions are available. In (7.2) it is convenient to write

$$f_2(\eta) = A^{1/5} f_1(\eta), \tag{7.4}$$

so that the equation becomes

$$\frac{d}{d\eta}(f_2'^6 f_2'') + f_2 f_2'' + \alpha f_2'^2 = 0. \tag{7.5}$$

Now if one solution of (7.5), with the correct behaviour near $\eta = 0$, has been found as $f_2(\eta)$, then, as in § 6, the general solution can be written as $X^7 f_2(X^{-5}\eta)$, for some constant X. The corresponding solution of (7.2) is

$$f_1(\eta) = A^{-1/5} X^7 f_2(X^{-5}\eta). \tag{7.6}$$

The conditions to be satisfied at the junction between the inner and outer layers will now be considered. Suppose that the join is to be at the velocity maximum, and here ψ and u are to be continuous. Thus at the velocity maximum $\eta = \eta_m$,

$$f_0'' = f_1'' = f_2'' = 0, \qquad f_0 = f_1 = A^{-1/5} X^7 f_2, \qquad f_0' = f_1' = A^{-1/5} X^2 f_2'. \tag{7.7}$$

Since the solutions f_0 and f_2 are known, the values of A and X can be found at once. The eddy viscosity is discontinuous at $\eta = \eta_m$, which is an apparent drawback. However, the shearing stress is continuous, being zero on each side of the join.

The eddy viscosity in the outer layer may now be determined as follows. Blasius's formula (6.2) shows that, near the wall,

$$\frac{\tau}{\rho} = \epsilon \frac{\partial u}{\partial y} = 0{\cdot}0225 u^2 \left(\frac{\nu}{uy}\right)^{1/4}. \tag{7.8}$$

With the expressions of § 6, this takes the form

$$A\lambda f_1'^4 f_1''(\eta f_1')^{1/4} = 0{\cdot}0225 \tag{7.9}$$

for small η. If $f_1' \eta^{-1/7} \to D$ as $\eta \to 0$, (7.9) gives

$$A\lambda D^{21/4} = 0{\cdot}1575, \tag{7.10}$$

and if $f_2' \eta^{-1/7} \to E$ as $\eta \to 0$, (7.6) shows that $D = A^{-1/5} X^{9/7} E$, and hence (7.10) becomes

$$\lambda = 0{\cdot}1575 A^{1/20} X^{-27/4} E^{-21/4}$$

$$= 0{\cdot}1575 E^{-21/4} \left(\frac{f_{2m}}{f_{0m}}\right)^{5/4} \frac{f_{0m}'}{f_{2m}'}, \tag{7.11}$$

from (7.6), where the suffix m denotes the value at the velocity maximum. All the terms of the right-hand side of (7.11) are supposed known, for any α, and thus λ is determined. Now, according to Prandtl's hypothesis, in the outer layer,

$$\epsilon = \kappa u_m \delta_t, \tag{7.12}$$

where u_m is the maximum velocity, δ_t a typical measure of the jet width, and κ a universal constant; i.e. one which should not depend on α. The jet Reynolds number may be defined, more precisely than previously, as $R = u_m \delta_t / \nu$, and it now follows from (6.7) and (7.1) that

$$\lambda = \kappa (\eta_t f_{0m}')^{3/4} R^{1/4}, \tag{7.13}$$

where η_t is the value of η corresponding to δ_t. Hence, from (7.11),

$$\kappa R^{1/4} = 0{\cdot}1575 E^{-21/4} \left(\frac{f_{2m}}{f_{0m}}\right)^{5/4} \frac{f_{0m}'}{f_{2m}'} (\eta_t f_{0m}')^{-3/4}. \tag{7.14}$$

8. Integrations and results

The integration of equations (7.3) and (7.5), for general values of α, will now be considered. As in § 4, we may choose the solution of (7.3) for which $f_0(\infty) = 1$. A series expansion, valid for large values of η, is readily obtained in the form

$$f_0(\eta) = 1 - e^{-\eta} + \tfrac{1}{4}(1+\alpha)e^{-2\eta} - \tfrac{1}{72}(1+\alpha)(5+4\alpha)e^{-3\eta} +$$
$$+ \tfrac{1}{1728}(1+\alpha)(34+53\alpha+21\alpha^2)e^{-4\eta} - \ldots, \tag{8.1}$$

where the coefficient of $e^{-\eta}$ has been arbitrarily taken as unity. This is equivalent to making a suitable choice of the zero of η. From the series, f_0 and its derivatives were calculated at a suitable set of values of η, and the solution of (7.3) was then extended to smaller values of η by numerical integration, until the zero of f_0'' was passed. The values of f_{0m}, f_{0m}' and η_t were then estimated, η_t being chosen as the interval between the point at which $f_0' = f_{0m}'$ and the point at which $f_0' = \frac{1}{2} f_{0m}'$. This procedure was carried out for $\alpha = 1{\cdot}1$, $1{\cdot}2$, $1{\cdot}4$, $1{\cdot}6$ and $1{\cdot}8$. The solution for $\alpha = 2$ was found in § 4, and, for $\alpha = 1$, equation (7.3) is that corresponding to a plane free jet, with solution $f_0 = \tanh \frac{1}{2}\eta$. The values of f_{0m}, f_{0m}' and η_t thus determined are shown in figure 3, and lie on smooth curves, considered

as functions of α. From this figure, the values corresponding to any required α in the range can be read off immediately, to sufficient accuracy.

A point which emerges from the integrations, is the great insensitivity to the value of α of the velocity profile in the region beyond the velocity maximum. In figure 4, where f_0'/f_{0m}' is plotted as a function of $(\eta-\eta_m)/\eta_t$,

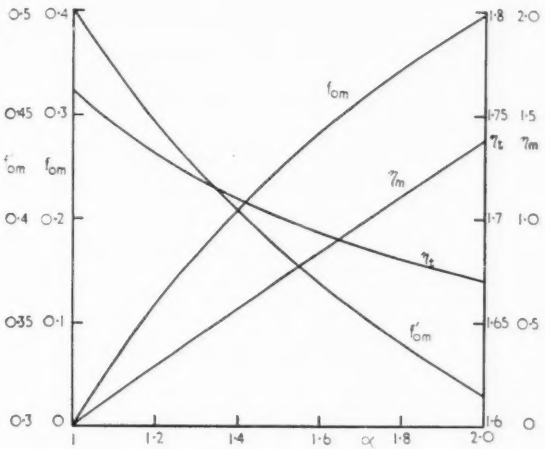

Figure 3. Results for a turbulent wall jet. Values of mass flux (f_{0m}) and velocity (f'_{0m}) at the velocity maximum. Also thickness of the inner layer (η_m) and outer layer (η_t).

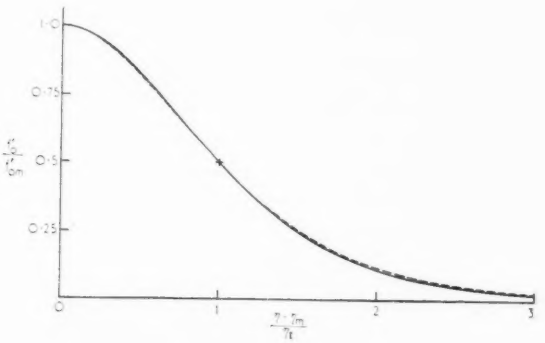

Figure 4. Comparison of velocity profiles. ——— $\alpha = 1$, – – – – $\alpha = 2$.

the curves for the extreme values $\alpha = 1$ and $\alpha = 2$ are seen to be so close to each other that no experiment could be expected to differentiate between them. Thus the outer part of the velocity profile of a laminar wall jet is virtually the same as that of a plane free jet.

For the inner part of the wall jet, we wish to determine the solution of (7.5) for which $f_2' \eta^{-1/7} \to$ constant as $\eta \to 0$. This implies that $f_2 f_2''/f_2'^2 \to \frac{1}{8}$ as $\eta \to 0$. Also, at the velocity maximum, which is the farthest point to which the solution need be carried, $f_2'' = 0$. Thus the second term of (7.5) is relatively unimportant compared with the third, throughout the range of integration. This suggests that a satisfactory approximation might be obtained by replacing the term $f_2 f_2''$ in (7.5) by $\theta f_2'^2$, where θ is a small positive constant, not depending on α. The equation then becomes

$$\frac{d}{d\eta}(f_2'^6 f_2'') + (\alpha + \theta) f_2'^2 = 0. \tag{8.2}$$

On writing
$$f_3(\eta) = B f_2(\eta), \qquad B^5 = (2+\theta)/(\alpha+\theta), \tag{8.3}$$

(8.2) becomes
$$\frac{d}{d\eta}(f_3'^6 f_3'') + (2+\theta) f_3'^2 = 0, \tag{8.4}$$

in which α does not appear. The reason for the particular choice of the substitution (8.3) is that, by reversing the arguments given above, equation (8.4) may be replaced by (7.5) with $\alpha = 2$. This is equation (6.13), of which the solution was found in § 6. Denoting this known solution by $f_3(\eta)$, we obtain the required solution of (7.5) from (8.3), once the value of θ has been chosen.

The accuracy of this approach can be judged by a consideration of the extreme case $\alpha = 1$. Equation (7.5) can in this case be integrated twice immediately, to give

$$\tfrac{1}{7} f_2'^7 + \tfrac{1}{2} f_2^2 = C\eta, \tag{8.5}$$

where C is a constant. As previously, C may be chosen arbitrarily, and the solution of (8.5) for a general value of C is then expressible as $Y^7 f_2(Y^{-5}\eta)$ for some constant Y. With $C = \frac{1}{7}$, equation (8.5) was integrated by a method of successive approximations. The following results were obtained.

$$\left.\begin{aligned} &\text{As} && \eta \to 0, && f_2' \eta^{-1/7} \to 1. \\ &\text{When} && f_3'' = 0, && f_2 = 0{\cdot}188, && f_2' = 0{\cdot}759, && \eta = 0{\cdot}269. \end{aligned}\right\} \tag{8.6}$$

These exact values may be compared with those we should deduce on the basis of the approximation developed above, using the relation $f_3(\eta) = BY^7 f_2(Y^{-5}\eta)$, and the following properties of $f_3(\eta)$ which were found in the integrations of § 6.

$$\left.\begin{aligned} &\text{As} && \eta \to 0, && f_3' \eta^{-1/7} \to 1{\cdot}322. \\ &\text{When} && f_3'' = 0, && f_3 = 0{\cdot}479, && f_3' = 1{\cdot}091, && \eta = 0{\cdot}478. \end{aligned}\right\} \tag{8.7}$$

With a suitable choice of the two constants B and Y, (8.7) should give values similar to those of (8.6) for the four quantities concerned. The value of η agrees if $Y = 1{\cdot}121$, and the values of B then required to give agreement of f_2, f_2' and $\lim_{\eta \to 0}(f_2' \eta^{-1/7})$ are 1·140, 1·142 and 1·140 respectively. This is a remarkable justification of the ideas we have used. Equation (8.3) now shows that $\theta = 0{\cdot}07$, a very acceptable value in view of the arguments leading to (8.2).

Thus for the inner layer, as for the outer, the form of the velocity distribution is effectively independent of α. However, the velocity distribution for the whole wall jet does vary with α, due to changes in the relative scaling factors in the two parts. The gradient near the wall becomes steeper as α decreases. A typical velocity profile, that corresponding to $\alpha = 1{\cdot}4$, is shown in figure 5. The width of the inner layer

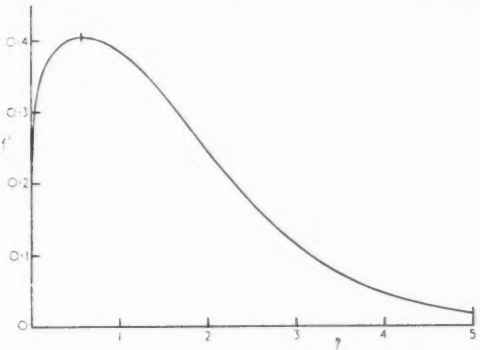

Figure 5. Velocity profile for a turbulent wall jet, $\alpha = 1{\cdot}4$.

is proportional to $\eta_m = 1{\cdot}09 f_{0m}/f'_{0m}$ and that of the outer layer to η_t, and so the velocity profiles corresponding to other values of α may readily be deduced from the curves of figure 3, where both η_m and η_t are given.

The results for the inner layer, obtained above, may now be inserted in (7.14) to give

$$\kappa R^{1\cdot4} = \frac{0{\cdot}0275}{\alpha + 0{\cdot}07} (f_{0m})^{-5\cdot4} (f'_{0m})^{1\cdot4} \eta_t^{-3\cdot4}, \tag{8.8}$$

and on substituting the values for the outer layer, from figure 3, we obtain the results shown in table 1.

α	$\kappa R^{1\cdot4}$	R ($\kappa = 0{\cdot}012$)	a	b
1·1	0·415	$1{\cdot}4 \times 10^6$	−1·050	1·005
1·2	0·170	$4{\cdot}1 \times 10^4$	−1·096	1·010
1·3	0·102	5200	−1·139	1·015
1·4	0·0707	1200	−1·178	1·019
1·5	0·0530	380	−1·214	1·023
1·6	0·0417	150	−1·247	1·026
1·8	0·0287	33	−1·307	1·033
2·0	0·0215	10	−1·359	1·038

Table 1

The value of the constant κ has to be determined empirically. Preliminary experiments (Bakke 1956), at a Reynolds number in the

neighbourhood of 5000, recorded a velocity profile in good agreement with that predicted for $\alpha = 1{\cdot}3$. This indicates that $\kappa = 0{\cdot}012$ is an appropriate choice, and the corresponding values of R are also shown in table 1. It may be noted that this value of κ is approximately one-half of that found to be appropriate for a circular jet, and one-third of that for a plane free jet. More accurate experiments might indicate a modified value to be preferable. The extreme insensitivity of α to the value of the Reynolds number powerfully supports the assumption of approximate similarity, on which our whole theory has been based.

Summing up, table 1 represents our main conclusions in regard to the behaviour of a turbulent wall jet, and it may be hoped that these would not prove unduly sensitive to changes in our assumptions as to the nature of the turbulent shearing stress. The predicted velocity distribution is given by figure 5, with suitable scaling of the inner and outer layers as discussed above. The similarity exponents, specifying the ratio of change of the maximum velocity and the jet width, are given as functions of α by equation (6.11); a few comments on the accuracy of this equation are made in the next and final section.

9. Values of similarity exponents

The one purely arbitrary feature of the matching procedure developed in § 7, was the decision to link the coordinate system to the inner layer, and to ignore variations in the outer layer. An equally valid alternative would be to choose coordinates appropriate for the outer layer, and to assume the skin-friction to have the value required by Blasius's formula at the particular Reynolds number. The whole analysis would go through as before, and identical velocity profiles would be deduced. In place of (6.11) we should have, as in § 5,

$$a = -\frac{2\alpha}{1+\alpha}, \qquad b = 1, \tag{9.1}$$

as is easily verified. Thus if $\alpha = 1{\cdot}3$, (6.11) gives

$$a = -1{\cdot}15, \qquad b = 1{\cdot}03, \tag{9.2}$$

while (9.1) gives

$$a = -1{\cdot}13, \qquad b = 1. \tag{9.3}$$

Although the difference between (9.2) and (9.3) is not great, it would be satisfying to see how it arises.

For $\alpha = 1{\cdot}3$, equation (9.2) shows that $R \propto x^{-0{\cdot}12}$. If R changes from that corresponding to $\alpha = 1{\cdot}3$ at $x = x_A$, to that corresponding to $\alpha = 1{\cdot}4$ at $x = x_B$, then approximately, from table 1,

$$\frac{x_B}{x_A} = \left(\frac{5200}{1200}\right)^{1{\cdot}0{\cdot}12} \doteqdot 200\,000. \tag{9.4}$$

Incidentally, this figure strikingly illustrates the slowness of the change in velocity profile. Consider a wall jet which has developed from x_A to x_B. On the theory of § 7, its profile at x_B is still that appropriate to $\alpha = 1{\cdot}3$. However, in fact the profile should be that corresponding to $\alpha = 1{\cdot}4$, with

the scales of f and η suitably adjusted. If the maximum velocity and width of the outer layer are $u_{1\cdot3}$ and $\delta_{1\cdot3}$ for $\alpha = 1\cdot3$, and $u_{1\cdot4}$ and $\delta_{1\cdot4}$ for $\alpha = 1\cdot4$, then if the adjustment is made so that the mass flux, and also the velocity gradient in the inner layer (for which the solution is known to be accurate), are unchanged, a rough calculation shows that, approximately,

$$\left.\begin{aligned} u_{1\cdot4}/u_{1\cdot3} &= 1\cdot12 \div (200\,000)^{0\cdot01}, \\ \delta_{1\cdot4}/\delta_{1\cdot3} &= 0\cdot84 \div (200\,000)^{-0\cdot015}. \end{aligned}\right\} \tag{9.5}$$

Adding these contributions from the changing profile to the values of (9.2), we have as revised estimates of the similarity exponents

$$a = -1\cdot14, \qquad b = 1\cdot015. \tag{9.6}$$

The fact that these figures are precisely intermediate between (9.2) and (9.3) must be considered entirely fortuitous, in view of the roughness of the calculations, but the order of magnitude of the differences arising from the alternative choice of coordinates is satisfactorily explained. Physically, we may argue from (7.1), that, with α constant, the velocity gradient in the outer layer becomes progressively too small as x increases, and hence an adjustment qualitatively similar to (9.5) is required. For the alternative approach, leading to (9.1), the velocity gradient in the inner layer becomes progressively too steep as x increases, and so necessitates an adjustment in the opposite direction.

The discrepancies between (6.11) and (9.1) are probably no larger than other errors inherent in the whole method of analysis, but in practice the mean of the two might well be adopted as the best prediction of our theory. These mean values are also given in table 1.

For a plane turbulent wall jet, the analysis of the last sections all applies unchanged, with appropriately modified values of the similarity exponents. Equation (6.11) is replaced by

$$a = -\frac{4\alpha}{5+4\alpha}, \qquad b = \frac{4+4\alpha}{5+4\alpha}, \tag{9.7}$$

and (9.1) is replaced by

$$a = -\frac{\alpha}{1+\alpha}, \qquad b = 1. \tag{9.8}$$

The value of the constant κ must be determined afresh, as there is no reason to suppose that it still has the same value as that for a radial wall jet.

References

Bakke, P. 1956 Private communication.

Bickley, W. 1937 *Phil. Mag.* (7) **23,** 727.

Blasius, H. 1913 *Forschungsarbeiten des Ver. deutsch Ing.* no. 131.

Görtler, H. 1942 *Z. angew. Math. Mech.* **22,** 244.

Prandtl, L. 1942 *Z. angew. Math. Mech.* **22,** 241.

Schlichting, H. 1933 *Z. angew Math. Mech.* **13,** 260.

Schlichting, H. 1955 *Boundary Layer Theory.* London : Pergamon Press.

Squire, H. B. 1955 50 *Jahre Grenzschichtforschung*, edited by H. Görtler & W. Tollmien, p. 47. Braunschweig : Vieweg.

The flow of conducting fluids in circular pipes under transverse magnetic fields

By J. A. SHERCLIFF
Department of Engineering, University of Cambridge

(*Received* 19 *September* 1956)

SUMMARY

The flow rate of liquid metals is commonly measured by electromagnetic flowmeters. In these the fluid moves through a region of transverse magnetic field, inducing a potential difference between two electrodes on the walls of the pipe. The ratio of signal to flow rate is dependent on the velocity profile, and this is affected by electromagnetic forces.

In this paper the ultimate steady velocity profile and its associated pressure gradient and induced potential are calculated for the case of laminar flow in a circular pipe whose walls are conducting but without contact resistance. Laminar flow is encouraged by a transverse field. When the fluid conductivity and field strength are sufficiently high, boundary layers occur with a thickness inversely proportional to normal field intensity. The induced potential difference is then 0·926 of the value corresponding to the case of uniform velocity if the walls are non-conducting.

The distance the fluid must travel after entering the transverse field before the steady state is reached is next estimated by a Rayleigh approximation. The inlet velocity is taken to be uniform and effects which occur at the edge of the field are neglected. The process falls into two stages, first a boundary-layer growth and then an adjustment of the velocity away from the walls, occupying a much greater length of pipe. The entry length is shorter than it is in the case of flow in a rectangular pipe, but is still too long for appreciable distortion of the velocity profile to occur within practical flowmeters except at low flow rates. The pressure drop associated with the adjustment of the velocity profile is found to be independent of field strength, if this is high, and about one-eighth of the drop which occurs in the non-conducting case.

Experiments are described in which steady-state pressure gradients and induced potential differences were measured in mercury flowing along Perspex pipes of 0·5 and 0·25 in. bore in transverse fields up to 14 500 gauss. The results confirmed the steady-state theory within the limitations of experimental

accuracy and the assumption in the theory of high conductivity and an intense field. The experiments also covered the entry region in many cases, and showed that the theoretical entry lengths were correct in order of magnitude but over-estimated. However, the exact entry condition was uncertain, and steady readings were difficult to obtain in the entry region.

1. Introduction

The rate of flow of a liquid may be measured by passing it along a pipe under a transverse magnetic field. The potential difference induced between two electrodes situated at the ends of a diameter of the pipe perpendicular to the flow and to the field may then be used to indicate the flow rate.

The ratio of the induced potential difference to the flow rate is affected by several factors, including the conductivity of the pipe walls and the form of the velocity profile. If the pipe is circular, the induced potential difference for a given flow rate is insensitive to the form of the velocity profile, provided the velocity is dependent only on distance from the axis of the pipe (Kolin 1945). This is usually the case for laminar or turbulent flow in the absence of upstream disturbances. If the profile departs from radial symmetry, the ratio of potential difference to flow rate can vary very widely (Shercliff 1954, 1955).

If the liquid is a good conductor and the magnetic field is sufficiently strong, the velocity profile can be appreciably distorted by electromagnetic forces (Hartmann 1937, Shercliff 1953), and the induced potential seriously affected. This can occur when electromagnetic flowmeters are used with mercury or liquid sodium.

The full distortion of an entry profile by a transverse field takes place over an entry length, which may be large or small in comparison with the distance the fluid traverses between the onset of the transverse field and the electrodes. The transverse field cannot have an abrupt edge, but nevertheless may change rapidly from negligible proportions to a high uniform intensity.

This paper examines theoretically the steady state of laminar flow in a circular pipe under a transverse field and, by means of a Rayleigh approximation, the entry length necessary to achieve it. Experiments are described which support the theoretical conclusions.

There is considerable interest in laminar flow since it persists at high Reynolds numbers in the presence of a transverse field (Murgatroyd 1953, Lock 1955). The experiments described include cases of laminar and turbulent flow.

In addition to the effect of a uniform transverse field on the velocity profile, there is another distorting effect due to secondary currents where the fluid enters the region of transverse field. This effect is ignored in the present analysis.

2. Governing equations

As figure 1 shows, we select Cartesian axes (x, y, z) such that the z-axis lies along the axis of the pipe, and the x-axis is parallel to the imposed uniform field H_0 existing outside the pipe.

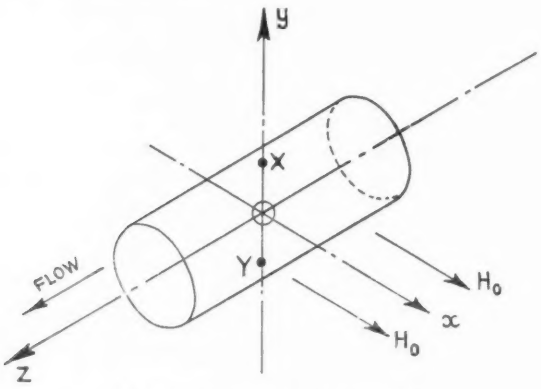

Figure 1. Axes and electrodes.

Various authors (e.g. Bullard 1955) have derived the basic equations for the motion of conducting fluids, pointing out that the displacement current and the convection of charges are negligible. In electromagnetic units Maxwell's equations therefore become

$$\operatorname{curl} \mathbf{E} = -\mu \partial \mathbf{H}/\partial t \tag{1}$$

and

$$\operatorname{curl} \mathbf{H} = 4\pi \mathbf{j}, \tag{2}$$

in which **E**, **H** and **j** are the electric field, magnetic field and current density vectors respectively, and μ is the permeability of the fluid. Ohm's law requires that

$$\mathbf{j} = \sigma(\mathbf{E} + \mu \mathbf{v} \times \mathbf{H}), \tag{3}$$

in which **v** is the fluid velocity and σ is the fluid conductivity. The dynamical equation is

$$\mu \mathbf{j} \times \mathbf{H} + \eta \nabla^2 \mathbf{v} - \operatorname{grad} p = \rho\{\partial \mathbf{v}/\partial t + (\mathbf{v} . \operatorname{grad}) \mathbf{v}\}, \tag{4}$$

in which p, ρ and η are the fluid pressure, density and viscosity respectively. We assume that ρ is constant, and μ is unity in both the fluid and the pipe walls. Consequently

$$\operatorname{div} \mathbf{v} = 0, \quad \text{and} \quad \operatorname{div} \mathbf{H} = 0. \tag{5}$$

For the motion of fluid in a straight pipe under a uniform transverse field, where conditions may vary in time but not in the z-direction (apart from the pressure gradient), the equations become linear in the unknown quantities. Differentiation of (4) with respect to z shows that grad$(\partial p/\partial z)$ vanishes, and hence that $\partial p/\partial z$ is a function of time only. It is compatible with the above equations, and with the boundary conditions, for v_x, v_y

and H_y to vanish and H_x to have the constant value H_0. Equations (1) to (5) then reduce to two equations in the unknown components H_z and v_z:

$$\nabla^2 H_z + 4\pi\mu\sigma H_0 \partial v_z/\partial x = 4\pi\mu\sigma \partial H_z/\partial t \tag{6}$$

and

$$\eta\nabla^2 v_z + (\mu H_0/4\pi)\partial H_z/\partial x = \partial p/\partial z + \rho \partial v_z/\partial t. \tag{7}$$

The Laplacian operators comprise two derivatives only.

The estimation of the entry length for velocity-profile distortion to occur after entry into a transverse field is a non-linear problem, as it stands. There is, however, an obvious analogy with the above linear case, in which there is variation with time instead of with z. We should therefore expect results of the right order if we calculate settling times in the linear problem, and convert these to entry lengths by multiplying by v_0, the mean velocity of flow in the pipe, which is necessarily constant. The variables z and t will be measured from the onset of the transverse field.

The equations (6) and (7) can be expressed non-dimensionally by means of the substitutions

$$v = v_z/v_0, \qquad h = H_z/4\pi v_0(\sigma\eta)^{1/2}, \qquad P = -(a^2/\eta v_0)\partial p/\partial z,$$
$$X = x/a, \qquad Y = y/a, \qquad T = \eta t/\rho a^2,$$
$$M = \mu H_0 a(\sigma/\eta)^{1/2}, \quad \text{and} \quad \beta = 4\pi\mu\sigma\eta/\rho,$$

where a is the internal radius of the pipe. We then have

$$\Delta h + M\partial v/\partial X = \beta\dot{h} \tag{8}$$

and

$$\Delta v + M\partial h/\partial X + P = \dot{v}, \tag{9}$$

in which $\Delta = \partial^2/\partial X^2 + \partial^2/\partial Y^2$, and a dot denotes differentiation with respect to T.

The dimensionless fluid property β is of the order of 10^{-6} for liquid metals. We shall therefore neglect the β-term in (8). This may be shown to be justified except at unusually large values of M, which is of the order of 10^2 in practical flowmeters. The role of h is now limited to that of a current stream-function, since

$$j_y = -v_0(\sigma\eta)^{1/2}\partial h/\partial x, \quad \text{and} \quad j_x = v_0(\sigma\eta)^{1/2}\partial h/\partial y. \tag{10}$$

In view of the interest in flowmeters, it is necessary to consider the electric potential V induced by the motion. This potential exists, because neglecting $\dot{h}$ implies that curl $\mathbf{E}$ is negligible. Then $\mathbf{E} = -\text{grad}\, V$, and from (3) it follows that

$$\partial V/\partial y = \mu H_0 v_z - j_y/\sigma. \tag{11}$$

It is convenient to express the flowmeter output V_{XY}, measured between the electrodes X and Y (figure 1), in terms of a sensitivity S, where

$$S = V_{XY}/2\mu H_0 a v_0. \tag{12}$$

This takes the value unity for uniform or radially-symmetric velocity profiles in a non-conducting circular pipe (Kolin 1945).

Spatial boundary conditions

One obvious condition is that v_z and v shall vanish at the wall. The other condition concerns the magnetic field and potential. In the absence of any contact resistance between the fluid and the walls, the potential is everywhere continuous. Also H_z and h must be continuous at the fluid-wall interface and zero at the exterior of the walls. This secures continuity of current flow between the fluid and the walls, and precludes the flow of current outside the walls. Any voltage measuring device would take a negligibly small current.

From (10) it follows that j_0, the total wall current per unit length of pipe, is equal to $(\sigma\eta)^{1/2}v_0 h$, in which h is taken at the fluid boundary. If *as* and *an* indicate distances along the boundary and inward normal respectively, as shown in figure 2, and we assume that the wall has conductivity σ_0 and

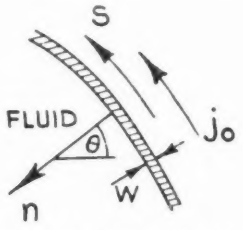

Figure 2. Portion of wall.

thickness w ($\ll a$), then $-j_0/w\sigma_0 = (\partial V/\partial s)/a$, V being in the wall or in the fluid at the wall. At the wall, v vanishes and $-\sigma \operatorname{grad} V = \operatorname{curl} \mathbf{H}/4\pi$, and hence $\partial V/\partial s = -(\eta/\sigma)^{1/2}v_0 \partial h/\partial n$. Eliminating $\partial V/\partial s$ and j_0, we see that at the fluid boundary

$$h = \frac{w\sigma_0}{a\sigma}\frac{\partial h}{\partial n}, \tag{13}$$

the other spatial boundary condition, if contact resistance is negligible. We shall write c for $w\sigma_0/a\sigma$, a dimensionless quantity.

In all that follows, complete symmetry in the x and y axes will prevail, with the result that v is even in X and Y, and that h is odd in X and even in Y.

3. The steady state solution

In an earlier paper (Shercliff 1953), (6) and (7) were solved for the case of steady flow in a rectangular channel with non-conducting walls. It was found that, when M is large, a core of uniform velocity occurs together with boundary layers at the walls. We should therefore expect similar behaviour in a circular pipe with thin conducting walls, the case which is now analysed.

We make the following assumptions.

(i) M is large in comparison with unity.

(ii) The boundary layer thickness is much smaller than the pipe radius, so that all variables may be treated locally as functions only of the distance *an* from the wall.

(iii) P is of the same order as Mv, as in the rectangular case, when M is large. P is here a constant, and v is of order unity.

(iv) In the core, Δv is negligible in (9), signifying that viscous forces are negligible.

The boundary layer region

The application of assumption (ii) to (8) and (9) for a point on a radius vector inclined at an angle θ to the x-axis (see figure 2) yields the equations

$$h'' - mv' = v'' - mh' + P = 0, \tag{14}$$

in which $m = M\cos\theta$, and dashes denote differentiations with respect to n. The boundary conditions are that $v = 0$ and $h = ch'$ when $n = 0$, and that v and h must become relatively steady outside the layer, approaching the local core values v_c and h_c. The solution is

$$v = v_c\{1 - \exp(-mn)\}, \tag{15}$$

$$h = h(0) - v + Pn/m. \tag{16}$$

The boundary-layer thickness is of the order of $1/m$, which is proportional to the reciprocal of the normal field intensity. The last term in (16) is negligible except where θ approaches $\frac{1}{2}\pi$, by virtue of assumption (iii) and because n is smaller than the boundary-layer thickness. Thus the pressure forces in the boundary layers are negligible, except where θ approaches $\frac{1}{2}\pi$. Equation (16) now gives $h = h(0) - v_c\{1 - \exp(-mn)\}$, and the condition (13) requires that $h(0) = -cmv_c = -v_c cM\cos\theta$. It follows that the total currents towards X per unit length of pipe are $(\sigma\eta)^{1/2}v_0(h_c - h_0)$, which is equal to $-(\sigma\eta)^{1/2}v_0 v_c$, in the boundary layer, and $-(\sigma\eta)^{1/2}v_0 v_c cM\cos\theta$ in the wall. The current in the layer is proportional to the core velocity, because the wall shear stress, proportional to (core velocity)/(layer thickness) and hence to (core velocity) × (normal field intensity), is balanced by the magnetic force on the layer, proportional to (current in layer) × (normal field intensity).

The core region

From assumption (iv) we have $\partial h_c/\partial X + P/M \doteqdot 0$, and hence $h_c = -PX/M$, since h_c is odd in X. This indicates that the current density in the core is uniform and parallel to the y-axis, and equal to $Pv_0(\sigma\eta)^{1/2}/Ma$. The electromagnetic force just balances the pressure gradient. Also, Δh_c vanishes, and (8) shows that, in the core, $v_z = v_c(Y)$, a function of Y only. The current in the core must all return in the two boundary layers and walls, as shown in figure 3. Across any section AB, remote from X or Y, the total core current per unit length of pipe is

$2X_0 Pv_0(\sigma\eta)^{1/2}/M$, in which $X_0 = (1 - Y^2)^{1/2}$, if we neglect the boundary-layer thickness in comparison with the length $2X_0$ of AB. Continuity of current flow, or of h, demands that $PX_0/M = v_c(1 + cM\cos\theta)$, and hence that

$$v_c = \frac{PX_0}{M(1 + cMX_0)}, \tag{17}$$

the required function of Y. Equation (17) ceases to be valid as Y approaches ± 1.

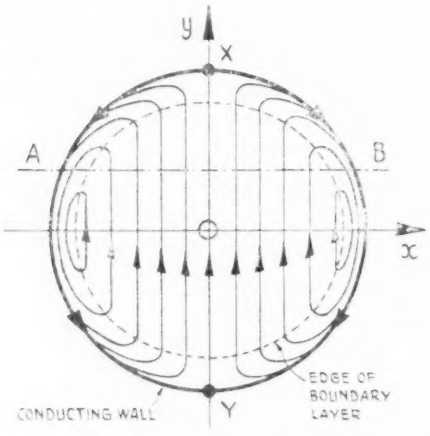

Figure 3. Current flow in walls, boundary layers and core.

The core velocity is not determined by local dynamical conditions, but indirectly by means of the current distribution. We may note in passing that when the walls are conducting, there is a downstream electromagnetic force on them with a corresponding net upstream force on the fluid. The pressure gradient has to counteract this as well as the viscous shear forces at the wall. When the walls do not conduct, there is no net electromagnetic force on the fluid. In neither case does the motion produce a force on the magnet supplying the transverse field, if edge effects are excluded.

It is now appropriate to examine some of the earlier assumptions. Equation (17) shows that Δv_c is of the order of P/M, and is negligible in (9), except when Y approaches ± 1. The boundary-layer thickness is small except where θ approaches $\frac{1}{2}\pi$. Obviously, the approximate treatment of the core and boundary layers fails near X and Y, but we assume that the solution is approximately valid elsewhere when M is large and the obscure regions are small.

Equation (17) is compatible with assumption (iii) provided cM is of the order of unity or less, and c is of the order of $1/M$ or less. For sodium flowing in a stainless steel pipe with reasonably thin walls, this condition is satisfied. The quantity cM is independent of the inside diameter of the pipe, and measures the relative conductivities of wall and boundary layer.

When cM is larger, the pressure gradient becomes important in the boundary layers, and the wall and core currents increase until the normal currents in the boundary layers become comparable with the tangential currents. Taking h as a function of n alone implies neglecting the normal currents.

Since the boundary layers are small, we may integrate (17) over the cross-section and relate P to the mean velocity v_0. This gives the relation

$$\frac{\partial p}{\partial z} = -\frac{3\pi\mu H_0 v_0(\sigma\eta)^{1/2}}{8a}(1+0{\cdot}883cM-0{\cdot}019(cM)^2+\ldots), \qquad (18)$$

which is nearly linear in cM.

The potential distribution may be found to the same accuracy from (11), in which $\mu H_0 v_z/(j_y/\sigma)$ is of the order of M. We therefore neglect j_y/σ and integrate along XY, assuming that no significant contribution to V_{XY} comes from the small obscure regions where v_z and j_y must be small. The variation of S with cM is shown in figure 4. When the walls are non-conducting, c vanishes and $S = 3\pi^2/32 = 0{\cdot}926$. Increasing the wall conductivity increases S, owing to the change in the velocity profile. Any decreasing tendency due to the short-circuit paths provided by the walls was neglected when j_y/σ was omitted from (11).

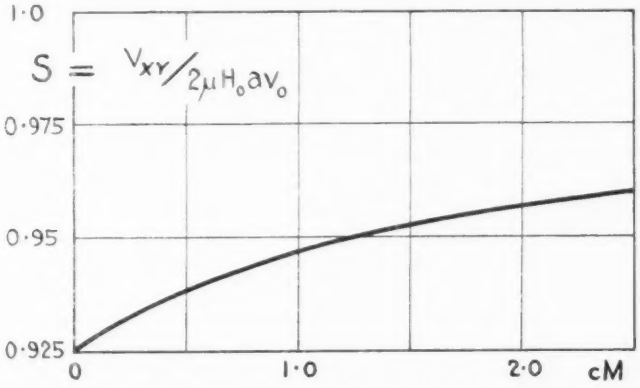

Figure 4. The effect of wall conductivity on sensitivity.

For low values of M, (8) and (9) may easily be solved in polar coordinates to yield solutions in series of ascending powers of M. In the steady state, the sensitivity is given by a series which begins with the terms

$$S = \frac{1}{1+c} - \frac{M^2}{576}\left(\frac{1}{1+3c}\right)+\ldots. \qquad (19)$$

4. The entry problem

The solution of (8) (less the β-term) and (9) is now considered for the case of a circular pipe with non-conducting walls, where the initial velocity is uniform and equal to v_0. It is not possible to impose an initial condition on h, since it is determined by (8). The spatial boundary conditions are that v and h shall vanish at the walls.

In order that the linear time-dependent case may be analogous to the original problem of entry into a region of transverse field, we must also impose the condition that v_0 and the integral of v over the pipe cross-section are constant.

It has been shown (Shercliff 1956) that when M is large and the fluid is flowing between parallel planes perpendicular to the field, a uniform entry-profile adjusts to its steady state in a dimensionless time T of the order of $1/M^2$. The dimensional time is of the order of $\rho/\mu^2 H_0^2 \sigma$, and the distance between the planes is irrelevant since the boundary-layer thicknesses are small in comparison. The settling process in this case simply involves the growth of boundary layers, the core velocity being virtually unaffected.

We should expect settling times for a circular pipe to be of the same order as for a square one, although somewhat less since the regions where the boundary layers are thick are smaller. For square pipes the dimensionless settling time is of the order of $1/M$ (Shercliff 1956).

The change from a uniform initial velocity in a circular pipe to the final steady profile, as already discussed, would be expected to fall into two stages as follows.

(*a*) During the first stage, lasting for a dimensionless time of the order of $1/M^2$, thin boundary layers are created as in the parallel-plane case, the core velocity being barely affected. Initially, no currents flow until viscous forces alone have produced a very small boundary layer. Subsequently, electromagnetic forces restrict the development of the layer to a thickness proportional to the reciprocal of the normal field intensity.

(*b*) In the second stage, occupying a much longer time of the order of $1/M$, the core profile is changed by electromagnetic forces to its final form, the boundary layer thickness being unchanged.

The motion in the regions near X and Y where the simple boundary layer theory fails is again left obscure on the assumption that the results are not seriously affected.

For both stages we shall make the following assumptions suggested by the steady state solution.

(i) M is large in comparison with unity.

(ii) The boundary layer thickness is always much smaller than a, so that all variables may be treated locally as functions only of T and n.

(iii) h and P/M are, at most, of the order of unity throughout. P may be related to the shear stresses at the walls by applying Green's theorem to the integral of (9) over the cross-section or the part in the first quadrant. This gives

$$\int_0^{\frac{1}{2}\pi} \frac{\partial v}{\partial n}\, d\theta = \frac{P\pi}{4}\,. \tag{20}$$

(iv) In the core, Δv_c is negligible in (9), and Δh_c is of the order of unity. The solution proves to be compatible with these assumptions except near X and Y. From (8) (less the β-term), it follows that $\partial v_c/\partial X$ is negligible and v_c is a function of Y and T only. We may note that this is true initially

and finally. Equation (9) degenerates to

$$M\partial h_c/\partial X + P = \dot{v}_c, \tag{21}$$

and we see that $\partial h_c/\partial X$ is also independent of X. Since h is odd in X, $\partial h_c/\partial X = h_c/X = h_0/X_0$, the value h_0 referring to the edge of the thin boundary layer. Equation (21) becomes

$$Mh_0/X_0 + P = \dot{v}_c. \tag{22}$$

On the basis of assumption (iii), this equation implies that $\dot{v}_c$ is of the order of M at most.

The first stage

This is expected to last a time of the order of $1/M^2$, and so the change in v_c will be of the order of $1/M$ and thus negligible. We shall therefore take v_c as unity during this stage.

Assumption (ii) applied to (8) and (9) for a point in the boundary layer on a radius vector inclined at an angle θ to the x-axis yields the equations

$$h'' - mv' = v'' - mh' - \dot{v} + P = 0. \tag{23}$$

Both h and v vanish when $n = 0$, and, when n is large, must approach the local core values h_0 and 1 respectively. From (23), $h' - mv = f(T)$, and hence $v'' - m^2v - v = mf(T) - P$ (independent of n) $= -m^2$, since when n is large, $v = 1$ and v'' and $\dot{v}$ vanish. In addition, $v = 1$ when $T = 0$. The solution is

$$v = 1 - \exp(-mn) + \frac{\exp(-m^2T)}{2(\pi m^2T)^{1/2}} \times$$
$$\times \int_0^\infty \exp(-u)\left[\exp\left(-\frac{(mn-u)^2}{4m^2T}\right) - \exp\left(-\frac{(mn+u)^2}{4m^2T}\right)\right] du,$$

in which the integral is obviously less than unity.

The form of the solution when T is a low multiple of $1/m^2$ is given closely by the first two terms. The boundary layer then resembles the steady-state one in extent, but the velocity rises to v_0 across every section of the layer. The first stage can be considered complete in a time of the order of $1/M^2$, even though $1/m^2$ is much larger in the obscure regions near X and Y.

Since P, which is of the order of M, is negligible in comparison with m^2 except near X and Y, then $f(T) \doteqdot -m$, and so $h' \doteqdot m(v-1)$. This equation and the condition $h = 0$ at the wall determine the behaviour of h, h_0 and hence h_c during the first stage. It can be shown that h_0 decreases steadily from zero, reaching -1 at the end of the first stage.

Figure 5 shows the current distribution at the end of the first stage. The boundary-layer current per unit length of the pipe is $(\sigma\eta)^{1/2}v_0$ at all sections of the boundary layer. There is singular behaviour near X and Y, where the currents issue into the core.

During the first stage, $\partial v/\partial n$ is of the order of m or M, except initially, when it is of the order of $T^{-1/2}$ and tends to infinity. Equation (20) shows

that P is, as assumed, of the order of M except when T is very small and M is an irrelevant variable.

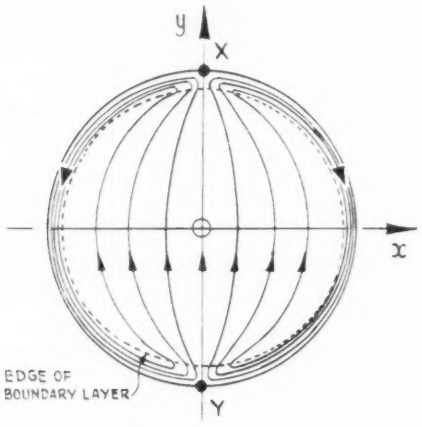

Figure 5. Current flow at the end of the first stage of the entry process.

The second stage

We shall see that v in the boundary layers is now of the same order as v_c. Hence $\dot{v}$ is, at most, of the order of M, and, like P, is negligible in (23). The boundary-layer analysis then gives $v = -h = v_c\{1-\exp(-mn)\}$, in which v_c varies with time, the extent of the boundary layers remaining constant. In particular $h_0 = -v_c$ and $\partial v/\partial n = mv_c$ at the wall. From (20) it follows that

$$P = \frac{4}{\pi}\int_0^{\frac{1}{2}\pi} M\cos\theta\, v_c\, d\theta = \frac{4M}{\pi}\int_0^1 v_c\, dY. \tag{24}$$

Again P is seen to be of the order of M. From (22) we may now deduce the linear equation

$$\frac{\dot{v}_c}{M} + \frac{v_c}{X_0} = \frac{4}{\pi}\int_0^1 v_c\, dY, \tag{25}$$

which governs the second stage of the motion. It is obvious that its duration will be of the order of $1/M$. The initial condition is $v_c = 1$, and no spatial boundary condition is necessary.

In calculating S we use (11) applied in the core, the term j_y/σ again being neglected. If no significant contribution to V_{XY} comes from the small obscure regions, it follows that

$$S = \int_0^1 v_c\, dY; \tag{26}$$

and we observe that P and S are simply proportional during the second stage. Equation (25) may be rewritten

$$\frac{\dot{v}_c}{M} + \frac{v_c}{X_0} = \frac{4}{\pi}S(MT), \tag{27}$$

which has the integrating factor $\exp(MT/X_0)$ and the solution

$$v_c = \exp(-MT/X_0)\left\{1+\frac{4}{\pi}\int_0^{MT} S(u)\exp(u/X_0)\,du\right\}$$

$$= \exp(-MT/X_0)+\frac{4}{\pi}\int_0^{MT} S(u)\exp\{(u-MT)/X_0\}\,du.$$

Application of the condition (26) yields the integral equation

$$S(MT) = H(MT)+\frac{4}{\pi}\int_0^{MT} S(u)H(MT-u)\,du, \tag{28}$$

where

$$H(p) = \int_0^1 \exp(-p/X_0)\,dY.$$

A numerical solution of (28) has been calculated, taking steps of 0·1 in MT and u. Initially S is unity, the velocity profile being almost wholly radially-symmetric (Kolin 1945); and finally the steady value $3\pi^2/32$ is reached. The continuous curve in figure 6 shows the variation of S or $-\{\pi a/4\mu H_0 v_0(\sigma\eta)^{1/2}\}\partial p/\partial z$ as a function of MT, or of Mz/Ra if we return to the non-linear entry problem by means of the Rayleigh approximation, setting $z = v_0 t$ and taking R to be the Reynolds number $\rho v_0 a/\eta$ based on pipe radius.

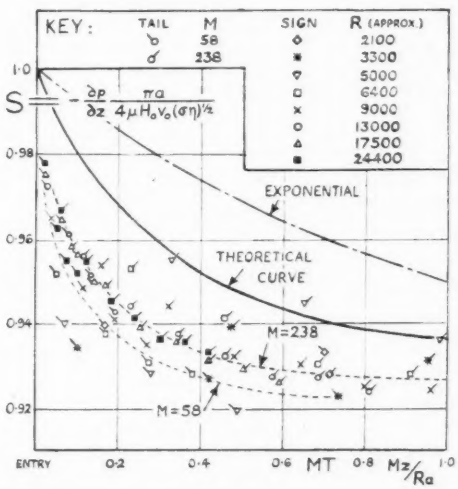

Figure 6. The entry process. S or dimensionless pressure gradient as a function of MT or Mz/Ra. The experimental points are from measurements of S at different values of M, R and z.

When T is small, the exact variation of S is not physically significant, because it is chiefly affected by the behaviour of v_c in the obscure regions near X and Y, and also because the first stage of the motion is still occurring. Moreover, the transverse field is not entered instantaneously in practice.

From figure 6 it will be observed that S is within 1% of its final steady value when $z \doteq Ra/M$. This makes an interesting comparison with the result for a rectangular pipe (Shercliff 1956) that departures from the ultimate steady velocity profile decrease by a factor $1/e$ in an entry length of the order of Ra/M. The departure of S from its ultimate value would be expected to decay similarly; and for comparison a chain-dotted exponential, decreasing by $1/e$ in a length Ra/M but having the terminal values appropriate to the circular case, has been added to figure 6. This emphasizes the fact that when M is large, entry lengths in rectangular pipes are considerably longer than in circular pipes.

The analysis has not been extended to cases where the entry velocity is not uniform. There is no reason for expecting the entry length to be very different. The analysis could easily be adapted for any initial variation of velocity in the y-direction. If the core velocity varies in the x-direction, such variations would probably be eliminated in the first stage by eddy currents in the xy-plane. This is suggested by the fact that for flow between parallel planes (Shercliff 1956), the entry length is of the order of Ra/M^2 when the core velocity varies in the x-direction.

Solutions in the form of series in ascending powers of M, valid when M is small, could be found, but the interest in such cases is slight.

Pressure loss at entry

In addition to the pressure loss due to the steady pressure gradient, there is a pressure loss δp associated with the profile adjustment from a uniform inlet velocity. No allowance will be made for the further large pressure loss due to eddy currents at the edge of the transverse field, as discussed by Hartmann (1937).

The drop δp may be found by integrating the excess of $\partial p/\partial z$ above its steady state value from zero to large values of z. No significant contribution comes from the very brief first stage of the motion, despite the singularity of P when $T = 0$. We can therefore use the second-stage result

$$P = 4MS/\pi. \tag{29}$$

From (27) we obtain

$$\frac{\partial(X_0 v_c)}{\partial(MT)} + v_c = \frac{4}{\pi} X_0 S,$$

which, when integrated from $Y = 0$ to $Y = 1$, shows that

$$\frac{\partial}{\partial T} \int_0^1 X_0 v_c \, dY = 0$$

because of (26). Hence

$$\int_0^1 X_0 v_c \, dY = \text{const.} = \tfrac{1}{4}\pi$$

initially, which expresses the equation of continuity since the boundary

layers are very thin. Also from (27), we get

$$\frac{\partial(X_0^2 v_c)}{\partial(MT)} + X_0 v_c = \frac{4}{\pi} X_0^2 S.$$

Integration of this equation from $Y = 0$ to $Y = 1$ gives

$$\frac{\partial}{\partial(MT)} \int_0^1 X_0^2 v_c \, dY = \frac{8S}{3\pi} - \frac{\pi}{4},$$

and hence

$$\frac{9\pi^2}{128} - \frac{2}{3} = \frac{8}{3\pi} \int_0^\infty \left(S - \frac{3\pi^2}{32} \right) d(MT),$$

since $v_c = 3\pi X_0/8$ finally, and the required integral has been determined. It follows that

$$\delta p / \tfrac{1}{2}\rho v_0^2 = \frac{27\pi^2}{128} - 2 = 0{\cdot}082,$$

which contrasts with the larger value 0·667 calculated by the Rayleigh approximation (Shercliff 1956) for flow into a circular pipe when magnetic effects are negligible. When M is large we see that δp is independent of M. A similar result would be expected for flow into rectangular pipes, in contrast with the result (Shercliff 1956) that $\delta p / \tfrac{1}{2}\rho v_0^2 = 1/M$ for flow between parallel planes when M is large. In this case there is no second stage of the motion, and δp is correspondingly smaller.

5. Experimental work

Experiments have been performed with the main object of verifying the theoretical values of S and $\partial p/\partial z$ in the steady flow of mercury in a non-conducting circular pipe under a transverse magnetic field at large values of M. The available values of M were limited by the saturation of the electromagnet and by the use of a tube small enough to produce measurable pressure gradients. Previous experiments (Hartmann and Lazarus 1937) reached a value of M of 18 only, and did not consider entry effects.

The apparatus also yielded approximate results for the variation of S and $\partial p/\partial z$ during the entry process, since only at the lower flow rates and greatest field intensities could steady conditions be reached within the extent of field available. At the lower flow rates and field intensities, the measured potential and pressure differences were liable to stray thermal and other effects, but nevertheless significant evidence in support of the theoretical work was obtained.

Experimental details

Figure 7 illustrates the mercury flow circuit schematically. The test-section indicated was either of two alternative Perspex pipes, installed in the gap of an electromagnet. One of 0·5 in. internal diameter with seven pairs of flowmeter-type electrodes at 1·5 in. pitch was used for measurements of S, and one of 0·25 in. diameter with four flush tappings at 3 in.

pitch for measurements of $\partial p/\partial z$. The electrodes were in fact small flush tappings also, this type having proved very successful. Tappings of $\frac{1}{32}$ in. diameter were the smallest that could be satisfactorily cleared of air. In each case the first tapping was 1·5 in. downstream of the edge of the magnet pole-faces.

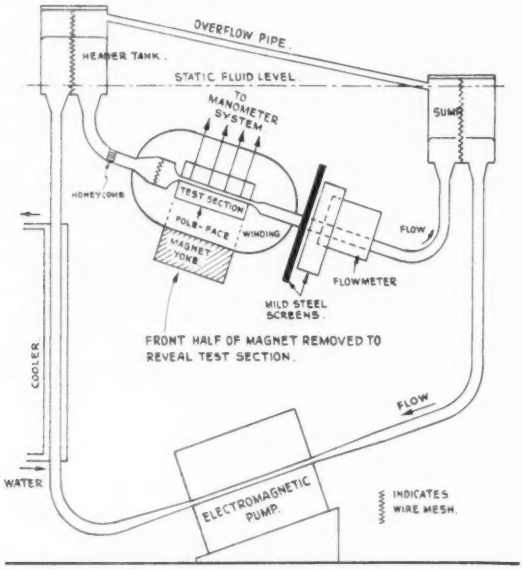

Figure 7. The fluid circuit (not to scale).

Steady flow occurred through the test-section under a gravity head of mercury maintained by an electromagnetic flat linear induction pump in the lower limb of the circuit. The cooler removed heat supplied by the pump. The mercury entered the test-sections through a streamlined contraction from a settling chamber with wire mesh grilles and preceded by a honeycomb to eliminate swirl. The velocity would presumably be nearly uniform after the contraction. Horizontal piping was avoided to aid the removal of air.

The flow rate was measured by an electromagnetic flowmeter in the upper limit of the circuit. Disturbance of this meter by the electromagnet was eliminated by the mild-steel screens shown and, when necessary, by taking the means of readings with the electromagnet energized alternatively in either direction.

The flowmeter was calibrated before and after the experiments with the screens in position using the apparatus illustrated in figure 8. The mercury flowed through the meter and the control cock under a constant head of 5·5 ft. Runs began when plug G was opened with plug H shut.

The mercury rose in the weir tank until a clock was started when contact was made with the electrode Z. This was surrounded by a sheath into which the mercury entered through a constriction at the bottom. The plug H was then opened, admitting mercury to the weigh tank until H was shut shortly before the header tank emptied. The clock stopped when contact was made at Z for the second time, there being the same amount of mercury in the weir tank at both timing instants. Thus the timed interval corresponded to the amount admitted to the weigh tank. After weighing, the mercury was blown back to the header tank through another pipe. Mercury has the advantage that electrical level indicators are easily arranged.

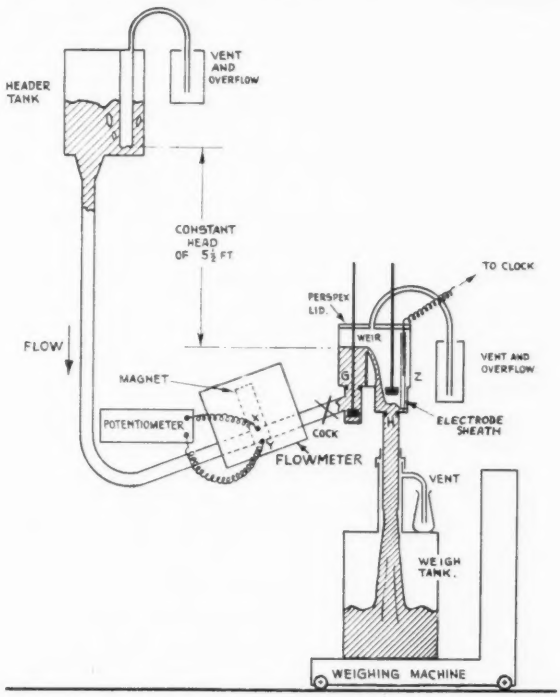

Figure 8. The flowmeter calibration rig (not to scale).

The apparatus worked well, even for runs as short as 18 sec. The flowmeter was found to give a relation between flow rate and output voltage which was linear over a wide range and reproducible within $\pm 0{\cdot}5\%$ of the mean in all positions relative to the upstream bend. This reliable calibration is to be attributed chiefly to the narrow fluid passage of the flowmeter, 1·10 in. deep and 0·04 in. in the field direction.

The electromagnet had pole faces 5 in. by 12 in. and a 1·25 in. gap. The water-cooled, low-voltage winding enabled fields of 14 800 oersted

to be attained. There was a sensibly single-valued relation between field intensity at the pole-face centre and exciting current for both directions of magnetization. Accordingly, the exciting current, measured in a temperature-insensitive shunt, was used to indicate field intensity after an initial calibration with a Cambridge fluxmeter and search coil had been performed. The experimental values of H_0 are considered accurate to 0·5%, except perhaps at low field intensities.

The field intensity fell off near the edges of the poles, the fall reaching 2% at the end electrode positions when the field was at its greatest value. A simple proportional correction was applied to voltages measured at the end electrodes, but not to the pressure differences. The effect of secondary currents at the field edges is difficult to allow for, but is small.

The test-section diameters were measured to 0·5% either by travelling microscope or weighing with a known length full of mercury. Mercury properties were taken from the *Liquid Metals Handbook* (Lyon 1952) and corrected for temperature changes.

All signals from the various electrodes were measured to 1 or 2 microvolts with a potentiometer, the readings at the higher flow rates or lower fields being more uncertain owing to increased unsteadiness of the flow. Care was necessary to ensure that the leads to the test-section electrodes did not link any of the main field as otherwise its small variations would produce large spurious signals. This is a point in favour of permanent magnets for flowmeters. Slight thermo-electric effects were observed when the magnet was running warm. All runs involving small signals were therefore made before the magnet had become warm.

Pressure gradients were measured with the sensitive manometer illustrated in figure 9. This instrument could record pressure differences to 0·001 in. of methylated spirits, a better fluid than water which is liable to wet non-uniformly. Owing to the presence of a warm magnet, however, it was impossible to eliminate stray errors of the order of 0·002 in., despite thorough lagging.

The four pipes from the flush tappings in the test-section led to the eight pinchcocks, which enabled the pressure difference between any two tappings to be measured, and also the 'zero' reading of the manometer to be established at any time. The manometer itself consisted of an inverted U-tube containing air above spirits. The spirits/mercury menisci were kept at fixed levels in reservoirs of large area by taking all readings with the air/spirits menisci brought to fixed positions in the two sloping parts of the U-tube. This also eliminated surface tension errors. It was achieved by adjusting the volume of air above the spirits and by altering the height of the right-hand sloping tube. Changes in the volume of the flexible tube below this had negligible effect, and thermal and other effects were reduced by the near-symmetry of the manometer system. A micrometer screw recorded the change in height of the sloping tube. The 'zero' reading was taken repeatedly as it was found to drift during long runs. The manometer took about 15 min to reach a steady state.

As the micrometer travel was limited, to measure the larger pressure differences the manometer was converted to a spirits/mercury one by allowing the spirits to rise, expelling the air, until the mercury menisci were in the sloping tubes. Readings taken by both methods were consistent. The smallest heads that were measured were about 0·05 in., read to the nearest 0·001 in. Care was taken to keep the mercury in the circuit at ambient temperature to minimize hydrostatic errors in the inclined test section.

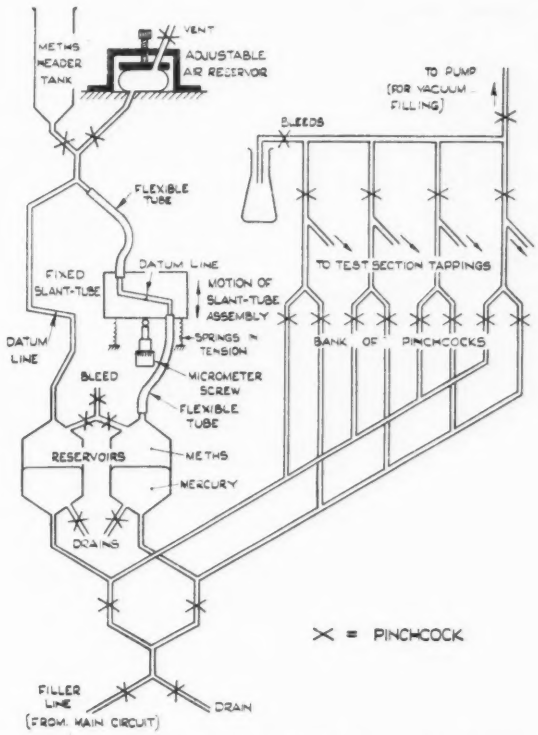

Figure 9. The manometer system, showing the air/methylated spirits arrangement (not to scale).

Observations were taken at four electromagnet field intensities and a range of flow rates, each 50% higher than the previous one. The upper limit was set by the available head, and the lower by the smallness of the signals to be measured by the potentiometer in the presence of stray potentials. The lowest signals were measurable only to 2% accuracy.

Experimental results: pressure gradients in the 0·25 *in. tube*

Figure 10 shows the readings reduced to dimensionless form, the three measured mean gradients between tappings being expressed as a multiple

of the theoretical gradient $3\pi\mu H_0 v_0(\sigma\eta)^{1/2}/8a$, valid for steady conditions when M is very large. Flow rate is represented by R, the Reynolds number based on radius. There are three zones in which the constant-M curves are horizontal, rising slowly and rising precipitately.

Where the experimental points are all marked as crosses, the three pressure differences showed a scatter but no clear falling tendency along the pipe. The central pressure difference tended to be slightly high. Horizontal lines fit the points reasonably well, and we deduce that this zone corresponds to steady flow that is laminar, because the gradient is independent of R and density.

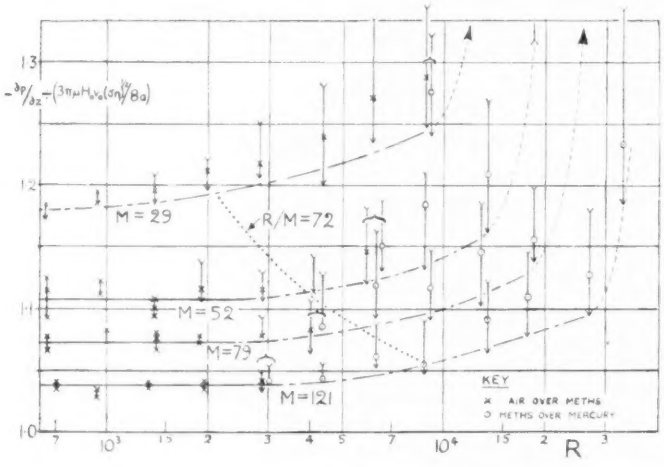

Figure 10. Experimental values of pressure gradient plotted non-dimensionally against flow rate at four field intensities.

At higher flow rates the pressure gradient was observed to fall along the pipe as steady conditions were approached, and here the three successive points are marked as arrow tail, cross (air/spirits) or circle (spirits/mercury) and arrow head. The points suggest that the flow was approaching a steady state with the same value of $(\partial p/\partial z)/(3\pi\mu H_0 v_0(\sigma\eta)^{1/2}/8a)$ as for the lower flow rates. Chain-dotted curves connect the arrow heads approximately. When M was 29, steady conditions were barely obtained even at the lowest flow rate. The pairs of arrows linked by brackets represent the fastest air/spirits readings and the slowest spirits/mercury readings, consistent within experimental error. During the runs where a steady state was still being approached, the readings both of pressure gradient and voltage were particularly prone to wander, even though the total flow rate was steady.

Finally the pressure gradients are seen to rise rapidly at a value of R that increases with M. Most of the experimental points are off the figure.

With $M = 29$ or 52 the gradients increased along the tube. There seems to be no doubt that a transition to turbulence was being observed. The rig did not permit an adequate study of the turbulent regime, and this was not attempted. It appears that provided $R < 250M$ approximately, laminar flow occurred under the conditions of the experiment, and that, in particular, there was laminar flow in all the runs with the 0·5 in. tube, described in the next section, except perhaps the fastest runs at the lowest field strength.

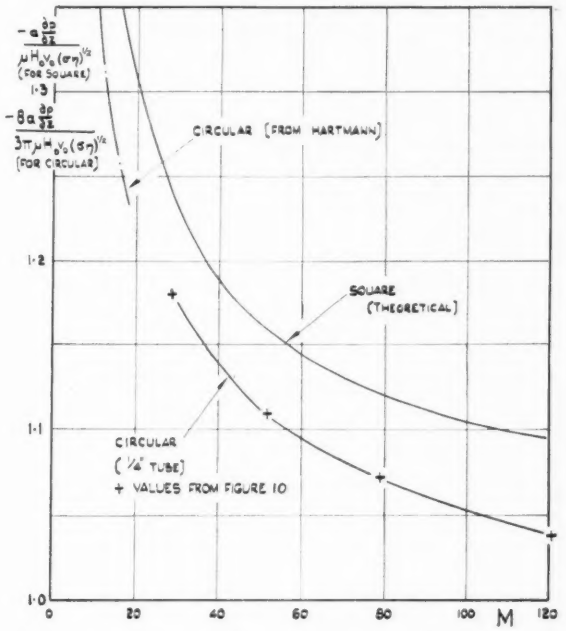

Figure 11. Ultimate pressure gradient plotted non-dimensionally against M for circular and square tubes.

The four steady values of $(\partial p/\partial z)/(3\pi\mu H_0 v_0(\sigma\eta)^{1/2}/8a)$ taken from figure 10 are plotted against M in figure 11. It appears likely that the curve does approach the value unity asymptotically as M increases. Experiments at higher values of M would almost inevitably involve the use of liquid sodium. Figure 11 also includes an approximate chain-dotted curve taken from the experiments of Hartmann & Lazarus (1937) for values of M up to 18. This is clearly compatible with the new results.

Experimental results: potential differences across the 0·5 *in. tube*

Values of S calculated from readings at the seven electrode pairs are plotted in figures 12(*a*) and 12(*b*) for values of M of 239 and 58. Similar intermediate results were obtained with M equal to 156 and 102. Curves

have been added to illustrate the trend of the results as R varies. The caption 'entry' refers to the leading edge of the pole faces.

Attention is directed first to figure 12 (*a*), since the readings are most reliable at the highest field strength. It is apparent that at the lower flow rates steady conditions were reached within the test-section, and that S then assumed the approximate value 0·92, confirming theoretical expectations reasonably well. At higher flow rates, decreasing values of S closer to unity occurred, as expected, because the velocity profile was not fully distorted from its presumed initial axial symmetry in the length available.

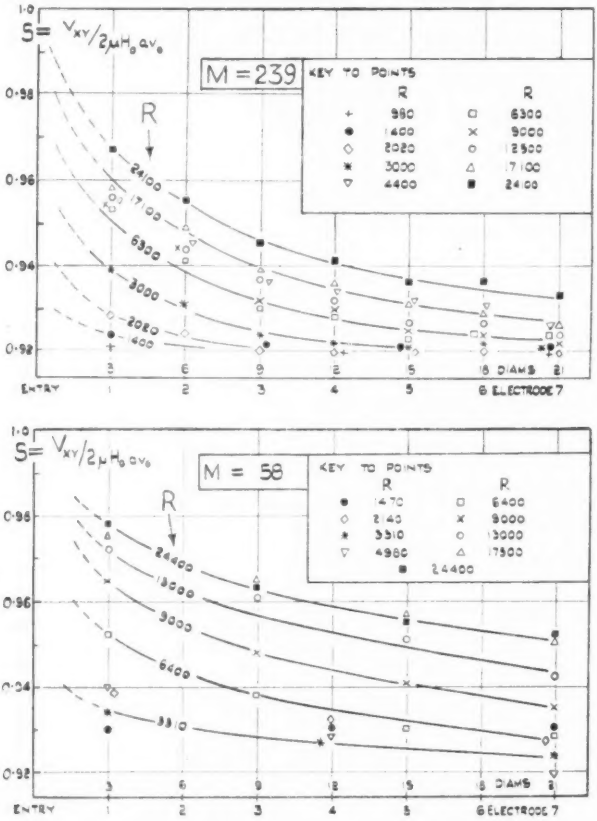

Figure 12. The fall in sensitivity along the 0·5 in. pipe.
(*a*) $M = 239$, (*b*) $M = 58$.

The accuracy fell as the field was reduced owing to the smallness of the quantities measured. Nevertheless figure 12 (*b*) is consistent with theoretical expectations. Another difficulty was the unsteadiness of the flow in runs where the settling process was protracted. It was impossible to achieve precise reproducible trends in these cases.

The entry process

The scatter of the results makes a close experimental check of the entry theory difficult. It is also complicated by the uncertainty of the entry conditions. As the streamlined contraction terminated about 1·25 in. before the edge of the pole-faces, there would presumably be some distortion of the velocity profile caused by the fringe flux before the main field was entered, and moreover the secondary currents at the field edges tend to distort the velocity profile. Nevertheless, in order to check the entry theory (itself approximate) we shall assume conventionally that the velocity was uniform at the section opposite the edge of the pole faces, and measure z from this section.

Experimental points for values of M of 239 and 58 have therefore been plotted in figure 6, z being measured from the edge of the pole faces. Dotted mean curves have been added. The theoretical entry length is seen to be correct in order of magnitude, if considerably overestimated. The experimental points also tend to confirm that the sensitivity S started to fall from unity while z was still negative.

A closer investigation of the entry process would require an elaborate technique to secure known, standard entry conditions. The dependence of S on the velocity profile provides a useful technique for studying such phenomena as the pipe-entry process, unless the velocity profile is radially symmetric.

Equation (28) indicates that $\partial p/\partial z$ and S should be mutually proportional at high values of M (except perhaps when the entry length is so long that the first stage with its higher value of $\partial p/\partial z$ becomes important). There is rough confirmation of this result in that $\partial p/\partial z$ and S both fall by amounts as large as 8% during the settling process. Figure 6 shows that S is usually within 1% of the steady state value when $Mz/Ra = 1$. A dotted curve for which $R/M = 72$, the value of z/a which corresponds to a point midway between the last two pressure tappings in the 0·25 in. tube, has therefore been added to figure 10. It is found to connect points where $\partial p/\partial z$ is roughly 1% above the steady state value. Thus both sets of readings give entry lengths of the same order of magnitude.

As M increases, the steady state value of S approaches its asymptotic value more rapidly than $(\partial p/\partial z)/(3\pi\mu H_0 v_0(\sigma\eta)^{1/2}/8a)$ tends to unity, simply because S (unlike $\partial p/\partial z$) only varies through a small range over the whole range of M. It was clearly impossible to find the variation of S with M from the present experiments. Hartmann & Lazarus did not measure potentials.

For comparison, a theoretical curve (Shercliff 1953) showing the variation of the steady $(\partial p/\partial z)/(\mu H_0 v_0(\sigma\eta)^{1/2}/a)$ against M for a square pipe of side $2a$, with the field parallel to a side, has been added to figure 11. This curve approaches the value unity less rapidly than the experimental curve for the circular pipe, presumably because the regions where the boundary layers are thick are smaller in circular than in square pipes.

6. Practical implications

It has been shown that distortion of the velocity profile can cause the sensitivity of a flowmeter of circular section to fall from the Kolin value by about 8%, provided the fluid traverses the magnetic field for a distance at least equal to Ra/M before encountering the electrodes, the theoretical distance being somewhat larger than the observed ones. It is important to consider whether the fall will occur commonly in practice. Typical figures for a small flowmeter of 1 in. bore bearing liquid sodium at 300° C at 100 cm/sec in a field of 3000 oersted are $R = 3{\cdot}3 \times 10^4$, $M = 500$ and $R/M = 66$. Since the field would probably extend for 2 or 3 rather than 33 diameters upstream of the electrodes, we see that only at much lower flow rates would appreciable distortion of the velocity profile and fall in sensitivity occur. Variation of sensitivity due to upstream disturbances or edge effects is likely to be much more serious (Shercliff 1954, 1955).

Further experiments to test the variation of S with wall conductivity would be interesting, but also very difficult owing to the importance of contact resistance.

The experiments described above were carried out with the help of facilities provided at Cambridge University by the Atomic Energy Research Establishment, Harwell.

References

Bullard, E. C. 1955 *Proc. Roy. Soc.* A, **233,** 289.

Hartmann, J. 1937 *Math.-fys. Medd.* **15,** No. 6.

Hartmann, J. & Lazarus, F. 1937 *Math.-fys. Medd.* **15,** No. 7.

Kolin, A. 1945 *Rev. Sci. Instr.* **16,** 109.

Lock, R. C. 1955 *Proc. Roy. Soc.* A, **233,** 105.

Lyon, R. N. 1952 *Liquid Metals Handbook,* Navexos P-733, U.S. Office of Naval Research.

Murgatroyd, W. 1953 *Phil. Mag.* **44,** 1348.

Shercliff, J. A. 1953 *Proc. Camb. Phil. Soc.* **49,** 136.

Shercliff, J. A. 1954 *J. Appl. Phys.* **25,** 817.

Shercliff, J. A. 1955 *J. Sci. Instr.* **32,** 441.

Shercliff, J. A. 1956 *Proc. Camb. Phil. Soc.* **52,** 573.

REVIEWS

Engineering Fluid Mechanics, by C. JAEGER. (Translated from the German by P. O. Wolf.) London: Blackie, 1956. 529 pp. 60*s*.

In English-speaking countries the term hydraulics has long been under a cloud. The disparagement from which it still suffers arose out of the difficulties of the subject that until relatively recently permitted investigators to give only their observations of depth, pressure and discharge. No analysis of the details of the motion or effective comparison with previous papers was possible, and all too often the records of their painstaking work terminated with nothing more than 'the author's formula', applicable only to the exact conditions of the experiment. It is presumably for this reason that a misleading title heads this revised and enlarged translation of Dr Jaeger's *Technische Hydraulik*, of which a French version has already appeared under the title *Hydraulique Technique*. The book is concerned wholly with the motion of water. After a preliminary account of the physical basis of hydraulics and the fundamental equations the author turns to his three principal topics, steady and unsteady flow in open channels, unsteady flow in pipes due to surge and water hammer, and seepage, which between them occupy nearly three quarters of the book.

For several reasons the practical problem of steady flow in a uniform open channel of uniform slope is far more extensive than that of steady flow in a circular pipe, and our knowledge of it is relatively scanty. The channel may be of rectangular, trapezoidal, circular or egg-shaped cross-section with almost unlimited variation in the proportions of the cross-section, and the free surface destroys any possible symmetry in the velocity distribution over the cross-section. Two types of flow can occur according as the velocity in the main stream is greater or less than that of a long wave moving under gravity on the surface. They may be given the descriptions 'superundal' and 'subundal', which seem clearer than the adjectives 'shooting' and 'streaming' which are more commonly used. They correspond to Froude numbers greater and less than unity, and an analogy exists with the flow of a gas which likewise is of two types according as the Mach number is greater or less than unity. In practice, friction effects are of vital importance because they determine the discharge through a channel of given shape and slope, but for a large canal the slope is so minute that it cannot easily be measured in existing works or correctly constructed in new works. Further complications ensue if the slope or cross-section of the channel is not uniform or if blockages, such as weirs are inserted. Unsteady flow may be due to the passage upstream of 'jumps' of various kinds (such as may be seen in nature as bores in esturaries) or to the passage downstream of disturbances caused by floods or by the removal of obstructions.

Unsteady flow in pipe-lines is of two kinds, dependent on the rapidity with which the control valve is moved. If the valve is shut suddenly,

a loud noise (water hammer) is heard which is familiar to many householders, and a pressure wave passes upstream, the intensity of which in pounds per square inch is roughly 60 times the original water velocity measured in feet per second. Now the velocity of sound in water in an almost rigid pipe is about 4500 ft/sec., and the original water velocity cannot be more than a very small fraction of this. Hence the aerodynamicist would describe the shock wave as weak; not so the hydraulic engineer as he surveys his shattered pipe and damaged power station. But normally the valve admitting water from the pipe-line to the turbine is moved relatively slowly by the governor, which can also open a bypass for a short time. The mass of water in the pipe-line is, however, so great that, to smooth out the resulting disturbances without excessive waste through the bypass, a surge tank is usually connected to the pipe-line. This is an open vertical pipe, much larger in cross-section than the pipe-line and placed as close to the power station as circumstances permit. Under steady conditions the water level in the surge tank stands lower than that in the reservoir by an amount equal to the friction loss of head in the intervening pipe-line. The installation can be regarded as a gigantic U-tube; one limb (the reservoir) is virtually of infinite cross-section, and from the base of the other (the surge tank) water is drawn off to the turbine. Any change in this demand leads to damped oscillations of level in the surge tank which are governed by non-linear differential equations. If the demand increases, the surge tank serves as a source close at hand, and initially the level in it falls; if the demand decreases, part of the flow from the reservoir passes into the surge tank, the level in which begins to rise.

Dr Jaeger deals with these subjects in great detail, and almost every possible case and sub-case is fully examined. The treatment is entirely analytical supplemented, when the working grows too complex, by graphical methods. The standard of mathematics that is employed is not high, but the algebra is often long and tedious. The author evidently believes that there is no satisfactory means of escape from these laborious calculations, for alternative methods are cursorily dismissed. Thus in the description of surge tanks six lines and five references suffice for an account of the importance and use of models and electrical analogues, as " there is not, however, sufficient space to include a description of these techniques here ". (Additional references on the first of these matters have strayed into the chapter on water hammer.)

The book does not contain examples to be worked out, and it is clearly meant, not for the general student, but for the designer and the advanced specialist. The designer will not, however, find here all that he wants. For many of the problems alternative methods of solution are provided, but he is given little help in choosing which is the best; the treatment is comprehensive rather than critical. Moreover, he is made aware that the theories are inevitably based on a variety of assumptions, yet they are left unsupported by experimental evidence. Thus a doubt may arise in his mind whether the lengthy computations are worth while—a doubt that will

not be lessened by the author's remark that " it is not within the province of this book to investigate the usefulness and practical results of the methods of analysis developed in " the chapters on surges and water hammer. It is to be hoped that Dr Jaeger will soon provide this much wanted assessment. He remarks with great truth that observations of surge and water hammer are, regrettably, too rarely published, but in his list of references there is sufficient information for at least some comparison to be made. This shortage of experimental evidence, which is seriously delaying the advance and spread of knowledge, seems to arise from financial pressure. A costly pipe-line must be put into commercial service the moment it has passed the simple tests required by the contract, and even a single day devoted to experiments would involve a serious loss of revenue. No lead in this matter has been given in the highest quarters, for in the course of a discussion on a paper on surge tanks read in 1933 before the Institution of Civil Engineers, a distinguished speaker expressed his hope of publishing surge observations on the Lochaber installation. This hope is long deferred, for these readings have not yet been communicated to the institution.

The book ends with appendices on empirical coefficients, flow over a movable bed, and density currents. A very valuable feature of the entire work is the enormous number of references extending up to 1955, which are presented in the form of footnotes. These are accompanied by brief biographical notices of the more eminent authors.

In his two prefaces Dr Jaeger describes his work as a handbook as well as a summary of his lectures at Zürich, and in a very large handbook of this sort it is inevitable that the author's chief interests are shown up by unevenness in the standard of treatment of the various topics. Thus, in the chapter on the basic equations when he is dealing with the loss of energy at a sudden expansion in a pipe, he is content to reproduce the usual dubious analysis that survives in text books seemingly because it leads to a tidy result. It depends on the assumption that the pressure on the annular surface at the enlargement is the same as that in the smaller pipe. This assumption, he writes, " is supported by experimental evidence ", but the references provided are scarcely convincing. Taylor's name might have been included in Chapter II amongst those who have gone deeply into that intractable subject, the theory of turbulence; and much more experimental confirmation of boundary-layer theory exists than can be found in Escande's 1938 book on dams, which is the only reference provided on this point. Little use is made of Froude number to simplify the analysis of flow in open channels, and Chapter IV on steady flow in channels ends in confusion as the calculation of the critical depth for various shapes of cross-section is apparently extended to include free and aerated jets. The detailed treatment of critical flow theory, which includes an interesting history of the problem, would have been improved by an account of the simple ideas introduced long ago by Hugoniot. The wretched weir formula involving a dimensional coefficient of discharge,

which engineers are accustomed to use, is stated without protest; and the opportunity is missed of explaining the advantage of comparing the actual discharge with that over the theoretical broad-crested weir having the same width and head. Lemoine's sinusoidal theory of undular jumps is noticed, but not its demolition by Benjamin and Lighthill. The important advance made by Southwell and Vaisey in their application of relaxation methods to free-surface problems is mentioned only in a footnote to a remark on a problem which they did not treat.

There is much to be said for the widely held view that the days are past when an author could produce a lengthy and balanced book covering the latest advances in many fields. It can no longer be expected that one man, no matter how scholarly and industrious he may be, can have everything at his fingers' ends at the same time. Of recent years the stream of original papers has greatly increased in width, depth and velocity, and the only way of control is by division of the flood. Two methods have been tried with success. The first is the large book covering a number of topics, each with a chapter to itself written by a different yet expert hand. Conspicuous examples are *Engineering Hydraulics* and *Modern Developments in Fluid Dynamics* under the respective editorship of Hunter Rouse and Goldstein, both of which have served as powerful springboards for further advances. A drawback of this method is the long delay that a big book encounters at the printer's hands. Moreover, the editor, if conscientious, must expect to be brought by his labours almost to the grave. The second method is the monograph of limited scope compiled and seen through the press by one man. The final stages are relatively brief, and the book need not be seriously out of date as soon as it is published. There is nothing to prevent a gifted author from producing a succession of monographs. In both methods it is unnecessary for the size of the book and therefore its price to be inflated by the inclusion of preliminary matter than can readily be found elsewhere.

A. M. Binnie

CORRIGENDUM

Equation (41) of my paper, "The influence of radiative transfer on cellular convection" (*J. Fluid Mech.* **1**, 1956, 424), should read as

$$R' = \frac{\int_{-\frac{1}{2}}^{+\frac{1}{2}} w'Q(w')\,d\zeta}{\int_{-\frac{1}{2}}^{+\frac{1}{2}} w'^2(\beta/\bar{\beta})\,d\zeta}. \qquad (41)$$

R. M. Goody

INDEX

Arie, Mikio and Rouse, Hunter Experiments on two-dimensional flow over a normal wall, 129.

Batchelor, G. K. On steady laminar flow with closed streamlines at large Reynolds number, 177.

Batchelor, G. K. A proposal concerning laminar wakes behind bluff bodies at large Reynolds number, 388.

Benjamin, T. Brooke On the flow in channels when rigid obstacles are placed in the stream, 227.

Betchov, R. An inequality concerning the production of vorticity in isotropic turbulence, 497.

Blackman, V. Vibrational relaxation in oxygen and nitrogen, 61.

Chester, W. Supersonic flow past a bluff body with a detached shock. Part I. Two-dimensional body, 353.

Chester, W. Supersonic flow past a bluff body with a detached shock. Part II. Axisymmetrical body, 490.

Coles, Donald The law of the wake in the turbulent boundary layer, 191.

Crease, J. Long waves on a rotating earth in the presence of a semi-infinite boundary, 86.

Evans, Cerda and Evans, Foster Shock compression of a perfect gas, 399.

Evans, Foster *See* **Evans and Evans.**

Francis, J. R. D. The speed of drifting bodies in a stream, 517.

Freeman, N. C. On the theory of hypersonic flow past plane and axially symmetric bluff bodies, 366.

Glauert, M. B. The laminar boundary layer on oscillating plates and cylinders, 97.

Glauert, M. B. The wall jet, 625.

Goody, R. M. The influence of radiative transfer on cellular convection, 424.

Greenspan, H. P. The generation of edge waves by moving pressure distributions, 574.

Hall, I. M. The displacement effect of a sphere in a two-dimensional shear flow, 142.

Holt, Maurice The method of characteristics for steady supersonic rotational flow in three dimensions, 409.

Jahn, Robert G. The refraction of shock waves at a gaseous interface, 457.

Landweber, L. and Yih, C. S. Forces, moments, and added masses for Rankine bodies, 319.

Laufer, John and McClellan, Robert Measurement of heat transfer from fine wires in supersonic flows, 276.

Lighthill, M. J. Drift, 31.

Lighthill, M. J. The wave drag at zero lift of slender delta wings and similar configurations, 337.

Longuet-Higgins, M. S. The refraction of sea waves in shallow water, 163.

Malkus, W. V. R. Outline of a theory of turbulent shear flow, 521,

McClellan, Robert *See* **Laufer and McClellan.**

Phillips, O. M. The intensity of Aeolian tones, 607.

Proudman, Ian The almost-rigid rotation of viscous fluid between concentric spheres, 505.

Rott, Nicholas Diffraction of a weak shock with vortex generation, 111.

Rouse, Hunter *See* **Arie and Rouse.**

Saffman, P. G. On the rise of small air bubbles in water, 249.

Saffman, P. G. On the motion of small spheroidal particles in a viscous liquid, 540.

Saffman, P. G. and Turner, J. S. On the collision of drops in turbulent clouds, 16.

Sakurai, Akira Propagation of spherical shock waves in stars, 436.

Shercliff, J. A. The flow of conducting fluids in circular pipes under transverse magnetic fields, 644.

Stewart, R. W. Irrotational motion associated with free turbulent flows, 593.

Townsend, A. A. The properties of equilibrium boundary layers, 561.

Turner, J. S. *See* **Saffman and Turner.**

Van Dyke, M. D. The slender elliptic cone as a model for non-linear supersonic flow theory, 1.

Whitham, G. B. On the propagation of weak shock waves, 290.

Woods, L. C. On the thrust due to an air jet flowing from a wing placed in a wind tunnel, 54.

Yih, C. S. *See* **Landweber and Yih.**

REVIEWS

The Theory of Hydrodynamic Stability, by C. C. Lin, 349.

Fluidization, edited by D. F. Othmer, 454.

The Structure of Turbulent Shear Flow, by A. A. Townsend, 554.

Engineering Fluid Mechanics, by C. Jaeger, 667.

The Philosophical Magazine

First Published in 1798

Editor:

PROFESSOR N. F. MOTT, M.A., D.Sc., F.R.S.

Editorial Board:

SIR GEORGE THOMSON, M.A., D.Sc., F.R.S.
PROFESSOR A. M. TYNDALL, C.B.E., D.Sc., F.R.S.
SIR LAWRENCE BRAGG, O.B.E., M.C., M.A., D.Sc., F.R.S.

Contents of November, 1956

Gamma Radiation from the Decay of $^{238}Pu_{94}$, $^{242}Cm_{96}$ and $^{244}Cm_{96}$. By J. O. Newton, B. Rose and J. Milsted, Atomic Energy Research Establishment, Harwell

The Elastic Scattering of 136 Mev Neutrons by Nuclei. By C. P. van Zyl, R. G. P. Voss and R. Wilson, Clarendon Laboratory, Oxford

The Nuclear Radius and Potential from Neutron Diffraction Scattering. By Richard Wilson, Cyclotron Laboratory, Harvard University, U.S.A.

An Investigation of Neutrons from the Reaction $^{10}B(d, n)^{11}C$ at 1·08 Mev Bombarding Energy. By A. Graue, Department of Physics, University of Bergen, Bergen, Norway

Isotopic Spin Selection Rules. VIII: Charge Independence and the Comparison of Isobaric Triplets. By D. H. Wilkinson, Cavendish Laboratory, Cambridge

The Nuclear Surface. By T. H. R. Skyrme, Atomic Energy Research Establishment, Harwell, Berks.

The Nuclear Spin–Orbit Coupling. By J. S. Bell and T. H. R. Skyrme, Atomic Energy Research Establishment, Harwell, nr. Didcot, Berks.

Correspondence

Book Reviews

Price per part £1

Price per annum £10 10s. post free

Printed and Published by

TAYLOR & FRANCIS LTD

RED LION COURT, FLEET STREET, LONDON, E.C.4

Physics in Medicine and Biology

The Journal of the Hospital Physicists' Association
published in association with the Philosophical Magazine

Editor:
J. E. ROBERTS, D.Sc.

Consultant Editor:
Professor N. F. MOTT, F.R.S.

Editorial Board:
W. A. LANGMEAD, M.Sc.
J. S. MITCHELL, C.B.E., F.R.S.
J. ROTBLAT, D.Sc.
D. A. MCDONALD, D.M.
G. J. NEARY, Ph.D.
F. W. SPIERS, D.Sc.
J. F. TAIT, Ph.D.

Contents of October, 1956

The Semicircular Canal System of the Organs of Equilibrium. By J. J. Groen, M.Sc., Universiteitskliniek voor keel-neus-en oorziekten, Utrecht, Netherlands

A Simple Differential Calorimeter for small Animals. By E. G. C. Clarke and A. E. Hawkins, Department of Physiology, Royal Veterinary College, University of London

The Radioactivity from Thorotrast and its Retention in Tissues. By J. Rotblat, Ph.D., D.Sc., F.Inst.P. and Gillian Ward, M.Sc., Ph.D., Physics Department, The Medical College of St. Bartholomew's Hospital, London

The Radioactivity of Thorotrast. By J. Rundo, B.Sc., A.R.C.S., A.R.I.C., Finsen Laboratory, Copenhagen ø, Denmark

Whole Body Radioactivity Measurement as Applied to Clinical Tracer Studies. By J. E. S. Bradley, Ph.D., Radioisotopes Laboratory, Postgraduate Medical School, Ducane Road, London, W.12, N. Veall, B.Sc., F.Inst.P., Guy's Hospital Medical School, London, S.E.1, and F. Whiting, B.Sc., Radioisotopes Laboratory, King's College Hospital and Medical School, London, S.E.5

A Calorimetric Method used in the Dosimetry of X-ray Beams from a 1 Million Volt Generator. By G. W. Dolphin, B.Sc., Ph.D. and G. S. Innes, B.Sc., A.M.I.E.E., Physics Dept., St. Bartholomew's Hospital Medical College

A Calibration of the Fricke Chemical Dosimeter. By H. C. Sutton, M.Sc., Ph.D., Hugh Adam Department of Cancer Research, University of Otago Medical School, Dunedin, N.Z.

Book Reviews

Abstracts Section

Subscription price per volume £3 10s. post free, *payable in advance*
4 parts per volume—£1 per part

Printed and Published by
TAYLOR & FRANCIS LTD
RED LION COURT, FLEET STREET, LONDON, E.C.4

Orders originating in U.S.A. and Canada should be sent to the Academic Press Inc., 111 Fifth Avenue, New York, 3, N.Y., U.S.A.

Advances in Physics

A Quarterly Supplement of the Philosophical Magazine

Editor:
PROFESSOR N. F. MOTT, M.A., D.Sc., F.R.S.

Editorial Board:
SIR GEORGE THOMSON, M.A., D.Sc., F.R.S.
PROFESSOR A. M. TYNDALL, C.B.E., D.Sc., F.R.S.
SIR LAWRENCE BRAGG, O.B.E., M.C., M.A., D.Sc., F.R.S.

Contents of October, 1956

Some Physical Properties of Diamonds. By F. C. Champion, King's College, London

On the Polaron Rest Energy and Effective Mass. By G. R. Allcock, Department of Physics, University of Liverpool

Some Aspects of Magnetohydrodynamics. By G. H. A. Cole, University College, London

---

Price per part £1

Price per annum £3 15s. post free

Printed and Published by

TAYLOR & FRANCIS LTD

RED LION COURT, FLEET STREET, LONDON, E.C.4

Journal of Electronics

A Philosophical Magazine Associated Journal

Devoted to Electron Sciences

Editor:
J. THOMSON, M.A., D.Sc., M.I.E.E., F.Inst.P.

Consultant Editor:
Professor N. F. MOTT, F.R.S.

Editorial Board:
Professor P. AIGRAIN (France)
Professor H. B. G. CASIMIR (Holland)
Dr. W. KLEIN (Germany)
Dr. R. KOMPFNER (U.S.A.)

Contents of November, 1956

Studies of Rectification in a Gas (Nitrogen) Discharge between Coaxial Cylindrical Electrodes. I. Theory of Rectification in a.c. Silent Discharges. By V. L. Talekar, Department of Physics, Maharaja's College, Jaipur, India

Studies of Rectification in a Gas (Nitrogen) Discharge between Coaxial Cylindrical Electrodes. II. Rectification in Semiozonizers. By V. L. Talekar, Department of Physics, Maharaja's College, Jaipur, India

The Photo-Thermoelectric Phenomenon in Semiconductors. By L. J. van der Pauw and D. Polder, Philips Research Laboratories, N.V. Philips' Gloeilampenfabrieken, Eindhoven, Netherlands

On the Effect of the Transition Region upon an Electron Beam constrained by Brillouin Flow. By B. W. Manley, Mullard Research Laboratories, Salfords

Anomalous Characteristics of Silicon Point Contact Rectifiers. By D. J. Kyte (Communication from the Staff of the Research Laboratories of The General Electric Company Limited, Wembley, England)

The Measurement of Drift Mobility in Germanium at High Electric Fields. By A. F. Gibson and J. W. Granville, Radar Research Establishment, Malvern, Worcs.

Tracer Experiments in Photocells. By W. E. Turk, English Electric Valve Co. Ltd., Chelmsford, England

Moving Striations in Low Pressure Mercury Vapour. By K. W. H. Foulds, Department of Electrical Engineering, Imperial College, London

Elastoresistance and Magnetoresistance in Multivalley Semiconductors with an Axis of Symmetry. By Robert W. Keyes, Westinghouse Research Laboratories, Pittsburg 35, Pennsylvania

Luminescence in ZnS: Cu, Cl Single Crystals. By T. B. Tomlinson, Communication from the Staff of the Research Laboratories of The General Electric Company Limited, Wembley, England

Correspondence:

Emitter-Base Impedances of Junction Transistors. By R. E. Burgess, Department of Physics, University of British Columbia, Canada

Book Notices

Price per part £1 5s.
Price per annum £7 post free

Printed and Published by

TAYLOR & FRANCIS LTD

RED LION COURT, FLEET STREET, LONDON, E.C.4

Orders originating in U.S.A. and Canada should be sent to the Academic Press Inc., 111 Fifth Avenue, New York, 3, N.Y., U.S.A.

JOURNAL OF FLUID MECHANICS

—o—

Orders originating

in

UNITED STATES OF AMERICA

and

CANADA

should be sent to the sole agents

ACADEMIC PRESS INC.

111 Fifth Avenue,

New York, 3,

N.Y., U.S.A.

JOURNAL OF FLUID MECHANICS
Volume 1, Part 6 December 1956

CONTENTS

The properties of equilibrium boundary layers
by A. A. TOWNSEND 561

The generation of edge waves by moving pressure distributions
by H. P. GREENSPAN 574

Irrotational motion associated with free turbulent flows
by R. W. STEWART 593

The intensity of Aeolian tones
by O. M. PHILLIPS 607

The wall jet
by M. B. GLAUERT 625

The flow of conducting fluids in circular pipes under transverse magnetic fields
by J. A. SHERCLIFF 644

Reviews 667

Index to Volume 1 671

5846